

The effect of environment on the structure of disc galaxies

Florian Pranger¹★, Ignacio Trujillo^{2,3}, Lee S. Kelvin⁴, María Cebrián^{2,3}

¹National Astronomical Research Institute of Thailand, 191 Huay Kaew Road, 50200 Chiang Mai, Thailand

²Instituto de Astrofísica de Canarias, c/Vía Láctea s/n, E-38205-La Laguna, Tenerife, Spain

³Departamento de Astrofísica, Universidad de La Laguna, E-38205 La Laguna, Tenerife, Spain

⁴Astrophysics Research Institute, Liverpool John Moores University, IC2, Liverpool Science Park, 146 Brownlow Hill, Liverpool L3 5RF, UK

23 January 2017

ABSTRACT

We study the influence of environment on the structure of disc galaxies, using IMFIT to measure the g- and r-band structural parameters of the surface-brightness profiles for ~700 low-redshift ($z < 0.063$) cluster and field disc galaxies with intermediate stellar mass ($0.8 \times 10^{10} M_{\odot} < M_{\star} < 4 \times 10^{10} M_{\odot}$) from the Sloan Digital Sky Survey, DR7. Based on this measurement, we assign each galaxy to a surface-brightness profile type (Type I \equiv single-exponential, Type II \equiv truncated, Type III \equiv anti-truncated). In addition, we measure (g-r) restframe colour for disc regions separated by the break radius. Cluster disc galaxies (at the same stellar mass) have redder (g-r) colour by ~0.2 mag than field galaxies. This reddening is slightly more pronounced outside the break radius. Cluster disc galaxies also show larger global Sérsic-indices and are more compact than field discs, both by ~15%. This change is connected to a flattening of the (outer) surface-brightness profile of Type I and - more significantly - of Type III galaxies by ~8% and ~16%, respectively, in the cluster environment compared to the field. We find fractions of Type I, II and III of $(6 \pm 2)\%$, $(66 \pm 4)\%$ and $(29 \pm 4)\%$ in the field and $(15^{+7}_{-4})\%$, $(56 \pm 7)\%$ and $(29 \pm 7)\%$ in the cluster environment, respectively. We suggest that the larger abundance of Type I galaxies in clusters (matched by a corresponding decrease in the Type II fraction) could be the signature of a transition between Type II and Type I galaxies produced/enhanced by environment-driven mechanisms.

Key words: galaxies: evolution – galaxies: photometry – galaxies: structure – galaxies: environment

1 INTRODUCTION

The last decade has witnessed the emergence of a new scheme to understand the structure of disc galaxies (e.g. Erwin et al. 2005; Pohlen & Trujillo 2006). Following this picture, disc galaxies can be classified according to the different slopes they present in their inner and outer regions. Galaxies which are best described by purely exponential surface-brightness profiles (e.g. Bland-Hawthorn et al. 2005; Weiner et al. 2001) are classified as Type I. Type II galaxies are those where the surface-brightness profile is characterised by a broken exponential with a steep outer and a shallower inner region (e.g. Pohlen et al. 2002). Finally, Type III are disc galaxies the surface-brightness profiles of which are anti-truncated, i.e. where the exponential decline of surface brightness is steeper in the inner region and shallower at larger galactocentric distances (e.g. Erwin et al. 2005).

The emergence of Type II galaxies has been studied by a number of authors using numerical simulations (e.g. Li et al. 2006; Bournaud et al. 2007; Foyle et al. 2008; Roškar et al. 2008; Martínez-Serrano

et al. 2009; Sánchez-Blázquez et al. 2009). To date, the general perception is that truncations that are not related to Lindblad-resonances (see e.g. Debattista et al. 2006) are the consequence of stellar migration and a radial star-formation threshold as the gas disc becomes thinner at large galactocentric radii. However, it is still being debated whether the other surface-brightness profile types also formed through internal mechanisms or are a consequence of external galaxy evolutionary processes. Theoretical work by e.g. Yoshii & Sommer-Larsen (1989) and Elmegreen & Hunter (2006) shows that in principle, single-exponential and antitruncated discs can form ab initio, albeit under very specific conditions. However, it is worth noting that Younger et al. (2007) have shown that antitruncations can be the consequence of external processes like tidal interactions and minor galaxy mergers. Furthermore, in S0 galaxies, antitruncated profiles might also be related to an extended bulge component (e.g. Erwin 2005; Maltby et al. 2015).

The first attempt to quantify the frequency of each profile type was done by Pohlen & Trujillo (2006) (hereafter PT06). Using ~90 nearby late-type (Sb-Sdm) spiral galaxies, they found that only ~10% are single-exponentials. The rest are ~60% Type II and ~30% anti-truncated galaxies. This study was conducted using

★ E-mail: florian@narit.or.th

disc galaxies of different environments. [Erwin et al. \(2008\)](#), using a sample of 66 barred S0-Sb disc galaxies from different environments, found a distribution of 27%, 42% and 24% of Type I, Type II and Type III profiles (with 6% combinations of Type II and III). In a follow-up to this work ([Gutiérrez et al. 2011](#)), the authors investigated a sample covering the full morphological range of disc galaxies (i.e. S0-Sm) and reported a correlation of morphology and surface-brightness profile type; Type I and Type III galaxies were found to be most frequent in early-type discs while the fraction of Type II profiles was found to increase with Hubble type, i.e. to be higher in late-type discs. Overall, they reported a distribution of 21%, 50% and 38% of Type I, Type II and Type III profiles, with 8% combined Type II and III galaxies that were counted twice.

A potential change on the structural break properties of the disc galaxies is expected when comparing the field with the cluster environment. There are many physical mechanisms in high density regions that should be particularly relevant for affecting the outermost (weakly bound) zones of galaxies; tidal galaxy-galaxy interactions, tidal interactions between galaxies in high-density cluster regions and with the gravitational potential of the cluster (i.e. galaxy harassment) as well as hydrodynamical interactions between galaxies and the intra-cluster or intra-group medium such as ram-pressure stripping (see e.g. [Toomre & Toomre 1972](#); [Gunn & Gott 1972](#); [Moore et al. 1996](#); [Lopes et al. 2014](#); [Head et al. 2014](#); [Hiemer et al. 2014](#)).

The effect of the environment on the structure of galaxy discs is still a debated question and recent analyses have led to somewhat incongruent conclusions. For a sample of spiral galaxies, [Maltby et al. \(2015\)](#) explored whether the frequency of each profile type changes in a cluster environment, finding $\sim 10\%$ Type I, $\sim 50\%$ Type II and $\sim 40\%$ Type III galaxies in their cluster and field samples. The authors also investigated a sample of S0 cluster and field galaxies, and found $\sim 25\%$ Type I, $< 5\%$ Type II and $\sim 50\%$ Type III galaxies with $\sim 20\%$ of the profiles exhibiting general curvature and hence remaining unclassified. Comparing their field and cluster galaxies, the authors concluded that the stellar distribution in the outer regions of disc galaxies is not significantly affected by the galaxy environment. However, [Erwin et al. \(2012\)](#) reported that truncated (Type II) S0 galaxies are nonexistent in Virgo Cluster while they account for roughly one third of S0s in the local field. The difference in the cluster was found to be almost entirely compensated by Type I galaxies. The authors reasoned different mechanisms driving the structural evolution of galaxies in the cluster and field environment. Other works have also pointed to environment-mediated mechanisms and their effect on the structural break properties of disc galaxies (e.g. [Roediger et al. 2012](#); [Laine et al. 2014](#); [Head et al. 2014](#)).

In this paper we want to investigate in detail whether the environment plays a role on the frequency of each profile (break) type. To isolate as much as possible the effects produced by the cluster environment, we select our sample of field and cluster galaxies to have the same redshifts and stellar mass ranges. We choose a narrow mass range since it has been shown that the structural parameters of disc galaxies change with mass (see PT06) and we want to minimise this effect in our analysis. We will show that the main effect of the cluster environment is to redden by around ~ 0.2 mag the (g-r) colour and to decrease the global size (as parameterised by the effective radius R_e) of the discs by $\sim 15\%$. These two global changes are accompanied by an increase (by a factor of ~ 2.5) in the fraction of Type I (pure exponential) disc galaxies in the cluster regions and an increase in the (outer) scale lengths of Type I ($\sim 8\%$) and Type III ($\sim 16\%$) profiles.

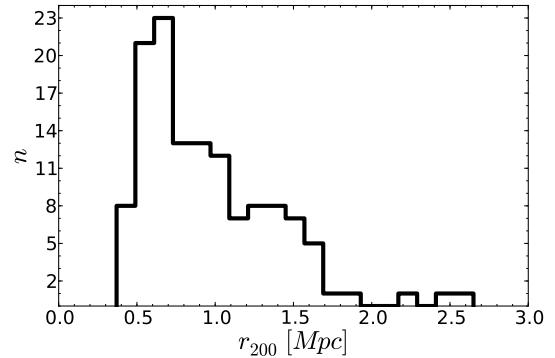


Figure 1. Distribution of the r_{200} values for all 130 host clusters.

In the subsequent section (Section 2) we present a description of the data including a discussion of our selection criteria, the sample compilation and the background subtraction techniques. Section 3 describes the methods used for structural galaxy fitting and for colour determination. The results are presented in Section 4 and discussed in Section 5. We summarise the results and conclusions in Section 6. Finally, we present prototypical profiles, further details of the analysis of the field sample and comprehensive data tables in an appendix to this paper. Throughout this paper we assume $H_0 = 70$ km/s/Mpc, $\Omega_m = 0.3$ and $\Omega_\Lambda = 0.7$.

2 THE DATA

To conduct our work, we used the NYU Value-Added Galaxy Catalogue (NYU-VAGC, [Blanton et al. 2005a](#)) based on the SDSS-DR7 ([Abazajian et al. 2009](#)) as the basis for our parent sample. This catalogue provides spectroscopic redshifts and photometry, global Sérsic-indices and corresponding effective radii (see [Blanton et al. 2005b](#) for a detailed description of the morphological fitting technique) as well as stellar masses ([Blanton & Roweis 2007](#)) calculated on the basis of a [Chabrier \(2003\)](#) IMF and a population synthesis model from [Bruzual & Charlot \(2003\)](#). Our parent sample is analogue to the one of [Cebrián & Trujillo \(2014\)](#). First, we selected only the galaxies contained within the region of the survey described by [Varela et al. \(2012\)](#), in order to avoid problems with the borders of the survey. Then, we only considered the objects above the mass-completeness limit presented in [Cebrián & Trujillo \(2014\)](#) (see Eq. 1 from that paper). This ensures that our sample is complete in stellar mass, avoiding biases due to the magnitude limit inherent to the SDSS catalogue. To assure that our initial sample of galaxies are predominantly disc-dominated and within a narrow range of stellar masses, we took only objects with Sérsic-index $n < 2.5$ and $0.8 \times 10^{10} M_\odot < M_\star < 4 \times 10^{10} M_\odot$. The lower mass limit corresponds to our completeness limit while the higher mass limit was chosen to minimise the influence of stellar mass on the results of our study.

We also estimated, for all the galaxies, the 3D spatial (X, Y, Z) position within the survey using the information provided by the R.A., Dec and redshift of each object. To do this, we used the following set of equations provided by [Varela et al. \(2012\)](#):

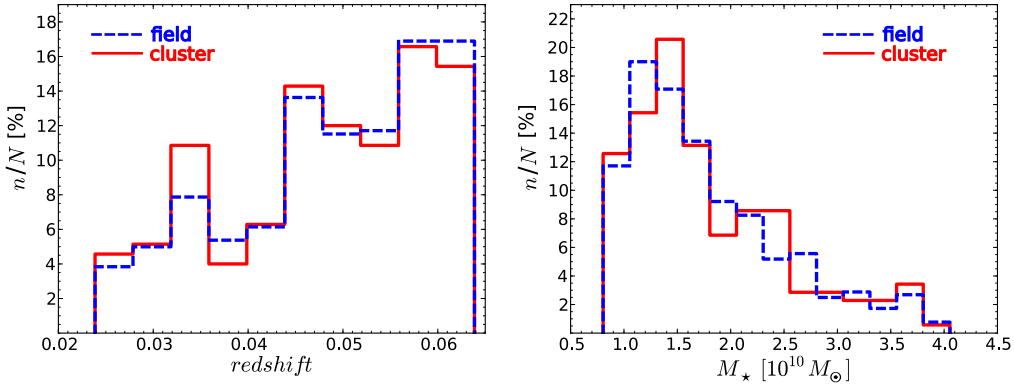


Figure 2. *Left panel:* normalised redshift distribution of the total cluster and total field sample. *right panel:* normalised distribution of stellar mass for the total cluster and total field sample.

$$\begin{aligned} X &= D(z) \cos \delta \cos \alpha \\ Y &= D(z) \cos \delta \sin \alpha \\ Z &= D(z) \sin \delta \end{aligned} \quad (1)$$

with α , δ and $D(z)$ being the equatorial coordinates and the co-moving radial distance, respectively. The spatial distribution of the galaxies is used to explore the environment inhabited by the objects.

2.1 The cluster sample

Following Cebrián & Trujillo (2014), we compiled a large sample of galaxy clusters in our explored volume using a number of catalogues: the Abell catalogue (Abell et al. 1989), a catalogue extracted from SDSS-DR6 (Szabo et al. 2011), three catalogues from SDSS III (Einasto et al. 2012; Tempel et al. 2012; Wen et al. 2012); the GMBCG cluster catalogue (Hao et al. 2010), and the XMMi-SDSS galaxy cluster survey (Takey et al. 2011). This is a total of 1877 galaxy clusters.

To build the sample of galaxies in clusters, we took only those galaxies from the parent sample that are located at a clustercentric distance less than 1 Mpc to the nearest galaxy cluster centre. Since the goal of this work is to conduct a detailed analysis of the structural properties of the disc of the galaxies, we selected the objects with the lowest redshifts. These selection criteria left us with 246 catalogue galaxies. To minimise the influence of dust and to ensure the reliability of morphological information, we followed PT06 in selecting face-on to intermediately inclined galaxies and we discarded close pairs and obvious galaxy mergers after a visual inspection. After doing this, we were left with 175 galaxies in 130 different clusters (25 clusters from Abell et al. 1989, 18 clusters from Szabo et al. 2011, 72 clusters from Tempel et al. 2012 and 15 clusters from Wen et al. 2012). The sample of 175 galaxies will henceforth be referred to as the total cluster sample. The selection of a reasonable number of cluster galaxies finally resulted in a redshift range of $0.021 < z < 0.063$. All galaxies in the total cluster sample are listed in the appendix. The r_{200}^1 -distribution of the 130 host clusters is shown in Fig. 1.

2.2 The field sample

In order to compare the properties of disc galaxies in the cluster environment to those of disc galaxies in the low-density to intermediate-density field environment, we created a sample of field galaxies drawn from the same parent galaxy catalogue as the initial cluster sample. In a first step, we confined the parent catalogue to galaxies with a 3D spatial distance greater than 3.5 Mpc to the nearest cluster centre to ensure our objects are beyond the virial radius of the nearest cluster. In order to have a field sample with stellar mass and redshift distribution similar to those distributions in the cluster sample, we generated random samples of 246 field galaxies (the same initial number as for the cluster galaxies), and selected three samples closely resembling the initial cluster sample. As we did for the cluster sample, we selected face-on to intermediately inclined galaxies and discarded close pairs and galaxy mergers after a by-eye inspection. We were left with 172, 172 and 177 galaxies in the three field samples (no overlap). They will henceforth be referred to as field sample 1, field sample 2 and field sample 3. By joining the three field samples we constructed a large field sample of 521 galaxies which will henceforth be referred to as the total field sample. All galaxies in the total field sample are listed in the appendix. The redshift and stellar mass distributions of the total cluster and field samples are compared in Fig. 2. The corresponding illustrations for the individual field samples are shown in Fig. B1.

We explored whether the global size of our field galaxies is representative of the general field population. With the redshift and stellar mass limits of our cluster sample, we had 14868 field galaxies. Their median size (as parametrised by R_e) is larger than the median size of the cluster sample by $\sim 13\%$. Our field samples have median global sizes larger than the median size of our total cluster sample by $\sim 15\%$. This difference in global size is in compliance with Cebrián & Trujillo (2014). All analyses presented in this paper were carried out on each of the initially selected samples (four in total). We use the three field samples to test for effects possibly introduced by random sampling and to estimate the robustness of the observed differences between the cluster and the field population.

2.3 Sky subtraction and limiting surface brightness

As this work aims to explore the outer regions of disc galaxies to characterise their properties, it is necessary to have an accurate sky subtraction and an estimation of the limiting surface brightness.

¹ Values adopted from the cluster catalogues, except for Abell-clusters for which values were taken from the literature.

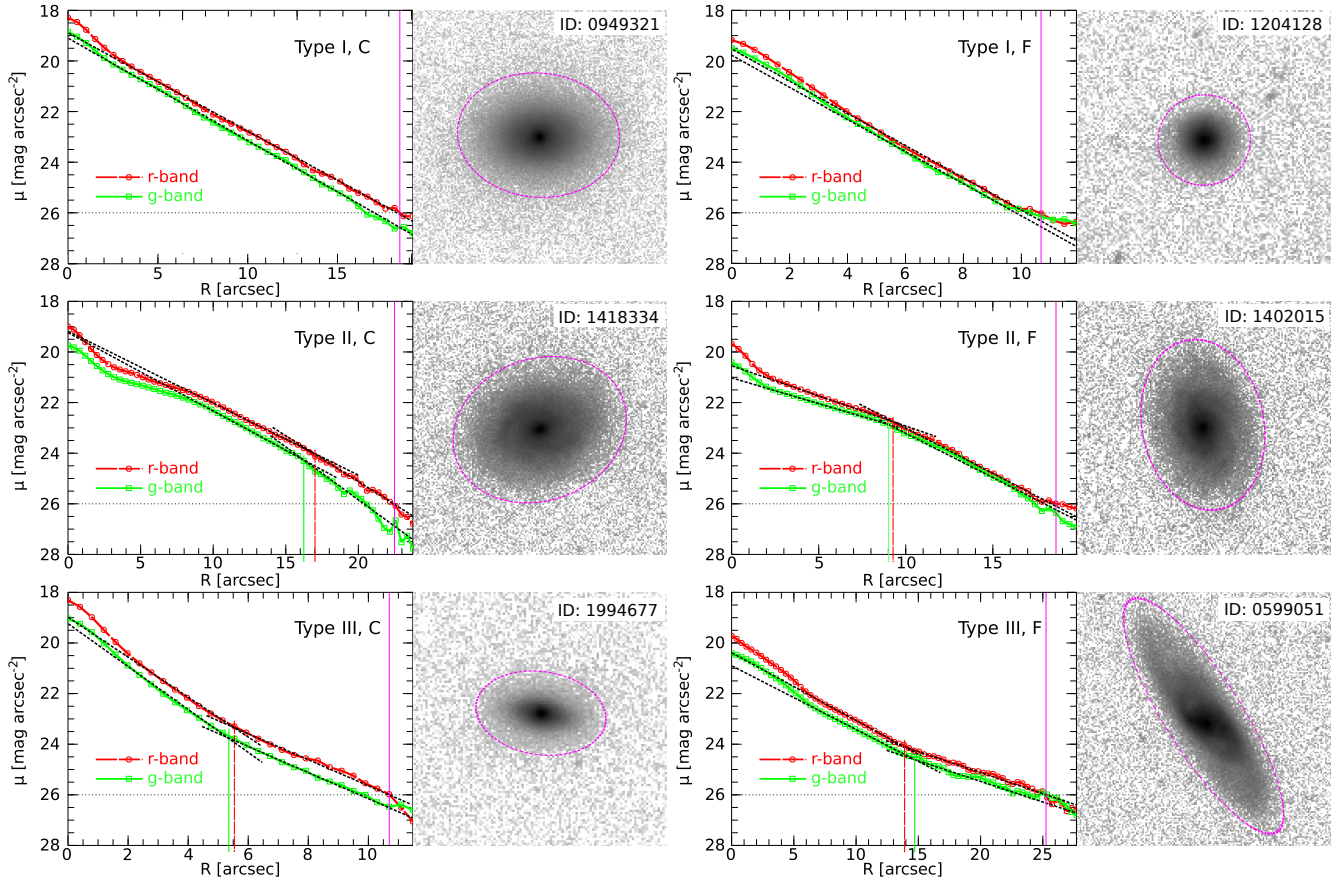


Figure 3. Prototypical examples for each galaxy type in both environments. *Left column, top to bottom:* Type I, Type II (double break) and Type III surface-brightness profiles and corresponding r-band cluster galaxy images. *Right column, top to bottom:* Type I, Type II and Type III surface-brightness profiles and corresponding r-band field galaxy images. The over-plotted short-dashed lines in the profile plots indicate the exponential disc regions resulting from the fitting routine. The short vertical lines represent the break radii in the different bands. The horizontal dashed line indicates our conservative confidence threshold. For scale reference, the purple ellipses in the images mark the mean radius corresponding to this threshold, indicated by a solid vertical line in the profile plots. The galaxies' NYU-VAGC-ID is inserted in the images.

Using the same SDSS imaging, PT06 showed that surface brightness profiles in the g- and r-band can be reliably traced down to 27 mag/arcsec² (see also Trujillo & Fliri 2016). In order to reach such accuracy, we followed the same strategy as PT06 to obtain an estimate of the sky from as close as possible to the galaxies under study. First, we measured the mean sky after three 3- σ clippings within 5 large rectangular sky boxes. Chosen sky boxes were placed as close as possible to the respective galaxy with the aim of including as little source flux as possible. This necessitates a variability in box size according to secondary source conditions unique to each pointing (typically in the range of 300-500 pixels on a side), with the total area fixed at 160k pixels per box. Any remaining extended sources within a sky box were masked out. For further details of this methodology, see PT06. As a second method, we investigated the radial profile of the galaxy image pixel counts (with masked adjacent sources) in 120 angular directions, separated by 3 degrees. We controlled whether the sky value measured with the first method was in compliance with the averaged value at which the radial profiles were visually found to flatten out. This was true within ± 0.16 counts for all galaxies in our total field and cluster samples, both for g- and r-band data. For the photometric calibration we followed again PT06. This error in the sky determination corresponds to $\sim 16\%$ of the sky and to a surface brightness of > 27

mag/arcsec². Since we do not attempt to extend our analyses beyond this value but limit ourselves to a conservative threshold of 26 mag/arcsec², this uncertainty has no effect on the results presented in this work.

3 STRUCTURAL GALAXY FITTING

In order to characterise the structural (break) properties of our sample of 696 disc galaxies (175 cluster and 521 field), we used the surface-brightness fitting code IMFIT (Erwin 2015). We applied this code to both, the g- and r-band data. The images provided to IMFIT were masked and sky-subtracted. The masks were created using SExtractor (Bertin & Arnouts 1996) in a hot and cold configuration mode. To account for the effect of the Point Spread Function (PSF), we built a PSF for each SDSS image frame using PSFExtractor (Bertin 2011) to estimate the FWHM of the PSF. Then, we used the image generator of the IMFIT package, MAKEIMAGE, to generate Moffat-PSF-images (SDSS standard β -values of 3.1 and 2.9 for the r- and g-band; see e.g. Trujillo et al. 2001; Erwin 2015 for more details) of 51 \times 51 pixels ($\sim 20'' \times 20''$). The surface-brightness distributions of the galaxies in our sample were modelled using a two-dimensional Sérsic-bulge and a broken

exponential (Erwin et al. 2008) for the disc component. These models were convolved with the PSF.

All 696 galaxies of the total cluster and field sample were successfully modelled by IMFIT in the g- and r-band. Each of the 1392 fits was set up individually, i.e. for each galaxy image we created an individual configuration file with initial parameter values based on visual estimates after a by-eye inspection of the azimuthally averaged 2D projected surface-brightness profile. The majority of the fits ran without any problems. For $\sim 30\%$ of the galaxies it was necessary to further refine the initial fitting parameters. Approximately 40% of these were to ensure that the innermost region of the galaxy (i.e. the bulge) was properly modelled by the Sérsic part, while the disc was to be (dominantly) modelled by the broken exponential function to exclude potential degeneracies. For the remaining 60%, the profiles showed more than one break in the galaxy’s disc region. In these cases, we manually forced IMFIT to model the *outermost* break above our limiting surface brightness. The profile types of the galaxies where the fit initially failed were Type II ($\sim 76\%$) and III ($\sim 24\%$).

For 56 galaxies (27 in the total cluster sample, 10, 10 and 9 in the field samples), the best fitting result was obtained for $h_1=h_2$ (i.e. the scale lengths in and outside the break have the same value). These galaxies were classified as Type I, following PT06. Another 199 galaxies (50 in the total cluster sample, 47, 50 and 52 in the field samples) showed an “up-bending” or “anti-truncated” profile, i.e. $h_1 < h_2$, and were classified as Type III. The remaining 441 galaxies (98 in the total cluster sample, 115, 112 and 116 in the field samples) exhibited a “down-bending” profile, i.e. $h_1 > h_2$, and thus were classified as Type II. The profile type number counts are the same in both bands. Depending on the analysed band, we notate the structural parameters as follows: $h_{1,g}$, $h_{2,g}$, $R_{b,g}$ and $h_{1,r}$, $h_{2,r}$, $R_{b,r}$, where $R_{b,g}$ and $R_{b,r}$ denote the break radii. Profile type fractions and average parameter values are shown in Table 1. In Fig. 3 we show prototypical examples for the surface-brightness profiles and the fitted scale lengths for all three types in both investigated environments.

In PT06, the authors applied several sub-classifications to Type II and Type III galaxies, based on their Hubble-type (barred vs. non-barred galaxies) and on the radial position of the break. Since the galaxy sample analysed for the present work are at a higher redshift ($0.021 \leq z \leq 0.063$) than the sample analysed by PT06 ($z \leq 0.01$), it was impossible to robustly determine the Hubble-type for all galaxies in our study. Thus, we did not apply any further sub-classification for Type II and Type III galaxies.

3.1 Galaxy colour

For all 696 galaxies in the combined total cluster and field sample, we measured (g-r) restframe colour, $(g-r)_{restframe}$, both outside ($(g-r)_o$) and inside ($(g-r)_i$) the break radius $\bar{R}_b = (R_{b,g} + R_{b,r})/2$. The k-correction was conducted following Chilingarian et al. (2010). In addition, to explore the effect of the bulge on the colour properties of the inner regions of the galaxies, we repeated the above colour measurements but this time masking the inner $R_{c1} = 0.5R_e$ (obtaining $(g-r)_{i,1}$) and $R_{c2} = 0.75R_e$ (obtaining $(g-r)_{i,2}$). For all investigated galaxies $R_b > R_{c1}$ and $R_b > R_{c2}$. The masking of the bulge regions results in a de-reddening of galaxy colours which is in general more pronounced in field galaxies and appears to be strongest in field Type II objects. This was to be expected, since Type II galaxies are predominantly late-type objects, which exhibit comparatively strong star-formation activity in their discs. The median colour val-

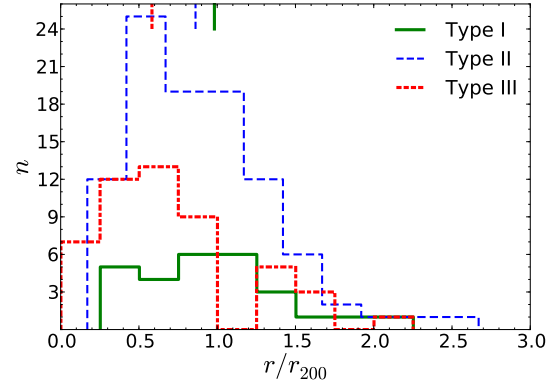


Figure 4. Normalised radial distributions of the different profile types in the total cluster sample (green solid, blue dashed and red short-dashed lines for Type I, II and III, respectively). The short vertical lines indicate the corresponding median values.

ues for the total cluster and total field sample are shown in Table 1, along with the other disc properties studied here.

4 GALAXY PROPERTIES AS A FUNCTION OF ENVIRONMENT

4.1 Global properties

There are several global results to highlight in this section. In relation to the global (break) structure: a) the number of Type I (single-exponential) galaxies in the cluster environment is significantly higher (by a factor of 2.5) than in the field; b) the number of Type II (truncated) galaxies is lower in the cluster environment by 10 percentage points, matching the increase of Type I objects; c) the number of Type III (anti-truncated) galaxies, however, is quite similar in both environments. It is worth noting that the average radial distribution of the different surface-brightness profile types within the clusters is different, with Type III galaxies residing at a median clustercentric distance (normalised to r_{200}) of 0.58 ± 0.05 , while the other types preferentially occupy regions at comparatively larger median normalised distances of 0.98 ± 0.09 and 0.86 ± 0.04 for Type I and II, respectively (errors estimated via 1000 1- σ bootstrapping iterations). The normalised radial distribution of the different profile types is illustrated in Fig. 4. The global size value, as mentioned before, measured by R_e , is $\sim 15\%$ larger in the field than in the cluster. Finally, also the global Sérsic-index (as provided by the NYU catalogue) is significantly higher in the cluster than in the field (by $\sim 15\%$). By construction of our subsamples, there is no global difference between cluster and field environment in average total stellar mass. The global structural and colour differences between the cluster and the field environment are illustrated in Fig. 5.

Independent of the surface-brightness profile type, in all the regions, the median $(g-r)_{restframe}$ colour is significantly (~ 0.2 mag) redder in the cluster than in the field (most significant for Type I and III). For Type II and III field galaxies, with the bulge suitably masked, we find the inner disc to be notably redder than the regions at galactocentric distances greater than the break radius. In the cluster sample no such difference is seen within the errors. This finding indicates that the reddening in the cluster is stronger in the outer parts of the disc, which is in compliance with the scenario of disc-fading (see e.g. Christlein & Zabludoff 2004), i.e. the fad-

Table 1. Listing of the median values of the structural properties of the galaxies analysed in this work. The total cluster and total field sample are abbreviated by TCS and TFS, respectively. The ratios of the inner and outer scale lengths in the g- and r-band surface-brightness profiles are listed as $ratio_g$ and $ratio_r$, respectively. Median colour values determined between R_b and R_{c1} are given as $(g-r)_{in,1}$, those determined between R_b and R_{c2} as $(g-r)_{in,2}$ (see Section 3.1). Type I galaxies were not considered for the calculation of the median $(g-r)_{out}$ colour for the total samples. We also list the number of galaxies in each sub-sample, N, and its percental equivalent (along with the corresponding Wilson 1927-confidence intervals), as well as the median global effective radius R_e , median Sérsic-index n and median stellar mass M_* . All errors were estimated through 1000 1- σ bootstrap iterations. Field values with an asterisk indicate significant differences between the cluster and the field as estimated by a standard KS-test (P-value <0.05).

	Cluster				Field			
Sample	Type I	Type II	Type III	TCS	Type I	Type II	Type III	TFS
N	27	98	50	175	29	343	149	521
%	15 $^{+7}_{-4}$	56 $^{+7}_{-7}$	29 $^{+7}_{-7}$	100	6 $^{+2}_{-2}$	66 $^{+4}_{-4}$	29 $^{+4}_{-4}$	100
R_e	2.20 \pm 0.13	2.79 \pm 0.09	2.02 \pm 0.08	2.44 \pm 0.07	2.41 \pm 0.14	3.20 \pm 0.06*	2.22 \pm 0.07	2.88 \pm 0.05*
n	2.07 \pm 0.04	1.83 \pm 0.04	2.17 \pm 0.03	1.99 \pm 0.03	1.60 \pm 0.06*	1.63 \pm 0.02	2.00 \pm 0.03*	1.73 \pm 0.02*
M_* [$10^{10} M_\odot$]	1.52 \pm 0.10	1.53 \pm 0.05	1.89 \pm 0.11	1.63 \pm 0.05	1.55 \pm 0.14	1.60 \pm 0.03	1.55 \pm 0.06	1.59 \pm 0.03
$(g-r)_{in}$	0.504 \pm 0.022	0.363 \pm 0.015	0.534 \pm 0.014	0.455 \pm 0.015	0.238 \pm 0.014*	0.266 \pm 0.007*	0.392 \pm 0.012*	0.288 \pm 0.006*
$(g-r)_{in,1}$	0.504 \pm 0.022	0.334 \pm 0.015	0.506 \pm 0.014	0.434 \pm 0.011	0.222 \pm 0.012*	0.235 \pm 0.007*	0.362 \pm 0.012*	0.265 \pm 0.006*
$(g-r)_{in,2}$	0.504 \pm 0.023	0.315 \pm 0.016	0.500 \pm 0.014	0.426 \pm 0.011	0.208 \pm 0.013*	0.217 \pm 0.007*	0.354 \pm 0.012*	0.247 \pm 0.006*
$(g-r)_{out}$	-	0.300 \pm 0.020	0.482 \pm 0.026	0.363 \pm 0.015	-	0.201 \pm 0.010*	0.288 \pm 0.015*	0.231 \pm 0.008*
$h_{1,g}$ [kpc]	1.55 \pm 0.08	2.75 \pm 0.14	1.38 \pm 0.06	-	1.47 \pm 0.05	2.85 \pm 0.07	1.37 \pm 0.04	-
$h_{2,g}$ [kpc]	-	1.37 \pm 0.05	2.18 \pm 0.11	-	-	1.46 \pm 0.03	1.83 \pm 0.05*	-
$ratio_g$	1	1.91 \pm 0.09	0.64 \pm 0.02	-	1	1.87 \pm 0.04	0.74 \pm 0.01*	-
$R_{b,g}$ [kpc]	-	5.21 \pm 0.19	4.68 \pm 0.20	-	-	5.33 \pm 0.10	4.41 \pm 0.15	-
$h_{1,r}$ [kpc]	1.57 \pm 0.09	2.66 \pm 0.12	1.37 \pm 0.06	-	1.45 \pm 0.05	2.66 \pm 0.06	1.32 \pm 0.04	-
$h_{2,r}$ [kpc]	-	1.37 \pm 0.04	2.12 \pm 0.08	-	-	1.38 \pm 0.02	1.87 \pm 0.05*	-
$ratio_r$	1	1.71 \pm 0.10	0.63 \pm 0.02	-	1	1.69 \pm 0.04	0.71 \pm 0.01*	-
$R_{b,r}$ [kpc]	-	5.72 \pm 0.19	4.74 \pm 0.20	-	-	5.53 \pm 0.10	5.22 \pm 0.15	-

ing/aging of a galaxy’s (outer) disc consequent to the stripping of gas by ram-pressure or to the consumption of gas through star formation (i.e. “strangulation”). Since we have selected our samples to minimise the influence of dust (see Section 2), we can assume that the observed reddening is truly caused by older stellar populations. Even though our data is not good enough to robustly determine the morphological type of the galaxies, we can further assume that the reddening is not solely related to a different morphological mix (i.e. a higher fraction of S0s) in the cluster environment; it has been shown that there exist hardly any Type II S0 galaxies in clusters (Erwin et al. 2012; Maltby et al. 2015), however, the reddening we detect is similarly seen in Type II and Type III galaxies. Moreover, given our selection limit in Sérsic-index and stellar mass, our sample is very likely biased towards late-type galaxies (see e.g. Ravindranath et al. 2004) and against S0s, which are among the most massive disc objects. The reddening observed in Type II and III cluster galaxies is slightly stronger in the outer disc regions, which is in compliance with galaxy evolutionary scenarios invoking ram-pressure stripping (see e.g. Steinhauser et al. 2016) or stellar migration (see e.g. Roškar et al. 2008). A summary of the global properties discussed here is illustrated in Fig. 9.

4.2 The different profile types

In total, the fractions of Type I, II and III galaxies in the total cluster and field sample are 15 $^{+7}_{-4}$ %, 56 $^{+7}_{-7}$ % and 29 $^{+7}_{-7}$ % and 6 $^{+2}_{-2}$ %, 66 $^{+4}_{-4}$ % and 29 $^{+4}_{-4}$ %, respectively (errors correspond to Wilson (1927)-confidence intervals). In Table 1 we list these fractions along with the median values of the structural parameters for the galaxies in both environments (numbers with an asterisk indicate significant differences between cluster and field, according to a standard KS-test P-value <0.05). We plot the distributions of the measured parameters for the different profile types in Figs. 6 to 8

and illustrate their median values in Fig. 9. The results for the three individual field samples can be found in Table B1 for comparison. Note that all trends reported in this paper are confirmed by the evaluation of the individual field samples.

4.2.1 Type I galaxies

The most interesting result in relation to this type of galaxies is the potentially larger scale length (a factor of ~ 1.08) in the clusters environment compared to the field. However, this result is not significant according to standard KS-testing (P-value: 0.481 and 0.361 for r- and g-band, respectively). Moreover, Type I cluster galaxies are as red as Type III cluster galaxies while in the field Type I colours are comparable to Type II field objects (see Figs. 6 and 9). Note that for Type I galaxies we measure the colour in the entire disc region.

4.2.2 Type II galaxies

The inner and outer scale length, h_1 and h_2 , (in both bands) are similar in clusters and in the field. In relation to the position of the break, R_b , there is not an obvious trend depending on environment. The most remarkable issue is that the location of the break position is independent of the band for the field galaxies (within the errors) but rather different in the clusters. However, the observed difference is not significant according to standard KS-testing. The decrease in R_e (field to cluster) is strongest for Type II cluster galaxies. For an illustration of these results, (see Figs. 7 and 9).

4.2.3 Type III galaxies

Following the trend found in Type I galaxies, the effect of the cluster environment in Type III galaxies is to significantly enlarge the value of the outer scale length, h_2 (KS-test P-values 0.007 and

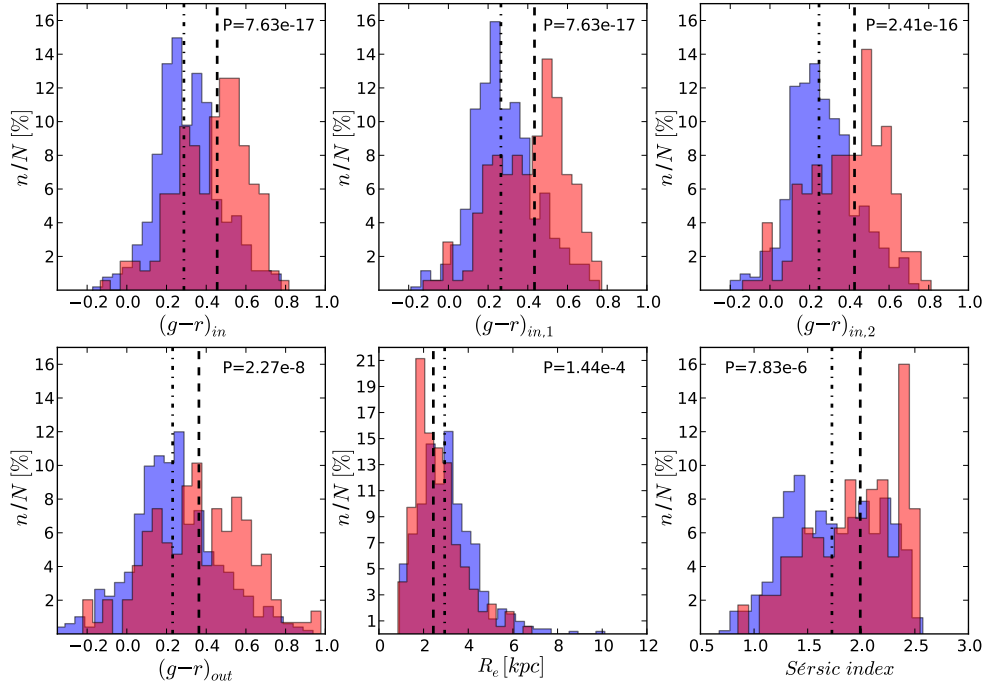


Figure 5. Normalised distributions of colour, R_e and Sérsic-index for the total cluster and field samples (field galaxies in the background in blue colour, cluster galaxies in the foreground in light-red colour, overlapping regions of the histograms in purple). The vertical lines indicate the median values (dash-dotted for field and dashed for cluster galaxies). The KS-test P-value is inserted in each panel. Type I galaxies are not included in the bottom-left panel.

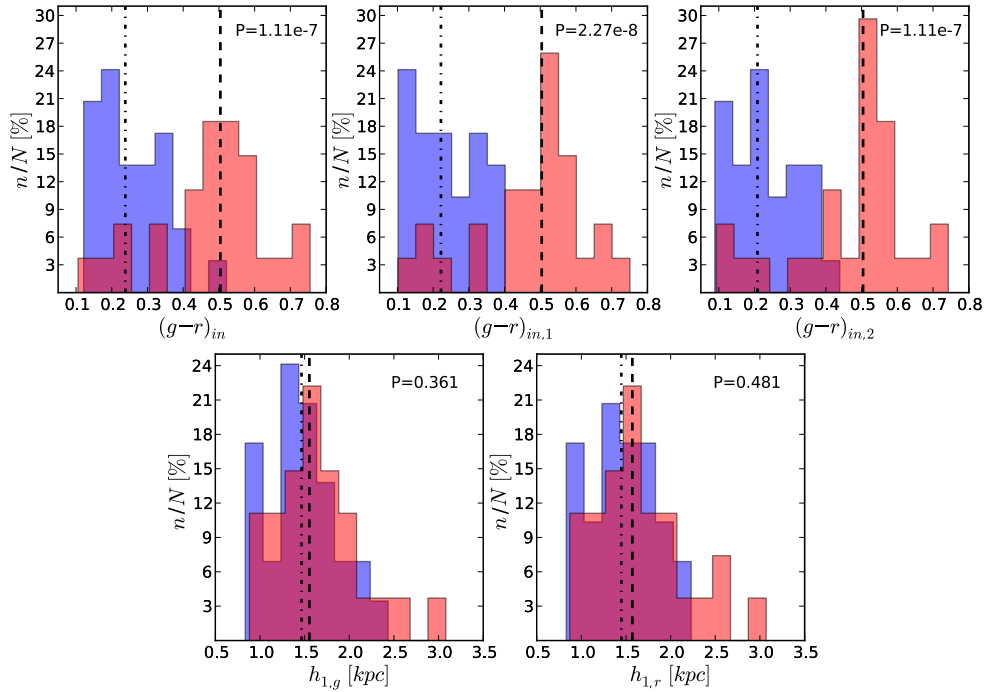


Figure 6. Normalised distributions of the measured disc properties for Type I galaxies (field galaxies in blue, cluster galaxies in red). The vertical lines indicate the median values (dash-dotted for field and dashed for cluster galaxies). The KS-test P-value is shown in the upper right corner of each panel.

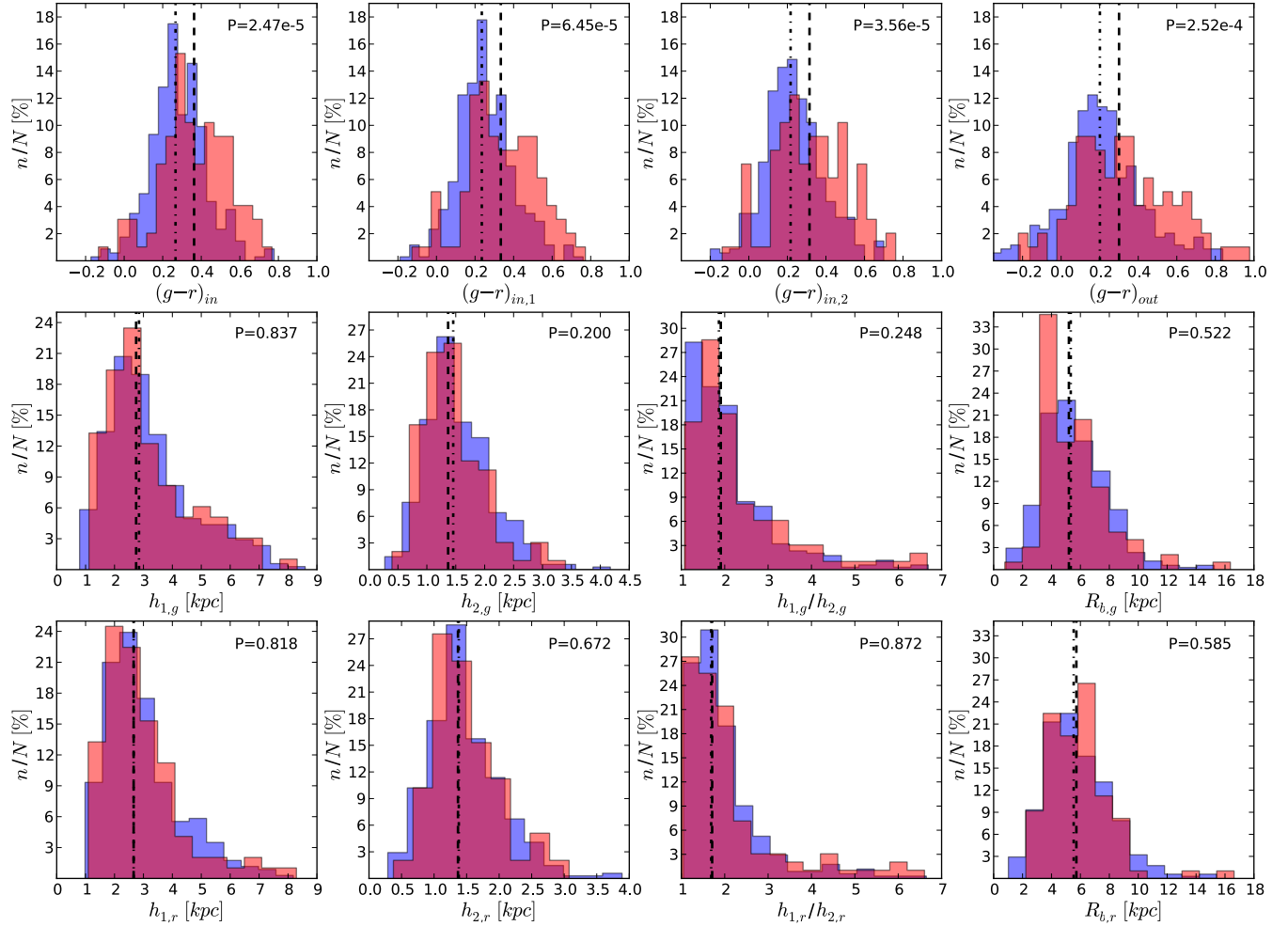


Figure 7. Same as Fig. 6 for Type II galaxies.

0.001 for r- and g-band, respectively). For Type III galaxies, the increase is by a factor of ~ 1.16 . We also find that the ratio of the inner-to-outer scale lengths is smaller in the cluster environment by $\sim 15\%$ (for both bands). These findings could be interpreted as tidal effects consequent to galaxy harassment (see Moore et al. 1996 for a detailed definition), as an increase of the rate of minor mergers building up the outer disc or as an increased contribution of an extended bulge component at larger galactocentric radii. However, the latter scenario is unlikely since it has been found to occur preferentially in S0 galaxies (see Maltby et al. 2012) and our sample is biased against those. While merger events could also explain why Type III galaxies in the cluster are more massive than those in the field (see 1), it has to be noted that the merger rate is assumed to be very small in inner cluster regions (where we find Type III galaxies to reside; see Fig. 4) due to high relative velocities. However, interactions of Type III galaxies with the intra-cluster medium and/or with other cluster galaxies (and the gravitational potential of the cluster) could have taken place in differently dense cluster regions over their comparatively long infall-time and thus might have been efficiently changing the galaxies' properties. The position of the break does not seem to be connected with the observed band for Type III cluster galaxies. This is different in the field, where R_b is smaller in the g-band. However, the data on the break radii show a

large scatter (resulting in large error bars), the observed differences in R_b between the environments are not significant according to KS-testing and hence the results on R_b have to be interpreted with caution. Illustrations of the results on Type III galaxies are given in (Figs. 8 and 9).

The comparison of the three individual field samples shows that for some measured properties there are notable differences (e.g. in R_e for Type I; in $h_{1,g}$, $h_{2,g}$ and R_b for Type II). However, the KS-test results (comparing each of the field samples to the corresponding cluster sample) are consistent for all of these quantities, except for one sole outlier, namely $h_{2,g}$ for Type II galaxies in field sample 2.

5 DISCUSSION

Comparing two different environments like the field (low to intermediate density) and the cluster (high density), we are in position to explore how the physical processes associated with high overdensity regions affect the peripheral parts of galaxy discs. There are three significant differences between our field and cluster samples:

- The global size of the galaxies, as parameterised by the effective radius, is smaller by $\sim 15\%$ in the cluster environment than in

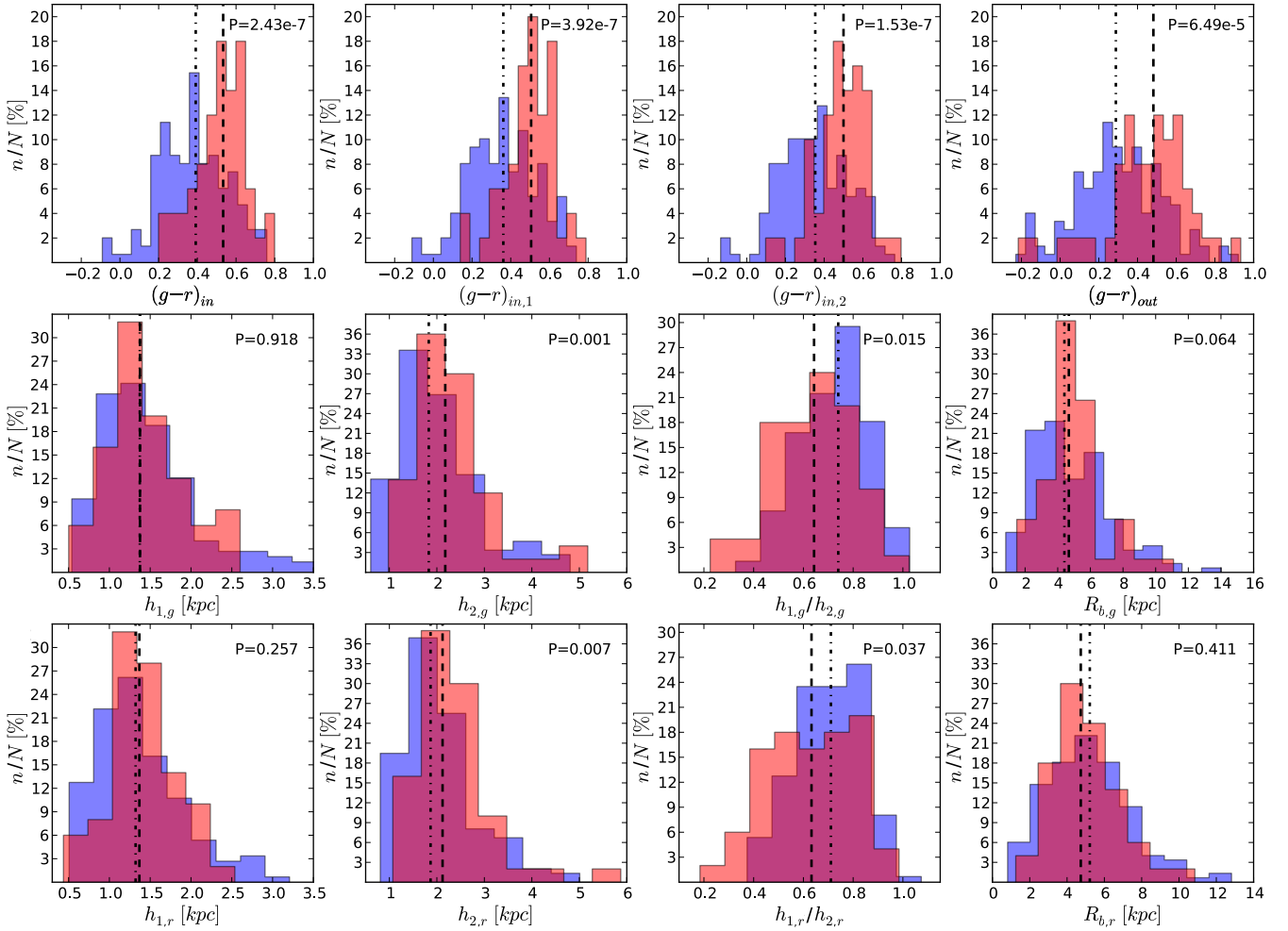


Figure 8. Same as Fig. 6 for Type III galaxies.

the field, while the global Sérsic-index is higher in the cluster by $\sim 15\%$.

- The global $(g-r)$ colour of the galaxies is redder by around 0.2 magnitudes in the clusters than in the field.
- We find ~ 2.5 times more Type I (pure exponential disc) galaxies in the clusters than in the field (15% vs. 5%). This difference is compensated by the lack of the corresponding percentage of Type II cluster galaxies (56% vs. 66%).

Our work allows us to probe, in detail, how and where the ageing and global size transformations have taken place. Figure 9 shows that the global size difference between the discs in the field and in the clusters, even though largest in Type II galaxies, seems to hold for all the profile types when explored separately. When taking a detailed look at the reddening of the individual profile types, Fig. 9 indicates that all the classes have undergone a similar reddening from the field to the cluster environments. It is worth noting that both Type I and II have a similar colour in the field, the Type III objects being notably redder. However, in the cluster environment this colour similarity is reversed so that Type I and III are the ones which share similar colours. It is remarkable that Type III field galaxies are redder than the other profile types even after masking the bulge. A possible explanation is that Type III field galaxies are formed by tidal interactions and minor mergers in the course of group pre-processing (see e.g. Younger et al. 2007; Lopes et al.

2014) which might have led to the observed reddening. The fact that Type II cluster galaxies are bluer than the other types in the same environment could indicate that the Type II feature is erased relatively quickly upon the cluster infall, allowing only for a limited reddening before the break vanishes. Note, however, that these are tentative interpretations.

As the inner scale length of the disc galaxies, h_1 , barely changes when moving from the field to the clusters, to understand the ultimate reason of the change in the global size of the galaxies we need to focus our attention on the outer scale length, h_2 . For Type I and Type III discs, we find that h_2 is larger (by a factor of ~ 1.08 and ~ 1.16 , respectively) in the clusters than in the field. If this was the only difference in the structure of the field versus the cluster galaxies, the global size of the cluster galaxies (at fixed stellar mass) should be larger than in the field. To understand why the cluster galaxies are yet more compact, we have to account also for the reddening of the objects. At decreasing the brightness of the galaxies' discs, the bulges of all these objects become more prominent. This effect moves the effective radius towards the inner regions of the objects.

Both the increment of h_2 and the global reddening of the discs in the cluster regions are suggestive of physical process connected to the cluster environment. The rise of h_2 in Type I and more significantly in Type III cluster galaxies could be understood as the result of an increased contribution of a prominent bulge component.

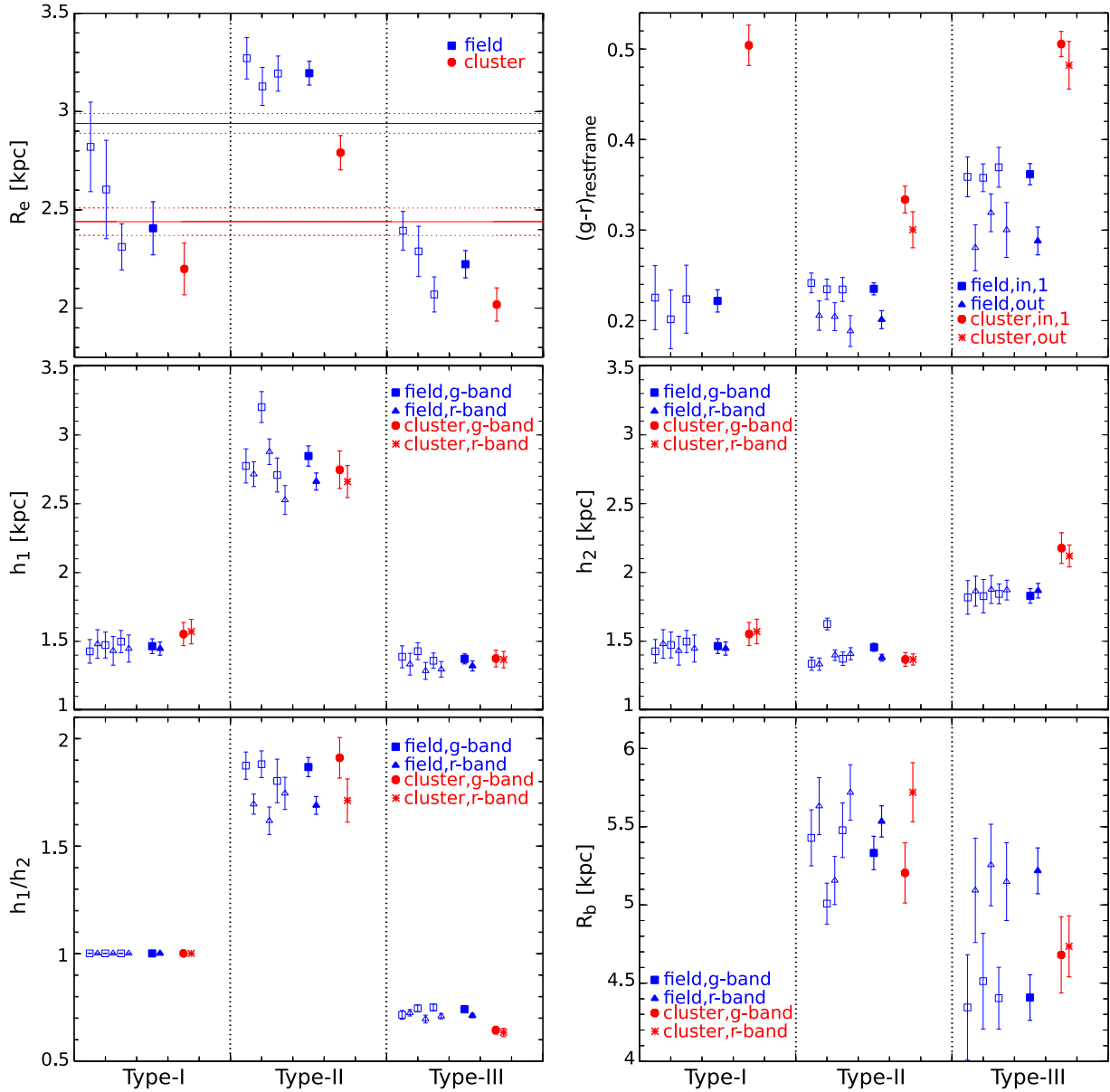


Figure 9. Median galaxy properties for both environments and all three surface-brightness profile types. Errors are 1-sigma bootstrap estimates (1000 iterations). Open symbols and thin error bars represent the individual field samples (1, 2 and 3 from left to right, respectively). *Top row:* effective radius, R_e , and $(g-r)_{\text{restframe}}$ colour. For Type II and Type III galaxies, $(g-r)_{\text{in},1}$ and $(g-r)_{\text{out}}$ are plotted. For Type I galaxies, we plot only $(g-r)_{\text{in},1}$, which in this case is the colour measured in the entire disc region (bulge masked at $0.5 R_e$). The horizontal lines in the first panel indicate the median R_e (and bootstrap errors) for the total cluster and total field sample, respectively. *Middle row:* inner (h_1) and outer (h_2) exponential scale length for both measured bands. *Bottom row:* Scale length ratio (h_1/h_2) and break radius (R_b) for both measured bands. For Type I galaxies, the break radius is not defined and the scale length ratio is by definition equal to unity.

Since we already accounted for the bulge component when fitting the surface-brightness profiles, this hypothesis is not sufficient to explain our findings. Other processes that might play an important role include tidal effects consequent to galaxy harassment (Moore et al. 1996) and minor merger events building up the outer disc. The global reddening of the cluster galaxies is potentially connected to the decrease of star formation in the cluster associated with the exhaustion of gas by ram-pressure stripping (see e.g. Bösch et al. 2013; Pranger et al. 2013; Steinhauser et al. 2016). It is worth noting that the reddening of the discs seems to be stronger outside the break radius of the galaxies. This is consistent with the view that

gas removal by ram-pressure stripping should be more efficient in the outer disc regions (see e.g. Steinhauser et al. 2012).

Another interesting aspect to discuss is the dramatic increase (by a factor of ~ 2.5) in the number of Type I discs in the clusters. This large variation in the frequency of Type I galaxies is accompanied by a substantial change in their colours. Whereas Type II and III have become redder by around 0.1-0.2 magnitudes, in the case of Type I this change is ~ 0.3 mag. The large increase in the number of Type I galaxies is compensated by a corresponding decrease of the percentage of Type II objects. This, together with our results on galaxy colour, indicates a transformation from Type II

to Type I as the galaxies fall onto the cluster. This hypothesis is in compliance with Maltby et al. (2015) who find indications for a transformation from spiral to S0 as the break is erased in Type II galaxies that fall onto a cluster, however, Maltby et al. (2015) (and Maltby et al. (2012)) conclude that the structural disc parameters are not significantly influenced by environment. This disparity could be explained by the higher mass and redshift range of the galaxies selected for their study that might have made it more difficult to detect environmental trends. Furthermore, our suggested scenario is in agreement with Erwin et al. (2012) who analysed S0 galaxies in the cluster and in the field and concluded that the lack of Type II cluster S0s indicates a transformation from Type II to Type I. A suppression of the survival of Type II objects in the cluster environment has also been reported by Roediger et al. (2012), analysing Virgo disc galaxies and, recently, by Clarke et al. (2017) using N-body SPH simulations. Supporting this view, it is worth noting that the scale length of the Type I discs has a value which is intermediate between the corresponding Type II and Type III values (both for the inner and outer scalelengths). This has also been found by Muñoz-Mateos et al. 2013. Also their comparatively large scatter in R_e can be interpreted as a hint for Type I galaxies experiencing a structural transformation. The unchanging frequency of Type III galaxies from field to cluster remains unexplained by our analysis and interpretation. We will address this point in our follow-up investigations.

Our results also have to be interpreted with respect to galaxy morphology. The quality of our data is not high enough to robustly assign all objects to morphological classes along the Hubble sequence, however, invoking the morphology-density relation (Dressler 1980) we can assume a higher fraction of early-type disc galaxies in the cluster environment. Referring to Gutiérrez et al. (2011) who find that Type I and III galaxies are more common in early-type discs while Type II galaxies are dominant in late-type discs, this would indicate that the trends we illustrate in Fig. 9 could - at least to some extent - be caused by morphological segregation between the two environments. On the other hand, as explained in Section 4, our sample is very likely biased against S0 galaxies due to our selection criteria in stellar mass and Sérsic-index. Moreover, the reddening for cluster Type II and III profiles is approximately the same. Since Type II galaxies are not found in cluster S0s (Erwin et al. 2012; Maltby et al. 2015), this indicates that the trends we find are not driven by S0 galaxies. In general, we conclude that our results are not significantly influenced by morphological segregation.

6 SUMMARY

We have selected four samples of disc galaxies within the same narrow stellar mass range ($0.8 < M_\star < 4$) $\times 10^{10} M_\odot$. While one of these samples consists of galaxies residing in galaxy clusters, the other three consist of galaxies outside of galaxy clusters, i.e. from the field. Each of the four samples holds around 175 galaxies which have been classified according to their disc structure (Type I \equiv single-exponential, Type II \equiv truncated, Type III \equiv anti-truncated). We find the following results:

- Disc galaxies are $\sim 15\%$ more compact in clusters than in the field. They are also ~ 0.2 mag redder in (g-r) colour and show higher Sérsic-indices (by $\sim 15\%$) in the cluster region. The reddening is observed both inside and outside the break radius.

- We find ~ 2.5 times more Type I (pure exponential disc) galaxies in the clusters than in the field. This difference is compensated by the lack of the corresponding percentage of Type II cluster galaxies. The fraction of Type III galaxies is the same in both environments.

- Type III cluster galaxies reside significantly closer to the cluster centre than the other break types.

- The structural parameter that changes most significantly, at comparing cluster versus field, is the outer scalelength of Type III discs, increasing by $\sim 16\%$ from field to cluster. Consequent to this change, the ratio of the inner and outer scale length of Type III galaxies changes by $\sim 15\%$.

- We suggest that Type I galaxies form from Type II galaxies, consequent to the physical mechanisms acting on the Type II population, produced/enhanced by environment.

In a follow-up to this work we will investigate the structural parameters of disc galaxies as functions of clustercentric distance. To ensure adequate statistics, our analyses will be carried out on an extended sample of galaxies, including a representative fraction of galaxies that reside in the transition region between cluster and field. For a consistent follow-up we will apply the same methods as presented and described in this paper.

A selection of prototypical surface-brightness profiles, the evaluation of the field control samples and comprehensive lists of the measured and analysed galaxy data can be found in the appendix.

ACKNOWLEDGEMENTS

We would like to thank the anonymous referee for detailed comments that contributed a lot to improving the quality of the present article. IT and MC acknowledge support from grant AYA2013-48226-C3-1-P and programme SEV-2011-0187 from the Spanish Ministry of Economy and Competitiveness (MINECO). This work is part of the research activities at the National Astronomical Research Institute of Thailand (Public Organization).

REFERENCES

- Abazajian K. N., et al., 2009, *ApJS*, **182**, 543
- Abell G. O., Corwin Jr. H. G., Olowin R. P., 1989, *ApJS*, **70**, 1
- Bertin E., 2011, in Evans I. N., Accomazzi A., Mink D. J., Rots A. H., eds, *Astronomical Society of the Pacific Conference Series* Vol. 442, *Astronomical Data Analysis Software and Systems XX*. p. 435
- Bertin E., Arnouts S., 1996, *A&AS*, **117**, 393
- Bland-Hawthorn J., Vlajić M., Freeman K. C., Draine B. T., 2005, *ApJ*, **629**, 239
- Blanton M. R., Roweis S., 2007, *AJ*, **133**, 734
- Blanton M. R., et al., 2005a, *AJ*, **129**, 2562
- Blanton M. R., Eisenstein D., Hogg D. W., Schlegel D. J., Brinkmann J., 2005b, *ApJ*, **629**, 143
- Bösch B., et al., 2013, *A&A*, **549**, A142
- Bournaud F., Elmegreen B. G., Elmegreen D. M., 2007, *ApJ*, **670**, 237
- Bruzual G., Charlot S., 2003, *MNRAS*, **344**, 1000
- Cebrián M., Trujillo I., 2014, *MNRAS*, **444**, 682
- Chabrier G., 2003, *PASP*, **115**, 763
- Chilingarian I. V., Melchior A.-L., Zolotukhin I. Y., 2010, *MNRAS*, **405**, 1409

- Christlein D., Zabludoff A. I., 2004, *ApJ*, **616**, 192
- Clarke A. J., Debattista V. P., Roškar R., Quinn T., 2017, *MNRAS*, **465**, L79
- Debattista V. P., Mayer L., Carollo C. M., Moore B., Wadsley J., Quinn T., 2006, *ApJ*, **645**, 209
- Dressler A., 1980, *ApJ*, **236**, 351
- Einasto M., et al., 2012, *A&A*, **542**, A36
- Elmegreen B. G., Hunter D. A., 2006, *ApJ*, **636**, 712
- Erwin P., 2005, *MNRAS*, **364**, 283
- Erwin P., 2015, *ApJ*, **799**, 226
- Erwin P., Beckman J. E., Pohlen M., 2005, *ApJ*, **626**, L81
- Erwin P., Pohlen M., Beckman J. E., 2008, *AJ*, **135**, 20
- Erwin P., Gutiérrez L., Beckman J. E., 2012, *ApJ*, **744**, L11
- Foye K., Courteau S., Thacker R. J., 2008, *MNRAS*, **386**, 1821
- Gunn J. E., Gott III J. R., 1972, *ApJ*, **176**, 1
- Gutiérrez L., Erwin P., Aladro R., Beckman J. E., 2011, *AJ*, **142**, 145
- Hao J., et al., 2010, *ApJS*, **191**, 254
- Head J. T. C. G., Lucey J. R., Hudson M. J., Smith R. J., 2014, *MNRAS*, **440**, 1690
- Hiemer A., Barden M., Kelvin L. S., Häußler B., Schindler S., 2014, *MNRAS*, **444**, 3089
- Laine J., et al., 2014, *MNRAS*, **441**, 1992
- Li Y., Mac Low M.-M., Klessen R. S., 2006, *ApJ*, **639**, 879
- Lopes P. A. A., Ribeiro A. L. B., Rembold S. B., 2014, *MNRAS*, **437**, 2430
- Maltby D. T., Hoyos C., Gray M. E., Aragón-Salamanca A., Wolf C., 2012, *MNRAS*, **420**, 2475
- Maltby D. T., Aragón-Salamanca A., Gray M. E., Hoyos C., Wolf C., Jogee S., Böhm A., 2015, *MNRAS*, **447**, 1506
- Martínez-Serrano F. J., Serna A., Doménech-Moral M., Domínguez-Tenreiro R., 2009, *ApJ*, **705**, L133
- Moore B., Katz N., Lake G., Dressler A., Oemler A., 1996, *Nature*, **379**, 613
- Muñoz-Mateos J. C., et al., 2013, *ApJ*, **771**, 59
- Pohlen M., Trujillo I., 2006, *A&A*, **454**, 759
- Pohlen M., Dettmar R.-J., Lütticke R., Aronica G., 2002, *A&A*, **392**, 807
- Pranger F., et al., 2013, *A&A*, **557**, A62
- Ravindranath S., et al., 2004, *ApJ*, **604**, L9
- Roediger J. C., Courteau S., Sánchez-Blázquez P., McDonald M., 2012, *ApJ*, **758**, 41
- Roškar R., Debattista V. P., Stinson G. S., Quinn T. R., Kaufmann T., Wadsley J., 2008, *ApJ*, **675**, L65
- Sánchez-Blázquez P., Courty S., Gibson B. K., Brook C. B., 2009, *MNRAS*, **398**, 591
- Steinhauser D., Haider M., Kapferer W., Schindler S., 2012, *A&A*, **544**, A54
- Steinhauser D., Schindler S., Springel V., 2016, *A&A*, **591**, A51
- Szabo T., Pierpaoli E., Dong F., Pipino A., Gunn J., 2011, *ApJ*, **736**, 21
- Takey A., Schwöpe A., Lamer G., 2011, *A&A*, **534**, A120
- Tempel E., Tago E., Liivamägi L. J., 2012, *A&A*, **540**, A106
- Toomre A., Toomre J., 1972, *ApJ*, **178**, 623
- Trujillo I., Fliri J., 2016, *ApJ*, **823**, 123
- Trujillo I., Aguerri J. A. L., Cepa J., Gutiérrez C. M., 2001, *MNRAS*, **328**, 977
- Varela J., Betancort-Rijo J., Trujillo I., Ricciardelli E., 2012, *ApJ*, **744**, 82
- Weiner B. J., Williams T. B., van Gorkom J. H., Sellwood J. A., 2001, *ApJ*, **546**, 916
- Wen Z. L., Han J. L., Liu F. S., 2012, *ApJS*, **199**, 34
- Wilson E. B., 1927, *Journal of the American Statistical Association*, **22**, 209
- Yoshii Y., Sommer-Larsen J., 1989, *MNRAS*, **236**, 779
- Younger J. D., Cox T. J., Seth A. C., Hernquist L., 2007, *ApJ*, **670**, 269

This paper has been typeset from a \LaTeX file prepared by the author.

APPENDIX A: PROTOTYPICAL PROFILES

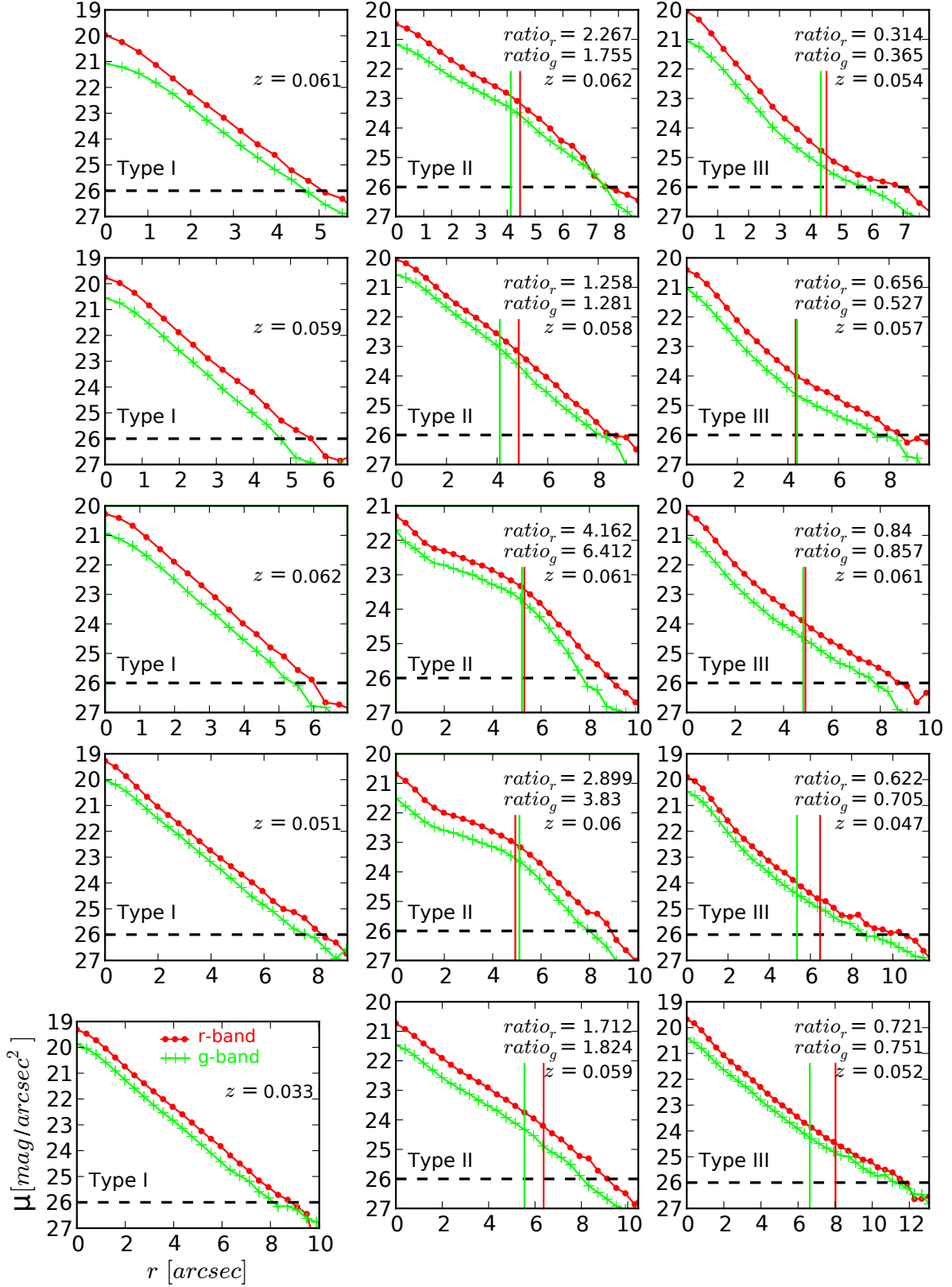


Figure A1: Prototypical cluster galaxy profiles as obtained and analysed in this work, sorted from top to bottom according to apparent size. The left, middle and right column contain Type I, Type II and Type III profiles, respectively. Vertical short lines indicate the break radii in the g-band (green) and r-band (red), the horizontal dashed line marks our conservative confidence threshold. In addition, galaxy redshifts and measured scale length ratios (h_1/h_2) are given.

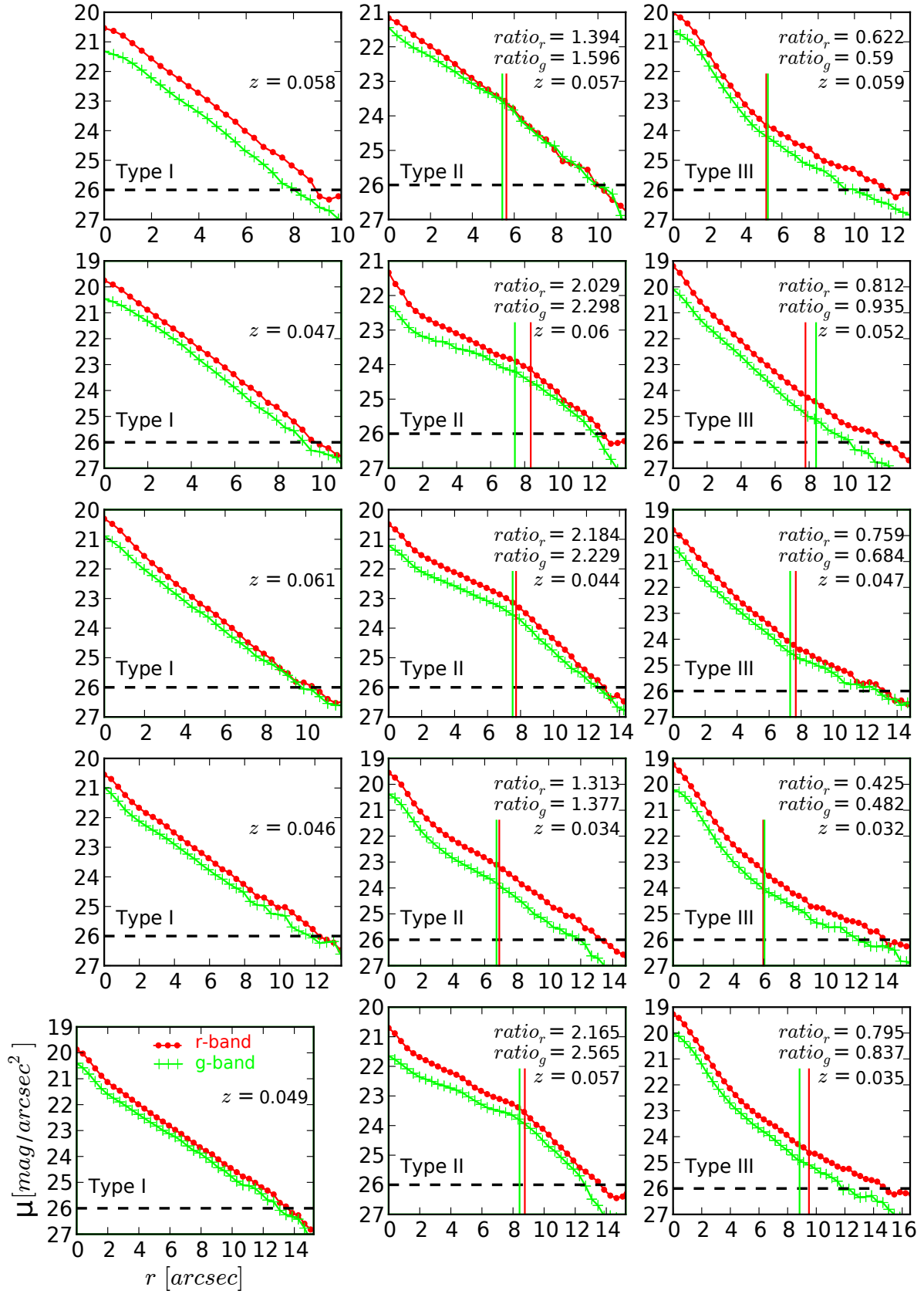


Figure A2: Same as Fig. A1 for field galaxies.

APPENDIX B: ANALYSIS OF THE SEPARATED FIELD SAMPLES

Table B1: Listing of the median values of the structural properties of the galaxies in the three initially selected field samples. See Table 1 for a detailed description.

Sample	Type I	Type II	Type III	all types
Field 1				
N	10	115	47	172
%	6^{+4}_{-3}	67^{+6}_{-8}	27^{+7}_{-6}	100
R_e [kpc]	2.82 ± 0.23	$3.27 \pm 0.11^*$	2.39 ± 0.10	$3.10 \pm 0.09^*$
n	1.81 ± 0.07	1.60 ± 0.03	$2.05 \pm 0.06^*$	$1.74 \pm 0.03^*$
M_\star [$10^{10} M_\odot$]	1.69 ± 0.16	1.62 ± 0.06	1.55 ± 0.08	1.60 ± 0.05
$(g-r)_{in}$	$0.235 \pm 0.041^*$	$0.282 \pm 0.010^*$	$0.379 \pm 0.022^*$	$0.283 \pm 0.010^*$
$(g-r)_{in,1}$	$0.225 \pm 0.035^*$	$0.242 \pm 0.011^*$	$0.359 \pm 0.022^*$	$0.270 \pm 0.010^*$
$(g-r)_{in,2}$	$0.214 \pm 0.037^*$	$0.223 \pm 0.010^*$	$0.355 \pm 0.022^*$	$0.249 \pm 0.010^*$
$(g-r)_{out}$	-	$0.199 \pm 0.016^*$	$0.281 \pm 0.025^*$	$0.232 \pm 0.015^*$
$h_{1,g}$ [kpc]	1.43 ± 0.09	2.77 ± 0.12	1.39 ± 0.08	-
$h_{2,g}$ [kpc]	''-	1.34 ± 0.05	$1.82 \pm 0.12^*$	-
$ratio_g$	1	1.87 ± 0.06	0.71 ± 0.02	-
$R_{b,g}$ [kpc]	-	5.43 ± 0.18	4.35 ± 0.33	-
$h_{1,r}$ [kpc]	1.48 ± 0.10	2.72 ± 0.09	1.33 ± 0.08	-
$h_{2,r}$ [kpc]	''-	1.33 ± 0.05	1.86 ± 0.11	-
$ratio_r$	1	1.69 ± 0.05	$0.72 \pm 0.01^*$	-
$R_{b,r}$ [kpc]	-	5.63 ± 0.18	5.09 ± 0.33	-
Field 2				
N	10	112	50	172
%	6^{+4}_{-3}	65^{+7}_{-7}	29^{+7}_{-6}	100
R_e [kpc]	2.60 ± 0.25	3.13 ± 0.10	2.29 ± 0.13	$2.91 \pm 0.08^*$
n	1.60 ± 0.11	$1.53 \pm 0.03^*$	$1.94 \pm 0.04^*$	$1.68 \pm 0.03^*$
M_\star [$10^{10} M_\odot$]	1.47 ± 0.18	1.60 ± 0.05	1.68 ± 0.09	1.61 ± 0.05
$(g-r)_{in}$	$0.214 \pm 0.031^*$	$0.256 \pm 0.011^*$	$0.389 \pm 0.016^*$	$0.275 \pm 0.010^*$
$(g-r)_{in,1}$	$0.201 \pm 0.032^*$	$0.235 \pm 0.011^*$	$0.358 \pm 0.015^*$	$0.253 \pm 0.011^*$
$(g-r)_{in,2}$	$0.202 \pm 0.033^*$	$0.213 \pm 0.012^*$	$0.348 \pm 0.015^*$	$0.242 \pm 0.010^*$
$(g-r)_{out}$	-	$0.197 \pm 0.015^*$	$0.302 \pm 0.021^*$	$0.215 \pm 0.013^*$
$h_{1,g}$ [kpc]	1.47 ± 0.09	3.20 ± 0.11	1.43 ± 0.06	-
$h_{2,g}$ [kpc]	''-	$1.42 \pm 0.04^*$	$1.83 \pm 0.12^*$	-
$ratio_g$	1	1.88 ± 0.06	$0.74 \pm 0.02^*$	-
$R_{b,g}$ [kpc]	-	5.01 ± 0.15	4.51 ± 0.26	-
$h_{1,r}$ [kpc]	1.43 ± 0.10	2.88 ± 0.09	1.29 ± 0.06	-
$h_{2,r}$ [kpc]	''-	1.40 ± 0.04	$1.88 \pm 0.10^*$	-
$ratio_r$	1	1.62 ± 0.06	0.69 ± 0.02	-
$R_{b,r}$ [kpc]	-	5.16 ± 0.15	5.26 ± 0.26	-
Field 3				
N	9	116	52	177
%	5^{+4}_{-2}	66^{+6}_{-8}	29^{+7}_{-6}	100
R_e [kpc]	2.31 ± 0.12	3.19 ± 0.09	2.07 ± 0.09	$2.74 \pm 0.07^*$
n	$1.33 \pm 0.09^*$	1.71 ± 0.03	$2.01 \pm 0.05^*$	$1.76 \pm 0.03^*$
M_\star [$10^{10} M_\odot$]	1.55 ± 0.12	1.59 ± 0.05	1.50 ± 0.08	1.56 ± 0.05
$(g-r)_{in}$	$0.238 \pm 0.038^*$	$0.269 \pm 0.012^*$	$0.401 \pm 0.021^*$	$0.294 \pm 0.012^*$
$(g-r)_{in,1}$	$0.224 \pm 0.038^*$	$0.234 \pm 0.013^*$	$0.369 \pm 0.022^*$	$0.271 \pm 0.012^*$
$(g-r)_{in,2}$	$0.224 \pm 0.037^*$	$0.213 \pm 0.014^*$	$0.351 \pm 0.020^*$	$0.252 \pm 0.013^*$
$(g-r)_{out}$	-	$0.189 \pm 0.017^*$	$0.300 \pm 0.030^*$	$0.238 \pm 0.015^*$
$h_{1,g}$ [kpc]	1.49 ± 0.08	2.71 ± 0.12	1.36 ± 0.06	-
$h_{2,g}$ [kpc]	''-	1.37 ± 0.05	$1.84 \pm 0.07^*$	-
$ratio_g$	1	1.80 ± 0.10	$0.75 \pm 0.01^*$	-
$R_{b,g}$ [kpc]	-	5.48 ± 0.18	4.40 ± 0.25	-
$h_{1,r}$ [kpc]	1.45 ± 0.10	2.53 ± 0.10	1.30 ± 0.06	-
$h_{2,r}$ [kpc]	''-	1.41 ± 0.04	$1.87 \pm 0.07^*$	-
$ratio_r$	1	1.74 ± 0.07	0.71 ± 0.01	-
$R_{b,r}$ [kpc]	-	5.72 ± 0.18	5.15 ± 0.25	-

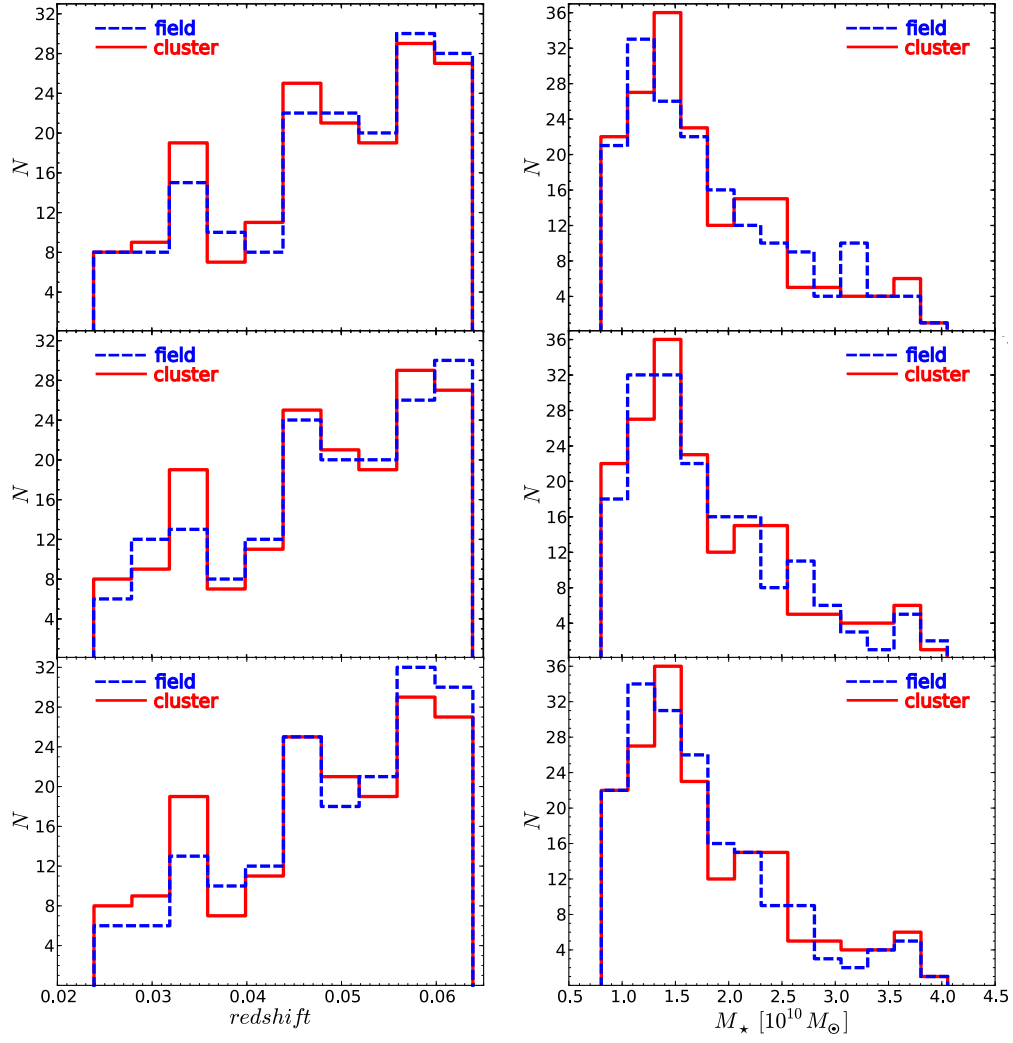


Figure B1: Redshift (left) and stellar mass (right) distributions of the total cluster sample and the three field samples (field sample 1, 2 and 3 from top to bottom).

APPENDIX C: GALAXY DATA

Table C1: Listing of coordinates, profile type, redshift, effective radius, Sérsic-index, colours and NYU-VAGC-ID of all 175 galaxies in the total cluster sample.

Total cluster sample											
Index	RA. [deg]	DEC. [deg]	Type	z	R_e [kpc]	n	$(g-r)_{in}$	$(g-r)_{in,1}$	$(g-r)_{in,2}$	$(g-r)_{out}$	ID
1	223.306	16.9354	I	0.0453	1.646	2.344	0.4951	0.4910	0.4882	-	2277479
2	207.954	37.5459	I	0.0615	2.798	1.990	0.4249	0.4139	0.4037	-	1837246
3	227.763	7.6391	I	0.0457	3.225	2.130	0.4338	0.4338	0.4338	-	1340835
4	239.843	17.9775	I	0.0465	3.245	1.768	0.3342	0.3342	0.3342	-	1998978
5	137.110	52.1416	I	0.0613	1.247	2.075	0.5695	0.5681	0.5664	-	0374342
6	235.227	21.7966	I	0.0416	1.846	2.445	0.5414	0.5414	0.5414	-	1965469
7	171.358	35.4429	I	0.0341	1.848	2.295	0.3463	0.3463	0.3463	-	1901033
8	173.629	49.1278	I	0.0334	2.249	2.078	0.5458	0.5458	0.5458	-	0955560
9	186.595	30.8729	I	0.0618	1.603	1.614	0.4111	0.4043	0.3956	-	1986663
10	239.538	16.3113	I	0.0373	2.314	1.926	0.5004	0.5004	0.5004	-	2020621
11	165.155	10.4372	I	0.0361	3.775	2.314	0.6267	0.6267	0.6267	-	0949321
12	183.190	59.9455	I	0.0607	1.175	1.844	0.4949	0.4796	0.4629	-	0921433
13	214.445	1.9345	I	0.0548	2.012	2.218	0.6794	0.6857	0.6939	-	0283316
14	213.119	24.5379	I	0.0531	2.200	1.389	0.1054	0.1012	0.0927	-	1991315
15	226.071	28.4281	I	0.0563	2.849	1.895	0.5488	0.5400	0.5374	-	1929467
16	174.201	55.1669	I	0.0572	1.554	2.379	0.7097	0.7113	0.7133	-	0821134
17	129.188	38.5303	I	0.0588	1.984	2.438	0.5819	0.5739	0.5735	-	0804437
18	223.680	18.4730	I	0.0526	3.968	1.503	0.2087	0.1600	0.1254	-	2312924
19	127.119	30.2956	I	0.0504	2.902	2.413	0.5035	0.5035	0.5035	-	1036567
20	209.802	32.6445	I	0.0495	1.416	1.642	0.1556	0.1556	0.1556	-	1925683
21	180.886	54.8527	I	0.0506	2.728	1.732	0.5041	0.5041	0.5041	-	0818930
22	222.117	11.3442	I	0.0521	1.127	2.423	0.5909	0.5853	0.5765	-	1419038
23	138.335	47.7194	I	0.0514	1.771	2.455	0.7060	0.6974	0.6896	-	0855566
24	235.432	28.3455	I	0.0328	2.553	1.461	0.2316	0.2316	0.2316	-	1323500
25	172.604	27.0024	I	0.0320	2.350	1.428	0.5300	0.5240	0.5180	-	2225418
26	207.225	26.6987	I	0.0623	1.553	2.363	0.5421	0.5364	0.5277	-	2010111
27	151.819	14.4081	I	0.0310	2.508	2.007	0.5611	0.5611	0.5611	-	2492023
28	218.245	3.8955	II	0.0296	2.252	1.577	0.4256	0.4003	0.3919	0.3526	0304600
29	246.849	40.6778	II	0.0299	2.419	2.182	0.1247	0.1158	0.1155	0.1895	0547924
30	241.263	33.2411	II	0.0602	2.192	2.195	0.4113	0.4022	0.4015	0.3845	1413028
31	243.095	30.6521	II	0.0510	3.186	2.433	0.4799	0.4328	0.3959	0.1684	1397013
32	229.343	5.2335	II	0.0515	2.099	2.478	0.5615	0.5490	0.5477	0.5157	1363878
33	138.695	47.6839	II	0.0517	1.713	1.581	0.4869	0.4809	0.4703	0.4602	0858869
34	202.119	37.7351	II	0.0573	3.087	2.189	0.3049	0.2800	0.2545	0.2346	1835724
35	243.407	30.9563	II	0.0511	3.091	1.589	0.2866	0.2664	0.2522	-0.0943	1398409
36	176.801	55.7686	II	0.0512	1.740	2.415	0.4624	0.4399	0.4034	0.2939	0967328
37	206.732	25.7824	II	0.0514	3.454	1.884	-0.0051	-0.0180	-0.0249	0.0823	1991080
38	239.332	19.9130	II	0.0502	3.033	1.835	0.2309	0.2109	0.2011	0.3147	1965670
39	129.036	38.7546	II	0.0574	2.757	1.667	0.2743	0.2474	0.2332	0.3062	0778811
40	224.204	9.1498	II	0.0492	2.770	1.424	0.3106	0.2935	0.2904	0.3450	1256997
41	241.416	33.3257	II	0.0606	1.999	1.878	0.2978	0.2666	0.2573	0.3639	1413029
42	162.302	22.2250	II	0.0478	2.437	1.167	0.2374	0.2125	0.1984	-0.0868	2261733
43	140.368	55.6322	II	0.0478	1.710	2.427	0.3286	0.3191	0.3139	0.1921	0204459
44	139.699	55.7060	II	0.0478	5.109	1.832	0.2623	0.1934	0.1655	0.0342	0206972
45	209.924	32.6738	II	0.0498	4.516	1.252	0.0360	-0.0049	-0.0298	-0.1645	1899535
46	209.721	32.6669	II	0.0499	2.398	1.227	0.0116	-0.0108	-0.0291	0.2207	1925686
47	204.118	34.8885	II	0.0604	3.100	1.445	0.2865	0.2686	0.2609	0.4600	1878852
48	209.646	32.6443	II	0.0493	2.288	0.937	0.2387	0.2304	0.2221	0.1411	1925682
49	170.551	2.9108	II	0.0494	2.694	1.801	0.6374	0.6137	0.5966	0.7170	0288564
50	139.161	20.3117	II	0.0300	1.923	1.266	0.2711	0.2555	0.2448	0.1724	2237340
51	207.318	25.7374	II	0.0518	4.859	2.108	0.2285	0.1609	-0.0203	0.1329	2006675
52	174.674	55.8989	II	0.0591	1.985	1.721	0.3843	0.3712	0.3530	0.6885	1165611
53	213.626	4.6529	II	0.0558	1.487	2.350	0.6164	0.6062	0.5958	0.7287	0491141
54	162.158	17.3099	II	0.0558	5.985	1.631	0.2708	0.2093	0.1741	0.1166	2352640
55	200.878	13.7729	II	0.0242	3.374	2.172	0.3636	0.3171	0.2931	0.3624	1418334
56	155.606	38.3386	II	0.0551	5.414	2.224	0.2161	0.1487	0.0932	0.0216	1180914
57	223.589	18.7770	II	0.0592	1.615	2.271	0.7319	0.7273	0.7211	0.7618	2290451
58	168.893	61.1311	II	0.0569	2.465	1.501	0.6609	0.6395	0.6165	0.6285	0553186
59	202.667	11.5949	II	0.0241	2.795	2.095	0.4499	0.4024	0.3637	0.1351	1224458

Total cluster sample (continued)											
Index	RA. [deg]	DEC. [deg]	Type	z	R_e [kpc]	n	$(g-r)_{in}$	$(g-r)_{in,1}$	$(g-r)_{in,2}$	$(g-r)_{out}$	ID
60	167.004	44.1476	II	0.0589	3.830	1.918	0.5561	0.5370	0.5330	0.5913	1248630
61	213.736	4.9446	II	0.0562	2.968	1.378	0.3315	0.3223	0.3043	0.3569	0306768
62	136.784	52.1685	II	0.0623	5.713	1.824	0.1104	0.0661	0.0414	0.0444	0432310
63	128.780	38.2247	II	0.0569	5.149	2.192	0.2922	0.2498	0.2342	0.3275	0804407
64	167.120	44.2202	II	0.0588	3.199	1.580	0.4344	0.4269	0.4186	0.5332	1248639
65	203.714	34.0555	II	0.0251	2.870	1.659	0.5307	0.5003	0.4947	0.3846	1928823
66	223.705	18.4942	II	0.0594	3.215	1.525	0.3331	0.3170	0.3010	0.2631	2312939
67	179.976	56.0882	II	0.0623	2.328	2.487	0.5387	0.5189	0.5066	0.4055	0822529
68	153.170	39.1042	II	0.0239	2.158	2.010	0.2905	0.2615	0.2471	0.2564	1092592
69	207.146	25.6637	II	0.0524	5.008	2.350	0.2413	0.1778	0.1470	0.0810	1991114
70	214.328	2.0340	II	0.0542	2.665	2.494	0.5767	0.5679	0.5678	0.5711	0269017
71	223.518	18.5686	II	0.0593	1.672	2.479	0.6941	0.6922	0.6911	0.9590	2312916
72	202.362	37.7317	II	0.0593	4.254	1.421	-0.0317	-0.0633	-0.0841	-0.2200	1835747
73	241.142	33.5988	II	0.0594	2.776	0.849	0.1583	0.1298	0.1132	0.1052	1404326
74	216.575	16.7779	II	0.0537	2.437	1.927	0.5591	0.5662	0.5764	0.6339	2339003
75	167.133	44.0961	II	0.0594	2.193	1.266	0.6484	0.6375	0.6292	0.4659	1248637
76	204.292	34.7301	II	0.0608	5.655	2.094	0.2222	0.1778	0.1558	0.1102	1901866
77	241.647	17.8925	II	0.0369	3.301	2.061	0.3477	0.3121	0.2969	0.2927	1974600
78	164.880	1.7405	II	0.0379	3.381	1.443	0.3639	0.3360	0.3207	0.3247	0427137
79	167.025	43.8946	II	0.0585	3.956	1.300	-0.1333	-0.1276	-0.1382	-0.2220	1233991
80	170.728	34.0593	II	0.0361	1.758	2.418	0.5251	0.5128	0.5060	0.6215	1894337
81	241.345	24.1314	II	0.0324	2.750	1.549	0.5874	0.5693	0.5629	0.9252	1315256
82	203.275	32.4404	II	0.0366	1.730	2.467	0.2120	0.2030	0.1912	0.2128	1916072
83	145.694	38.8420	II	0.0417	1.919	1.964	0.4552	0.4219	0.3987	0.4709	1092086
84	204.016	36.6196	II	0.0617	3.479	1.149	0.4615	0.4463	0.4385	0.6882	1879987
85	226.081	28.4544	II	0.0583	1.574	2.207	0.7021	0.7123	0.7223	0.8430	1929466
86	136.935	51.8537	II	0.0617	2.379	1.326	0.3252	0.3051	0.2866	0.1334	0374326
87	164.919	1.4534	II	0.0406	4.310	1.738	0.0485	0.0088	-0.0109	-0.0170	0426490
88	156.430	10.9559	II	0.0319	2.891	1.719	0.3096	0.2697	0.2516	0.1229	1117110
89	229.820	25.7379	II	0.0338	3.252	1.664	0.4808	0.4850	0.4962	0.5469	1908663
90	171.135	35.1609	II	0.0340	3.221	1.915	0.3570	0.3323	0.3159	0.3737	1930732
91	235.410	28.3205	II	0.0326	2.646	1.225	0.5403	0.5085	0.4923	0.5808	1323499
92	226.097	28.4373	II	0.0586	1.824	0.911	0.3671	0.3653	0.3639	0.3484	1929470
93	167.144	21.4789	II	0.0331	2.368	1.249	0.4919	0.4737	0.4625	0.3385	2282591
94	238.789	41.4485	II	0.0336	3.389	1.328	0.3619	0.3351	0.3235	0.2809	1185350
95	170.650	34.3934	II	0.0349	3.318	1.815	0.2672	0.2263	0.2118	0.1146	1898577
96	233.974	25.1072	II	0.0350	1.780	2.119	0.4336	0.4249	0.4190	0.4734	1911425
97	170.184	34.4938	II	0.0351	2.662	1.803	0.4031	0.3773	0.3608	0.2946	1898550
98	254.117	39.2935	II	0.0620	2.381	2.460	0.6717	0.6390	0.6177	0.6548	0504465
99	230.762	8.4566	II	0.0343	0.852	2.391	0.4930	0.4870	0.4828	0.4963	1305220
100	242.873	29.4501	II	0.0324	2.901	2.485	0.4862	0.4704	0.4555	0.5328	1210969
101	236.185	4.4688	II	0.0419	4.058	2.145	0.3380	0.2881	0.2633	0.1516	0599896
102	155.504	15.1915	II	0.0462	2.787	1.309	0.4259	0.3827	0.3507	0.2402	2501013
103	240.015	17.7825	II	0.0463	2.425	2.100	0.5850	0.5769	0.5821	0.6519	1998984
104	126.640	18.0547	II	0.0579	2.539	1.125	0.2906	0.2380	0.2007	0.2109	2130989
105	200.214	31.3908	II	0.0454	3.202	1.829	0.2166	0.1649	0.1384	0.0603	1938919
106	157.870	56.8973	II	0.0458	3.668	2.377	0.4689	0.4547	0.4582	0.5847	0917704
107	137.320	52.0707	II	0.0614	4.328	1.614	0.2203	0.1631	0.1341	0.1306	0374343
108	151.338	54.4382	II	0.0476	2.694	1.896	0.6227	0.5876	0.5731	0.2821	0509387
109	150.618	54.7214	II	0.0477	6.469	2.201	0.4029	0.3512	-0.0100	0.3333	0511486
110	139.817	55.4342	II	0.0477	3.610	2.053	0.2875	0.2526	0.2184	0.0503	0191882
111	247.530	40.8801	II	0.0301	1.898	1.901	0.4729	0.4518	0.4363	0.4034	0565318
112	244.036	49.3433	II	0.0579	1.947	1.927	0.4284	0.4180	0.4045	0.5471	0533711
113	204.212	34.9362	II	0.0609	4.820	1.128	0.1880	0.1759	0.1713	0.2565	1878854
114	170.670	34.1820	II	0.0437	2.949	2.276	0.4272	0.3907	0.3843	0.4450	1924762
115	170.351	34.2080	II	0.0441	3.648	1.629	0.2072	0.1823	0.1751	0.2092	1924736
116	223.335	16.9993	II	0.0441	2.224	1.915	0.3691	0.3561	0.3556	0.4831	2277481
117	243.881	49.1696	II	0.0580	1.973	2.220	0.5248	0.5023	0.4734	0.2145	0217167
118	212.773	55.1491	II	0.0422	3.793	1.250	0.1904	0.1728	0.1600	0.1310	1193602

Total cluster sample (continued)											
Index	RA. [deg]	DEC. [deg]	Type	z	R_e [kpc]	n	$(g-r)_{in}$	$(g-r)_{in,1}$	$(g-r)_{in,2}$	$(g-r)_{out}$	ID
119	205.241	29.8189	II	0.0433	2.983	1.383	0.0524	0.0193	-0.0075	-0.0126	1936820
120	218.608	52.9602	II	0.0452	4.647	1.532	0.2610	0.2135	0.1893	0.1116	1191490
121	167.395	21.6654	II	0.0317	1.967	1.531	0.3743	0.3490	0.3411	0.2330	2306478
122	230.383	7.8144	II	0.0453	2.311	1.461	0.4713	0.4632	0.4636	0.5016	1343316
123	203.894	36.7494	II	0.0615	4.136	1.072	0.2907	0.2486	0.2271	0.2091	1879979
124	200.225	31.2495	II	0.0452	3.729	1.535	0.2155	0.1844	0.1559	0.1109	1948165
125	242.986	29.4545	II	0.0317	3.021	2.480	0.5603	0.5289	0.5223	0.6522	1210976
126	125.249	35.8317	III	0.0616	3.240	2.398	0.5329	0.4838	0.4496	-0.2165	0778702
127	254.146	39.3527	III	0.0621	2.179	2.082	0.6206	0.6038	0.5975	0.5978	0584877
128	172.615	36.7160	III	0.0612	2.379	2.140	0.5492	0.5277	0.5112	0.3652	1867661
129	208.309	37.5091	III	0.0620	1.739	2.043	0.5204	0.5243	0.5289	0.2971	1837274
130	208.038	37.5184	III	0.0617	1.792	2.217	0.6182	0.6270	0.6380	0.7401	1837250
131	186.330	32.1986	III	0.0616	3.442	2.349	0.3429	0.3705	0.4046	0.5430	1947852
132	177.591	54.6320	III	0.0600	3.085	1.798	0.5583	0.5209	0.5053	0.3667	0818838
133	233.051	58.7692	III	0.0590	3.730	2.050	0.2012	0.1390	0.0977	0.0289	0252358
134	223.644	18.6196	III	0.0590	1.412	2.358	0.7741	0.7706	0.7656	0.9308	2290466
135	209.174	36.5481	III	0.0621	2.574	1.907	0.1994	0.1794	0.1565	-0.1208	1436875
136	207.206	26.5618	III	0.0621	1.021	2.037	0.7527	0.7387	0.7246	0.6100	1995663
137	241.647	33.1914	III	0.0601	2.473	1.966	0.5901	0.5758	0.5714	0.5301	1413046
138	235.072	22.0277	III	0.0418	2.026	1.991	0.6032	0.5692	0.5397	0.4859	2001752
139	227.082	20.4379	III	0.0421	1.752	2.215	0.6047	0.5759	0.5570	0.6185	2004647
140	155.426	23.8793	III	0.0402	1.086	2.451	0.6205	0.5980	0.5692	0.5477	2233390
141	226.981	20.4657	III	0.0418	4.190	1.896	0.4441	0.4096	0.3943	0.4871	2004643
142	241.389	16.3668	III	0.0451	1.644	2.474	0.5341	0.5063	0.4960	0.4911	1994677
143	227.869	7.2622	III	0.0464	1.315	1.949	0.5669	0.5649	0.5632	0.6809	1337935
144	146.560	54.6639	III	0.0467	2.492	2.183	0.6149	0.5784	0.5615	0.3865	0517806
145	230.581	7.6296	III	0.0452	1.921	2.313	0.3273	0.3151	0.3017	0.1303	1356600
146	152.514	54.4545	III	0.0461	1.586	1.943	0.3531	0.3471	0.3364	0.3381	0916315
147	233.341	4.9340	III	0.0395	2.314	1.991	0.6736	0.6365	0.6267	0.3378	1364052
148	214.472	7.4088	III	0.0253	1.823	2.474	0.4870	0.4840	0.4901	0.6920	0603017
149	214.638	7.2868	III	0.0257	2.886	2.382	0.5974	0.6300	0.6216	0.5597	1366376
150	195.033	28.0786	III	0.0241	1.003	2.443	0.4602	0.4509	0.4456	0.4782	2229499
151	188.994	26.9660	III	0.0246	2.643	2.006	0.4420	0.4074	0.3910	0.2892	2240993
152	195.735	53.9820	III	0.0300	2.151	2.385	0.6878	0.6490	0.6388	0.6806	0968581
153	171.589	35.4571	III	0.0341	2.468	2.267	0.5496	0.5336	0.5284	0.5332	1901061
154	167.557	28.3360	III	0.0345	1.990	2.414	0.5158	0.4909	0.4827	0.4215	2202171
155	247.255	40.4951	III	0.0302	1.838	1.573	0.5095	0.5047	0.5043	0.6277	0564276
156	235.215	28.3410	III	0.0329	2.489	1.930	0.5734	0.5380	0.5227	0.5742	1323491
157	214.355	1.9550	III	0.0546	1.795	1.964	0.5689	0.5647	0.5641	0.3374	0283308
158	244.556	50.5234	III	0.0554	1.955	1.496	0.3876	0.3469	0.3280	0.1677	2413557
159	214.235	2.1275	III	0.0540	2.657	1.666	0.3814	0.3279	0.3007	0.0461	0269009
160	124.515	47.3310	III	0.0544	1.474	2.465	0.7132	0.6965	0.6810	0.7977	0195386
161	196.431	9.5637	III	0.0557	1.591	1.527	0.4848	0.4636	0.4382	0.2689	0941499
162	129.064	38.2725	III	0.0569	1.970	2.274	0.4738	0.4521	0.4446	0.4329	0777863
163	167.137	43.7842	III	0.0570	2.033	2.163	0.4953	0.4857	0.4776	0.2890	1246473
164	214.324	8.1464	III	0.0565	1.292	2.375	0.6223	0.6295	0.6323	0.5929	1335472
165	214.411	8.1166	III	0.0566	1.647	2.356	0.6341	0.6320	0.6271	0.6837	1335495
166	194.856	31.3031	III	0.0530	2.136	2.424	0.4658	0.4659	0.4669	0.4303	1946197
167	127.114	30.7482	III	0.0489	3.547	2.382	0.4287	0.4357	0.4405	0.5618	1038034
168	219.397	60.8314	III	0.0493	1.333	2.374	0.2783	0.2855	0.2966	0.4464	0213567
169	168.941	29.3732	III	0.0469	2.012	2.434	0.5152	0.4806	0.4551	0.4425	2208030
170	169.237	29.2675	III	0.0477	1.897	2.349	0.4487	0.4333	0.4261	0.4643	2174009
171	222.627	9.6074	III	0.0502	3.800	1.826	0.6774	0.6300	0.6018	0.3749	1304879
172	176.599	55.4062	III	0.0524	2.004	2.027	0.5008	0.4910	0.4860	0.5905	0821250
173	222.390	11.2685	III	0.0526	2.034	2.134	0.6349	0.5948	0.5695	0.6519	1419068
174	222.666	9.5706	III	0.0504	2.293	2.155	0.2845	0.2995	0.3256	0.5225	1304883
175	133.470	49.1218	III	0.0523	3.466	2.195	0.5428	0.4972	0.4764	0.2886	0430547

Table C2: Listing of coordinates, profile type, redshift, effective radius, Sérsic-index, colours and NYU-VAGC-IDof all 172 galaxies in field sample 1.

Field sample 1											
Index	RA. [deg]	DEC. [deg]	Type	z	R_e [kpc]	n	$(g-r)_{in}$	$(g-r)_{in,1}$	$(g-r)_{in,2}$	$(g-r)_{out}$	ID
1	135.394	2.3800	I	0.0609	1.274	1.598	0.2026	0.1990	0.1940	-	0452293
2	165.776	5.2676	I	0.0517	3.028	2.193	0.4791	0.3620	0.3592	-	0450752
3	210.160	18.8510	I	0.0613	2.614	1.785	0.1842	0.1663	0.1503	-	2365545
4	148.309	22.5635	I	0.0620	3.949	1.823	0.1600	0.1643	0.1577	-	2235614
5	244.952	34.3156	I	0.0333	1.345	1.578	0.3092	0.3056	0.3053	-	0984438
6	146.060	24.1013	I	0.0515	1.728	1.999	0.2683	0.2518	0.2338	-	2204509
7	245.484	31.3006	I	0.0327	3.090	2.043	0.3443	0.3073	0.2940	-	1370346
8	195.727	46.3929	I	0.0611	3.206	1.481	0.1774	0.1432	0.1240	-	1203516
9	229.497	49.6772	I	0.0615	4.174	1.795	0.1391	0.1260	0.1012	-	1195827
10	169.333	47.3545	I	0.0344	2.202	1.853	0.3550	0.3397	0.3313	-	1172603
11	235.444	25.2152	II	0.0333	1.996	1.905	0.3367	0.3239	0.3345	0.2639	1450267
12	128.996	24.8625	II	0.0615	2.979	1.227	0.3072	0.2832	0.2657	0.3293	1814850
13	128.942	25.7911	II	0.0378	3.231	1.207	0.2822	0.2329	0.2114	0.1298	1818197
14	233.067	10.3102	II	0.0442	4.145	1.661	0.2827	0.2439	0.2235	0.1961	1423548
15	231.973	41.1151	II	0.0565	4.044	1.181	0.2339	0.1992	0.1783	0.2144	1372385
16	237.823	32.4569	II	0.0548	3.491	1.237	0.1529	0.1391	0.1282	0.0877	1393223
17	249.010	26.3614	II	0.0577	5.076	2.300	0.3987	0.3266	0.2822	0.1082	1397279
18	222.367	27.7561	II	0.0310	1.725	2.444	0.4789	0.4573	0.4500	0.3815	1916598
19	210.317	31.9882	II	0.0334	3.085	1.644	0.1842	0.1377	0.1013	-0.0281	1922043
20	210.031	29.1894	II	0.0616	3.146	1.316	0.2644	0.2479	0.2440	0.6268	1946609
21	131.720	23.2510	II	0.0614	4.282	1.380	0.2972	0.2416	0.2118	0.1263	1871679
22	155.872	12.5419	II	0.0452	2.247	1.137	0.4263	0.3970	0.3843	0.3808	1821127
23	170.866	35.5844	II	0.0520	3.148	1.644	-0.0489	-0.0775	-0.0990	-0.1128	1839656
24	132.023	27.7731	II	0.0560	3.548	1.516	0.5330	0.4922	0.4664	0.8339	1857841
25	172.613	42.2623	II	0.0443	1.970	1.535	0.3673	0.3372	0.3147	0.2230	1276839
26	189.720	7.1151	II	0.0240	2.377	1.201	0.3791	0.3549	0.3310	0.2580	1282501
27	168.546	38.4120	II	0.0338	5.364	1.634	0.3318	0.2935	0.2650	0.1879	1317298
28	191.218	42.4222	II	0.0536	3.160	2.452	0.5037	0.4897	0.4886	0.4522	1276275
29	196.717	44.0724	II	0.0606	2.376	1.316	0.2029	0.1872	0.1794	0.0961	1244843
30	207.657	43.7641	II	0.0486	2.780	2.253	0.3366	0.2867	0.2627	0.2660	1251658
31	220.187	10.5235	II	0.0536	4.504	1.350	0.1894	0.1390	0.1020	-0.3098	1263032
32	197.767	46.4257	II	0.0606	1.189	2.093	0.5294	0.5210	0.5133	0.2528	1175083
33	196.303	56.7135	II	0.0620	3.212	1.396	-0.0628	-0.0949	-0.1155	-0.1585	1198439
34	163.359	46.4558	II	0.0450	3.901	1.816	0.2458	0.1770	0.1273	0.0616	1172490
35	156.850	37.6114	II	0.0593	1.996	1.375	-0.0796	-0.0947	-0.1230	-0.3266	1178905
36	173.023	45.1020	II	0.0572	6.068	0.990	0.3826	0.3529	0.3309	0.2703	1236624
37	239.029	43.5781	II	0.0600	7.667	1.983	0.1999	0.1132	0.0766	0.0056	1194131
38	157.187	37.2316	II	0.0550	3.073	1.880	0.4238	0.3702	0.3455	0.2217	1325919
39	217.969	16.5218	II	0.0487	3.168	2.203	0.4728	0.4274	0.4074	0.3838	2339088
40	133.224	14.0602	II	0.0593	2.272	1.402	0.2619	0.2183	0.1919	0.2332	2300826
41	209.605	18.3384	II	0.0615	2.995	2.205	0.3220	0.2863	0.2814	0.2569	2363549
42	212.748	19.0106	II	0.0549	3.451	1.354	0.3179	0.2952	0.2804	0.5093	2347334
43	132.261	14.4966	II	0.0604	3.793	2.174	0.2180	0.1862	0.1616	0.1018	2274307
44	155.337	22.5073	II	0.0562	1.306	2.023	0.4154	0.4275	0.4442	0.7155	2258188
45	172.392	21.3621	II	0.0342	2.207	1.415	0.2568	0.2145	0.1982	0.2718	2297738
46	183.213	22.8700	II	0.0563	2.205	1.539	0.2502	0.2535	0.2620	0.3575	2286334
47	139.127	13.0992	II	0.0499	4.346	2.186	0.2338	0.2103	0.1953	0.1235	2504287
48	137.448	11.0953	II	0.0480	3.389	1.589	0.1531	0.1219	0.1048	0.0417	2497026
49	223.008	11.5279	II	0.0468	3.412	1.376	0.2333	0.2143	0.2004	0.1289	1419970
50	190.784	2.9136	II	0.0477	3.646	1.710	0.3949	0.3608	0.3408	0.3378	0289187
51	208.022	15.2309	II	0.0437	2.094	1.289	0.2241	0.1778	0.1442	0.1199	2371415
52	226.277	14.4799	II	0.0442	3.988	1.394	0.2467	0.2075	0.1853	0.1873	2368160
53	208.686	16.1057	II	0.0592	1.855	2.445	0.2908	0.2767	0.2637	0.4846	2383692
54	230.193	18.7565	II	0.0544	2.780	1.015	0.2751	0.2338	0.2144	0.1856	2379640
55	205.561	24.3023	II	0.0461	7.493	1.864	0.2315	0.1705	0.1424	0.1207	2249162
56	211.053	27.6265	II	0.0368	2.842	2.023	0.1855	0.1615	0.1514	0.1604	1982623
57	238.355	19.2866	II	0.0613	2.366	1.585	0.3366	0.3065	0.2854	0.3972	1974442
58	208.984	24.9510	II	0.0291	3.925	1.713	0.2829	0.2519	0.2377	0.2445	1989338
59	196.636	29.9454	II	0.0558	2.453	1.598	0.3933	0.3620	0.3317	0.3877	1984904

Field sample 1 (continued)											
Index	RA. [deg]	DEC. [deg]	Type	z	R_e [kpc]	n	$(g-r)_{in}$	$(g-r)_{in,1}$	$(g-r)_{in,2}$	$(g-r)_{out}$	ID
60	243.436	51.0830	II	0.0474	3.111	2.110	0.4440	0.3918	0.3681	0.4065	1958893
61	225.951	24.5416	II	0.0583	2.573	1.440	0.1958	0.1857	0.1826	0.2164	1954643
62	166.244	31.4176	II	0.0468	3.960	1.705	0.1621	0.1404	0.1375	-0.0322	1962270
63	165.740	31.3927	II	0.0461	4.507	1.893	0.2330	0.1799	0.1446	-0.3618	1962260
64	143.999	26.6740	II	0.0336	1.887	2.161	0.2530	0.2345	0.2187	0.2141	2136922
65	138.720	23.4598	II	0.0349	3.383	1.764	0.1229	0.0725	0.0454	-0.1470	2134713
66	146.998	21.9527	II	0.0248	3.292	1.827	0.3541	0.3288	0.3193	0.3794	2218043
67	167.770	28.2080	II	0.0317	2.014	1.872	0.3613	0.3561	0.3602	0.3467	2168475
68	207.215	26.8721	II	0.0579	4.004	1.537	0.3456	0.2878	0.2678	0.1700	1997728
69	221.541	22.2327	II	0.0613	4.499	1.414	0.3630	0.3210	0.2870	0.2044	1989811
70	226.217	21.0695	II	0.0347	3.540	1.596	0.1820	0.1390	0.1160	0.1142	2005874
71	231.251	21.0022	II	0.0418	1.334	2.032	0.5429	0.5352	0.5293	0.6118	1998689
72	143.632	46.4616	II	0.0265	3.463	1.779	0.3764	0.3297	0.3118	0.3171	0803771
73	224.650	5.3965	II	0.0589	2.889	1.255	0.0183	0.0006	0.0066	0.2327	0599370
74	134.928	46.0484	II	0.0523	3.604	1.587	0.1235	0.0995	0.0908	0.2132	0859503
75	182.907	56.6036	II	0.0511	5.532	1.203	0.0513	0.0122	-0.0183	-0.0493	0836056
76	194.085	5.4765	II	0.0242	3.366	1.541	0.3614	0.3181	0.3000	0.3734	0526837
77	153.624	56.9896	II	0.0455	2.235	2.141	0.1980	0.1470	0.1156	0.0300	0517952
78	253.663	34.5611	II	0.0308	1.484	2.415	0.4845	0.4673	0.4680	0.7167	0565569
79	178.059	61.3786	II	0.0425	4.842	1.479	0.2640	0.2200	0.1848	0.1896	0539445
80	134.771	39.1801	II	0.0581	7.190	1.729	0.3465	0.2960	0.2727	0.1543	0862668
81	186.472	62.4292	II	0.0334	4.697	2.010	0.2504	0.1962	0.1678	-0.0277	0951585
82	196.690	9.9837	II	0.0485	2.599	1.361	0.2370	0.1961	0.1745	0.1581	0944647
83	183.195	48.9245	II	0.0603	6.009	1.240	0.1351	0.1027	0.0835	-0.0039	0953767
84	181.979	67.8165	II	0.0595	5.426	2.000	0.3097	0.2684	0.2406	0.0701	0953113
85	147.469	54.2924	II	0.0482	3.210	1.180	0.2868	0.2712	0.2605	0.2310	0918275
86	195.863	49.4553	II	0.0598	2.431	0.809	0.2318	0.2068	0.1897	0.2571	0895315
87	167.990	8.4287	II	0.0479	2.942	1.672	0.3970	0.3846	0.3608	0.2951	0934866
88	185.461	61.1398	II	0.0438	4.131	1.537	0.2641	0.2342	0.2189	0.1956	0923338
89	179.895	60.3780	II	0.0506	1.886	1.521	0.7481	0.7097	0.6767	0.4669	0516557
90	129.952	54.5808	II	0.0446	1.554	2.079	0.3676	0.3798	0.3995	0.4136	0244952
91	170.938	67.0768	II	0.0557	4.343	2.489	0.2417	0.1836	0.1593	0.0573	0229048
92	221.795	62.5847	II	0.0221	2.679	1.573	0.2815	0.2497	0.2375	0.3527	0250049
93	217.912	63.5311	II	0.0465	2.165	0.812	0.2357	0.2201	0.2096	0.2931	0249995
94	180.100	0.4907	II	0.0257	1.861	1.760	0.3437	0.2747	0.2510	0.0939	0518886
95	218.091	0.1781	II	0.0549	6.822	1.911	0.1618	0.1114	0.0661	0.0421	0049431
96	132.125	0.1709	II	0.0581	3.934	1.580	0.0206	-0.0319	-0.0653	-0.1406	0181973
97	142.691	1.1856	II	0.0513	3.272	0.806	0.2099	0.1889	0.1695	0.1760	0083396
98	255.377	38.9158	II	0.0352	2.913	1.130	0.4481	0.3736	0.3548	0.3912	0260988
99	145.459	53.0277	II	0.0464	3.141	1.262	0.2224	0.1840	0.1683	0.1662	0471045
100	129.997	49.0009	II	0.0513	5.321	1.239	0.2741	0.2290	0.1882	0.1728	0433868
101	125.158	41.8362	II	0.0591	2.586	2.487	0.3698	0.3407	0.3362	0.5267	0515442
102	150.403	54.5831	II	0.0563	3.655	1.438	0.1383	0.1199	0.1031	0.0573	0511478
103	234.164	3.3603	II	0.0323	7.210	1.753	0.1967	0.1511	0.1371	0.1059	0306271
104	211.220	3.7856	II	0.0519	2.706	2.294	0.3696	0.3431	0.3368	0.4837	0303648
105	135.451	51.9320	II	0.0579	5.509	1.308	0.2984	0.2328	0.1921	-0.0079	0433124
106	135.232	50.2354	II	0.0412	2.325	2.026	0.2367	0.1888	0.1488	0.1940	0430631
107	173.921	48.8037	II	0.0367	5.178	2.357	0.3458	0.2873	0.2683	0.3768	0954536
108	162.739	13.6083	II	0.0600	3.679	1.743	0.2665	0.2351	0.2251	0.3913	1126747
109	130.047	29.8610	II	0.0499	2.834	0.960	0.2876	0.2647	0.2551	0.2444	1096967
110	123.670	26.4252	II	0.0405	2.352	1.847	0.5248	0.5008	0.4896	0.1844	1090092
111	136.531	32.6943	II	0.0495	5.038	1.540	0.1714	0.1444	0.1272	0.0838	1155179
112	184.796	55.4484	II	0.0451	2.354	1.431	0.3464	0.2934	0.2694	0.2642	0965952
113	206.288	52.8672	II	0.0503	3.325	0.913	0.2106	0.1909	0.1939	0.2564	0985890
114	224.461	53.9532	II	0.0491	3.603	1.828	0.4120	0.3782	0.3507	0.2275	0992287
115	121.739	25.0140	II	0.0362	3.182	2.177	0.3519	0.3511	0.3526	0.4730	1052633
116	152.192	9.1769	II	0.0606	4.497	1.499	0.2169	0.1738	0.1451	0.1471	1056688
117	152.260	9.0855	II	0.0564	2.153	1.913	0.5910	0.5685	0.5574	0.6998	1056691
118	236.891	46.4051	II	0.0378	3.606	1.642	0.3435	0.2747	0.2402	0.1701	1015222

Field sample 1 (continued)											
Index	RA. [deg]	DEC. [deg]	Type	z	R_e [kpc]	n	$(g-r)_{in}$	$(g-r)_{in,1}$	$(g-r)_{in,2}$	$(g-r)_{out}$	ID
119	132.199	30.8083	II	0.0539	4.814	1.366	0.2011	0.1768	0.1667	0.1753	1087420
120	158.216	43.6308	II	0.0537	9.824	2.050	0.1944	0.1499	0.1267	0.2402	1064537
121	185.665	55.0830	II	0.0367	3.312	2.125	0.0917	0.0687	0.0555	0.0625	0964454
122	184.269	55.1235	II	0.0521	3.037	1.192	0.3138	0.2909	0.2800	0.3792	0964422
123	200.705	49.8553	II	0.0595	3.484	1.213	0.1100	0.0736	0.0473	-0.2302	1162715
124	172.780	56.5250	II	0.0493	6.029	1.957	0.4247	0.3096	0.2738	-0.2185	1166396
125	157.698	47.2257	II	0.0618	3.736	2.122	0.3350	0.2770	0.2404	0.2055	0957431
126	165.849	46.4911	III	0.0534	3.040	2.479	0.5903	0.5449	0.5217	0.4721	1171599
127	163.135	16.6297	III	0.0582	1.323	2.163	0.5987	0.5803	0.5724	0.5060	2407018
128	220.890	17.9274	III	0.0563	4.084	2.294	0.4065	0.3762	0.3579	0.0828	2280853
129	162.051	45.5953	III	0.0501	3.196	2.004	0.1937	0.1634	0.1482	0.1844	1171511
130	161.743	62.6157	III	0.0567	3.542	1.145	0.1973	0.1701	0.1464	-0.0047	0484295
131	209.680	0.3195	III	0.0332	1.092	2.184	0.3773	0.3639	0.3549	0.3469	0075524
132	178.481	24.3691	III	0.0578	3.552	1.747	0.0612	0.0954	0.1197	-0.1455	2263148
133	222.269	49.9470	III	0.0305	5.509	2.165	0.3945	0.3358	0.2946	0.2559	1197165
134	212.878	16.5617	III	0.0553	3.689	2.048	0.2694	0.1843	0.1442	-0.1047	2358244
135	212.679	15.3362	III	0.0602	1.284	2.439	0.6384	0.6274	0.6045	0.5507	2382504
136	151.789	37.8573	III	0.0520	2.415	2.147	0.5728	0.5704	0.5806	0.5287	1157916
137	138.265	32.6365	III	0.0491	2.172	2.353	0.6519	0.6451	0.6391	0.6987	1182538
138	131.223	55.0541	III	0.0256	1.470	2.363	0.5726	0.5354	0.5152	0.5147	0228486
139	202.817	12.5115	III	0.0463	2.294	1.303	0.4436	0.4726	0.4925	0.6157	1225656
140	172.577	1.4098	III	0.0618	3.412	2.484	0.5201	0.4716	0.4714	0.4653	0426807
141	230.907	16.4293	III	0.0400	1.146	1.750	0.4466	0.4416	0.4368	0.4374	2287670
142	223.204	16.8082	III	0.0413	2.191	1.989	0.7197	0.7163	0.7141	0.6231	2345983
143	189.072	14.1754	III	0.0471	1.706	2.323	0.2849	0.2718	0.2671	0.1457	1125044
144	206.089	22.1340	III	0.0368	2.394	1.170	0.1025	0.0820	0.0723	-0.0114	2316098
145	221.145	10.4483	III	0.0566	3.414	1.729	0.2215	0.2182	0.2239	0.2606	1263057
146	199.710	31.9662	III	0.0359	1.378	1.893	0.5413	0.5035	0.4806	0.3851	1939891
147	201.709	31.2126	III	0.0610	2.458	1.611	0.4706	0.4480	0.4337	0.2880	1938960
148	151.525	5.7078	III	0.0590	2.311	1.314	0.4123	0.3973	0.3893	0.3345	0925629
149	163.580	29.7014	III	0.0307	3.911	1.803	0.1809	0.1379	0.1158	0.1196	1959320
150	233.012	4.9341	III	0.0502	1.934	2.263	0.3427	0.3088	0.2995	0.2779	1364042
151	204.169	31.2643	III	0.0618	3.972	1.046	0.2294	0.2179	0.2136	0.0797	1940071
152	202.148	42.2725	III	0.0350	2.898	1.907	0.1954	0.1720	0.1598	0.0294	1391062
153	129.625	24.2861	III	0.0612	2.361	2.284	0.2941	0.2814	0.2774	0.2555	1876792
154	185.350	60.8813	III	0.0623	1.619	2.226	0.2682	0.2570	0.2468	0.2805	0951959
155	164.027	53.1697	III	0.0621	1.763	2.080	0.4381	0.4275	0.4144	0.2958	0964003
156	204.517	32.5399	III	0.0448	4.226	1.566	-0.0594	-0.1076	-0.1350	0.0486	1896227
157	238.829	24.6264	III	0.0441	3.202	1.469	0.3017	0.2801	0.2738	-0.1789	1892835
158	146.535	32.8973	III	0.0368	2.917	2.120	0.3785	0.3588	0.3670	0.3877	1882821
159	218.613	9.4639	III	0.0550	3.130	1.280	0.3143	0.3049	0.3054	0.2713	1344969
160	237.502	20.0682	III	0.0617	3.005	1.512	0.5448	0.5406	0.5347	0.8633	2000035
161	163.658	55.6628	III	0.0478	3.115	2.203	0.2709	0.2446	0.2360	-0.0233	0799002
162	154.923	54.2081	III	0.0251	1.596	2.303	0.3960	0.3552	0.3549	0.2851	0799262
163	219.928	9.5951	III	0.0515	2.775	2.185	0.5051	0.4759	0.4626	0.5827	1303297
164	145.708	25.3924	III	0.0283	0.941	1.778	0.3998	0.3909	0.3833	0.4065	2134115
165	171.003	37.9591	III	0.0360	1.945	1.328	0.3786	0.3620	0.3480	0.2790	1310346
166	201.690	8.7394	III	0.0565	1.097	2.292	0.2206	0.2181	0.2148	0.5129	1333350
167	191.374	9.8650	III	0.0541	1.312	1.176	0.1732	0.1685	0.1638	0.2031	1336800
168	197.287	28.8925	III	0.0248	2.065	2.146	0.4319	0.4219	0.4165	0.3787	1968833
169	194.849	9.7773	III	0.0464	2.310	1.289	0.2395	0.2942	0.3636	0.2357	1336910
170	126.536	40.9784	III	0.0572	1.042	2.237	0.7096	0.6842	0.6522	0.2830	0827940
171	190.870	29.4668	III	0.0312	3.531	2.160	0.4322	0.3978	0.3821	0.2610	1979632
172	187.721	28.8740	III	0.0594	3.065	1.061	0.1678	0.1308	0.1088	0.1110	1976938

Table C3: Listing of coordinates, profile type, redshift, effective radius, Sérsic-index, colours and NYU-VAGC-ID of all 172 galaxies in field sample 2.

Field sample 2											
Index	RA. [deg]	DEC. [deg]	Type	z	R_e [kpc]	n	$(g-r)_{in}$	$(g-r)_{in,1}$	$(g-r)_{in,2}$	$(g-r)_{out}$	ID
1	131.463	31.9604	I	0.0472	2.340	1.403	0.2391	0.2152	0.2078	-	1091789
2	166.242	6.1212	I	0.0298	2.407	1.492	0.1312	0.1194	0.1165	-	0924271
3	158.996	34.9529	I	0.0492	2.068	1.216	0.1839	0.1877	0.1965	-	1890683
4	200.407	47.7353	I	0.0620	3.788	1.040	0.2832	0.2723	0.2641	-	1208166
5	199.225	47.5285	I	0.0618	1.027	2.295	0.3528	0.3491	0.3453	-	1177594
6	232.567	35.4766	I	0.0605	2.802	1.701	0.1736	0.1467	0.1206	-	1393032
7	198.543	32.2280	I	0.0611	3.200	1.430	0.3835	0.3734	0.3720	-	1951670
8	183.319	41.4936	I	0.0494	3.670	1.924	0.1666	0.1372	0.1169	-	1292041
9	152.685	24.8738	I	0.0474	3.696	2.060	0.1898	0.1706	0.1578	-	2165893
10	183.000	24.1835	I	0.0514	0.917	2.417	0.3583	0.3559	0.3543	-	2319450
11	182.463	11.2567	II	0.0597	2.893	1.215	-0.1722	-0.1892	-0.1999	-0.0768	1218406
12	179.972	25.6608	II	0.0585	2.984	1.891	0.2532	0.2332	0.2214	0.2039	2248535
13	210.149	45.9764	II	0.0423	2.596	1.492	0.1340	0.0972	0.0853	-0.1207	1208408
14	226.822	10.6043	II	0.0256	4.363	1.857	0.4183	0.3908	0.3847	0.6333	1268252
15	150.608	23.0746	II	0.0414	3.133	1.348	0.2276	0.1856	0.1606	0.2343	2235677
16	179.812	42.5669	II	0.0304	3.974	2.121	0.0350	0.0136	-0.0001	0.1287	1275962
17	213.412	41.6752	II	0.0404	3.001	1.429	0.3548	0.3079	0.2862	0.2487	1234965
18	220.150	10.1097	II	0.0505	3.943	2.084	0.2738	0.2375	0.2221	0.1805	1259841
19	190.725	25.6621	II	0.0594	3.072	1.326	0.2258	0.1805	0.1614	0.2146	2248860
20	170.712	46.5745	II	0.0333	1.238	2.406	0.4609	0.4374	0.4257	0.2905	1066535
21	162.168	12.5123	II	0.0536	2.294	1.434	0.4080	0.3764	0.3495	0.1554	1076294
22	144.697	34.9171	II	0.0419	4.616	1.862	0.1772	0.1523	0.1361	0.1112	1156845
23	164.032	10.0217	II	0.0314	2.853	1.522	0.2854	0.2590	0.2371	0.3587	1061359
24	246.093	40.9272	II	0.0617	4.476	1.364	0.3404	0.3198	0.3234	0.3723	1011580
25	216.057	20.0453	II	0.0539	6.363	1.952	0.5343	0.4722	0.4560	0.3785	2312614
26	163.184	9.1753	II	0.0467	2.749	1.181	0.2864	0.2606	0.2471	0.4201	1059458
27	143.987	34.2373	II	0.0503	2.527	1.246	0.1233	0.1117	0.1026	-0.1190	1180609
28	140.003	32.9698	II	0.0502	4.005	1.869	0.2460	0.2337	0.2145	0.2937	1181508
29	190.333	57.5019	II	0.0431	2.828	1.621	-0.1091	-0.1358	-0.1517	-0.1347	1199232
30	202.331	45.0518	II	0.0596	3.326	1.286	0.2078	0.1881	0.1844	0.2442	1173570
31	134.601	17.5970	II	0.0479	4.798	1.483	0.1453	0.1002	0.0775	0.0475	2258701
32	228.186	40.1099	II	0.0622	2.567	1.364	0.3703	0.3458	0.3234	0.1019	1163483
33	137.089	17.4861	II	0.0563	4.445	2.247	0.3767	0.3391	0.3319	0.1828	2256419
34	175.145	41.1196	II	0.0523	5.411	1.291	-0.0818	-0.1244	-0.1598	-0.2790	1291892
35	239.901	19.2143	II	0.0352	2.634	1.642	0.3537	0.3462	0.3463	0.4869	1965020
36	128.481	25.1679	II	0.0432	1.524	1.879	0.3885	0.3858	0.3843	0.2098	1855099
37	195.861	36.1303	II	0.0505	2.510	1.990	0.2149	0.1701	0.1498	0.1223	1866125
38	160.477	14.0994	II	0.0540	3.897	1.275	0.0313	-0.0095	-0.0403	-0.0805	1824635
39	198.504	28.2056	II	0.0572	3.758	1.867	0.0715	0.0241	-0.0013	0.0017	1977215
40	237.723	24.9632	II	0.0459	4.594	2.075	0.1941	0.1612	0.1403	0.1246	1453216
41	242.772	18.4994	II	0.0360	4.891	2.329	0.2048	0.1388	0.1265	0.0539	1976736
42	207.604	30.7369	II	0.0561	1.372	1.349	0.3759	0.3736	0.3690	0.2970	1934456
43	184.562	33.1693	II	0.0604	5.322	1.768	0.1478	0.1159	0.0864	0.1796	1940574
44	182.557	32.0837	II	0.0610	8.896	2.072	0.2102	0.1507	0.1273	0.0745	1947744
45	214.910	28.8666	II	0.0557	4.131	1.616	0.2368	0.2120	0.2117	0.2828	1933916
46	177.796	36.0032	II	0.0622	3.764	1.633	0.2686	0.2362	0.2112	0.1324	1901240
47	228.580	26.7496	II	0.0312	2.096	1.458	0.3551	0.3315	0.3190	0.2985	1909969
48	214.434	30.2190	II	0.0618	3.184	2.186	0.2845	0.2297	0.1831	0.1704	1916334
49	201.508	51.3021	II	0.0304	6.357	1.897	0.1927	0.1568	0.1291	0.1472	1374021
50	228.872	20.3357	II	0.0476	4.255	2.114	0.1895	0.1645	0.1462	0.1977	2005967
51	245.498	30.6598	II	0.0554	2.631	2.224	0.3245	0.3192	0.3205	0.4323	1404489
52	229.523	5.2140	II	0.0458	2.168	1.236	0.2222	0.1899	0.1757	0.2964	1363892
53	188.388	39.6678	II	0.0613	1.767	2.255	0.5773	0.5577	0.5335	0.5702	1317705
54	183.447	40.4892	II	0.0465	2.309	1.590	0.3012	0.2912	0.2885	0.2150	1326551
55	132.182	18.9904	II	0.0618	4.920	1.720	0.3359	0.2975	0.2795	0.2111	2170362
56	209.586	36.2732	II	0.0608	3.044	2.187	0.4227	0.3989	0.3905	0.4804	1436901
57	241.298	24.9601	II	0.0338	4.741	2.439	0.2545	0.2048	0.1810	0.1084	1441060
58	217.809	36.0586	II	0.0551	2.777	1.147	0.2378	0.1871	0.1601	0.0777	1444101
59	223.688	11.8032	II	0.0504	6.254	2.316	0.1927	0.1274	0.0857	-0.0406	1428783

Field sample 2 (continued)											
Index	RA. [deg]	DEC. [deg]	Type	z	R_e [kpc]	n	$(g-r)_{in}$	$(g-r)_{in,1}$	$(g-r)_{in,2}$	$(g-r)_{out}$	ID
60	243.559	32.7621	II	0.0621	4.821	1.422	0.2663	0.2373	0.2050	0.2335	1414848
61	199.574	13.4167	II	0.0498	2.909	1.439	0.2522	0.2215	0.2073	0.2049	1415975
62	201.786	28.2623	II	0.0369	2.867	1.732	0.0466	0.0115	-0.0135	-0.0852	1977874
63	154.050	3.6506	II	0.0320	2.089	1.645	0.2535	0.2378	0.2361	0.2864	0445454
64	154.318	4.7619	II	0.0623	3.839	1.353	0.3548	0.3301	0.3147	0.3517	0450405
65	236.194	22.8382	II	0.0452	4.033	1.531	0.3497	0.3147	0.2992	0.2881	1967239
66	239.316	29.3858	II	0.0584	3.688	1.193	0.4089	0.3545	0.3279	0.2904	1424358
67	164.556	2.6478	II	0.0349	2.761	1.472	0.2586	0.2162	-0.0238	0.2511	0428254
68	118.317	36.4922	II	0.0467	3.486	1.286	0.1800	0.1444	0.1226	0.0812	0435735
69	138.735	31.3599	II	0.0622	3.086	1.276	0.3694	0.3569	0.3455	0.3602	1859710
70	132.309	3.9338	II	0.0587	2.067	1.408	0.2815	0.2695	0.2641	0.3652	0451275
71	148.893	14.3590	II	0.0433	1.199	2.190	0.1647	0.1611	0.1564	0.0920	2493368
72	241.327	52.1344	II	0.0463	3.720	1.236	0.2550	0.2299	0.2070	0.2048	0500400
73	141.583	50.5709	II	0.0476	3.124	2.150	0.2373	0.1919	0.1692	0.0520	0509198
74	193.633	3.9975	II	0.0495	2.007	0.869	0.1085	0.0938	0.0853	0.1854	0485141
75	167.517	4.1473	II	0.0296	2.164	1.893	0.5392	0.5202	0.5150	0.6137	0455659
76	118.318	35.5726	II	0.0458	2.280	1.481	0.2277	0.2504	0.2773	0.4568	0473359
77	137.091	50.2600	II	0.0494	3.505	1.422	0.2841	0.2506	0.2374	0.1885	0473957
78	155.009	2.9866	II	0.0459	6.114	1.582	0.3489	0.2868	0.2300	0.1545	0389636
79	205.884	1.1266	II	0.0480	6.383	1.916	0.1911	0.1315	0.1143	0.1157	0244576
80	136.751	57.4515	II	0.0462	4.133	1.664	0.3169	0.2424	0.1921	0.0736	0246940
81	191.358	52.9575	II	0.0535	3.297	2.276	0.4035	0.3600	0.3319	0.2814	0851147
82	216.157	55.7291	II	0.0434	3.068	0.819	0.2386	0.2117	0.1953	0.0674	0989463
83	217.321	0.6973	II	0.0559	4.130	1.048	0.3684	0.3399	0.3149	0.2686	0080975
84	133.005	51.3255	II	0.0566	6.077	2.224	0.5691	0.5036	0.4703	0.5146	0191392
85	176.283	21.8753	II	0.0516	3.858	1.094	0.1969	0.1516	0.1174	0.0205	2302096
86	241.288	54.4891	II	0.0339	2.012	2.294	0.5308	0.5215	0.5210	0.5766	0254593
87	162.692	60.6839	II	0.0563	1.832	1.310	0.3059	0.2712	0.2180	-0.0924	0377145
88	148.004	1.5598	II	0.0479	3.182	1.385	0.3921	0.3396	-0.0113	0.2858	0386564
89	131.652	1.7761	II	0.0512	2.119	1.661	0.4026	0.3922	0.3902	0.3157	0387880
90	213.582	24.3125	II	0.0617	3.847	1.316	0.1616	0.1440	0.1297	0.0700	2005346
91	224.610	6.2380	II	0.0578	2.960	1.258	0.4540	0.4171	0.4072	0.6709	0602336
92	195.951	2.5289	II	0.0417	3.072	1.666	0.4949	0.4999	0.5059	0.5512	0286187
93	166.032	3.3347	II	0.0570	2.545	0.674	0.1661	0.1520	0.1420	0.2148	0290815
94	126.914	41.9036	II	0.0359	4.070	2.010	0.3412	0.2845	0.2468	0.1560	0510986
95	192.903	18.6545	II	0.0444	2.717	1.345	0.0775	0.0349	0.0101	-0.0587	2357658
96	181.915	57.0284	II	0.0621	3.309	1.867	0.3902	0.3494	0.3290	0.2110	0836713
97	149.521	53.2621	II	0.0451	2.917	1.017	0.2055	0.1829	0.1645	0.2580	0860604
98	218.585	16.8025	II	0.0538	2.279	1.358	0.2139	0.2356	0.2560	0.4515	2341284
99	185.009	54.1117	II	0.0610	3.236	1.252	0.1748	0.1606	0.1479	0.1599	0816921
100	161.227	51.4917	II	0.0251	3.420	2.067	0.2010	0.1723	0.1634	0.1630	0816508
101	178.222	56.3693	II	0.0555	4.838	1.968	0.1986	0.1462	0.1131	0.0451	0835919
102	169.035	55.4903	II	0.0576	2.408	2.306	0.1807	0.1517	0.1240	-0.0916	0835630
103	180.406	20.2032	II	0.0557	3.884	1.318	0.1863	0.1401	0.1250	-0.0005	2331923
104	228.888	46.0635	II	0.0517	4.853	2.446	0.3595	0.3286	0.3057	0.1523	0980959
105	156.423	52.0777	II	0.0568	3.085	2.471	0.4260	0.4011	0.3987	0.3785	0965269
106	227.614	49.7751	II	0.0521	2.794	1.444	0.2974	0.2724	0.2539	0.1297	0999348
107	237.016	41.3743	II	0.0326	1.932	1.452	0.1638	0.1182	0.0903	0.0511	0981164
108	183.835	59.8700	II	0.0570	3.870	1.302	0.3548	0.3111	0.2891	0.2172	0921475
109	181.813	24.7424	II	0.0486	3.660	1.402	0.4695	0.4502	0.4453	0.5814	2321126
110	200.603	23.4513	II	0.0372	3.055	1.301	0.2342	0.2101	0.2186	0.1835	2319865
111	195.485	8.6812	II	0.0525	2.728	1.973	0.0598	0.0315	0.0198	0.1205	0936812
112	164.456	55.8810	II	0.0614	4.365	1.413	0.1507	0.1155	0.0926	0.1025	0799013
113	206.924	57.7418	II	0.0614	2.632	1.377	0.0899	0.0703	0.0419	0.0398	0512345
114	228.274	54.5213	II	0.0387	2.483	2.075	0.2458	0.2120	0.1892	0.1679	0555697
115	230.879	52.4210	II	0.0273	2.289	1.332	0.3556	0.3650	0.3786	0.4195	0536291
116	240.978	51.6140	II	0.0297	2.500	1.504	0.2561	0.2308	0.2247	0.2489	0533631
117	163.805	16.1302	II	0.0581	4.159	1.444	0.3112	0.2669	0.2472	0.2437	2393996
118	231.808	2.2768	II	0.0614	3.793	1.280	0.3978	0.3414	0.3096	0.3946	0562516

Field sample 2 (continued)											
Index	RA. [deg]	DEC. [deg]	Type	z	R_e [kpc]	n	$(g-r)_{in}$	$(g-r)_{in,1}$	$(g-r)_{in,2}$	$(g-r)_{out}$	ID
119	253.295	40.6836	II	0.0614	4.831	1.014	0.2438	0.2066	0.1862	0.2005	0584808
120	231.638	4.7850	II	0.0416	1.764	1.993	0.4663	0.4444	0.4290	0.5231	0599710
121	202.718	58.3555	II	0.0592	1.437	1.889	0.5591	0.5437	0.5274	0.5436	0512268
122	241.187	49.4584	II	0.0242	3.604	1.848	0.3199	0.2948	0.2883	0.2777	0530131
123	125.054	18.0934	III	0.0610	3.158	1.311	0.4732	0.4850	0.5016	0.5017	2163133
124	188.588	29.0042	III	0.0607	1.297	2.292	0.3951	0.3857	0.3704	0.3837	2199946
125	202.652	31.0356	III	0.0382	3.433	2.095	0.4526	0.4135	0.4000	0.4157	1948234
126	134.977	20.5999	III	0.0250	1.570	1.417	0.2175	0.2271	0.2186	0.1828	2207187
127	215.695	23.7814	III	0.0358	1.293	1.910	0.4375	0.4098	0.3971	0.3017	2005420
128	151.333	23.8170	III	0.0456	1.892	2.161	0.4057	0.3888	0.3782	0.2217	2237623
129	242.211	12.4744	III	0.0339	1.767	1.367	0.2210	0.1822	0.1651	0.1352	2390821
130	208.543	23.9576	III	0.0565	1.103	2.143	0.6390	0.6363	0.6301	0.6728	2017625
131	187.706	33.3123	III	0.0596	2.611	1.027	0.2393	0.2334	0.2402	0.5390	1953263
132	244.687	41.7982	III	0.0607	2.295	2.353	0.6808	0.6636	0.6509	0.4813	1957995
133	128.333	36.1152	III	0.0533	2.447	1.829	0.4256	0.3949	0.3733	0.1572	0865178
134	157.358	5.9632	III	0.0354	1.996	1.931	0.3867	0.3690	0.3657	0.2557	0908182
135	145.963	52.0744	III	0.0458	1.702	1.616	0.2916	0.2845	0.2818	0.2309	0860533
136	221.747	58.0606	III	0.0599	1.696	1.918	0.2407	0.2273	0.2091	0.1013	0559031
137	154.807	48.5368	III	0.0617	1.926	2.353	0.4799	0.4634	0.4489	0.1049	0848007
138	151.126	37.0652	III	0.0413	6.048	1.966	0.1889	0.1325	0.1067	-0.0157	1157019
139	178.390	47.3187	III	0.0473	3.280	2.465	0.4082	0.3533	0.3344	0.1257	1170771
140	163.966	8.9023	III	0.0318	1.787	2.112	0.4794	0.4614	0.4638	0.3602	1058575
141	156.075	51.9816	III	0.0456	2.963	1.393	0.4716	0.4828	0.4861	0.5520	0965258
142	250.811	33.5826	III	0.0528	5.185	1.937	0.1842	0.1603	0.1490	0.2107	0999976
143	191.824	3.1513	III	0.0331	1.653	1.611	0.3363	0.3422	0.3451	0.4862	0273237
144	177.606	3.3247	III	0.0467	2.944	2.296	0.3285	0.2836	0.2434	0.0635	0291185
145	237.654	56.7973	III	0.0520	4.803	1.776	0.4035	0.3539	0.3217	0.1951	0254506
146	131.216	51.2895	III	0.0550	2.144	1.178	0.2227	0.2428	0.2666	0.5079	0192857
147	244.385	46.6295	III	0.0577	2.198	2.453	0.5813	0.5715	0.5671	0.4556	0207864
148	199.656	3.9951	III	0.0457	2.283	2.383	0.5055	0.4794	0.4587	0.4165	0485305
149	206.632	5.2097	III	0.0309	2.879	2.208	0.2458	0.2008	0.1870	0.1833	0527196
150	163.634	5.2076	III	0.0241	1.645	1.340	0.6157	0.6099	0.6223	0.5266	0450694
151	227.054	56.4229	III	0.0295	1.933	2.394	0.2620	0.2532	0.2562	0.1806	0440237
152	177.221	64.1185	III	0.0414	2.324	1.689	0.5225	0.4974	0.4803	0.4219	0440587
153	218.304	31.4727	III	0.0611	1.858	1.636	0.2089	0.2167	0.2304	0.5366	1448401
154	166.660	14.2487	III	0.0585	1.715	1.688	0.2181	0.2020	0.1798	0.2630	1824215
155	201.117	13.6963	III	0.0596	1.558	2.216	0.1997	0.1829	0.1652	-0.1355	1418354
156	248.922	25.9019	III	0.0518	2.140	2.071	0.3801	0.3617	0.3507	0.3298	1396006
157	236.390	30.1474	III	0.0316	4.041	2.428	0.2782	0.2254	0.1966	0.0092	1402014
158	226.142	26.0271	III	0.0575	3.044	2.013	0.5742	0.5610	0.5561	0.5894	1935052
159	210.469	29.4533	III	0.0617	2.351	2.337	0.5174	0.4854	0.4670	0.5031	1938121
160	155.166	33.1453	III	0.0447	2.716	1.798	0.5513	0.5227	0.5009	0.4681	1888860
161	199.692	13.6149	III	0.0548	3.291	1.135	-0.0280	-0.0562	-0.0686	-0.1678	1828591
162	157.371	37.5032	III	0.0558	2.515	2.284	0.6942	0.6758	0.6585	0.5032	1858285
163	232.001	8.3969	III	0.0350	2.224	2.165	0.3917	0.3735	0.3708	0.3341	1260295
164	206.199	7.9807	III	0.0372	2.054	2.199	0.3121	0.2743	0.2572	0.3085	1287915
165	222.224	38.7683	III	0.0317	4.009	2.065	0.3767	0.3312	0.3013	0.2021	1235127
166	195.056	46.4813	III	0.0503	2.154	1.839	0.4934	0.4921	0.4904	0.4583	1203505
167	204.249	46.9606	III	0.0589	3.869	1.627	0.4157	0.3786	0.3544	0.3578	1208248
168	227.193	5.4043	III	0.0371	2.455	1.095	0.2635	0.2531	0.2590	0.2610	1363747
169	232.078	32.9591	III	0.0587	2.803	2.065	0.1887	0.1418	0.1061	0.0296	1391769
170	231.338	6.6677	III	0.0336	1.139	1.893	0.5791	0.5601	0.5429	0.5016	1351628
171	208.987	8.1936	III	0.0234	2.700	1.948	0.3255	0.3010	0.3027	0.3492	1333535
172	203.729	7.5230	III	0.0503	4.192	1.606	0.2014	0.1715	0.1650	0.1582	1346838

Table C4: Listing of coordinates, profile type, redshift, effective radius, Sérsic-index, colours and NYU-VAGC-ID of all 177 galaxies in field sample 3.

Field sample 3											
Index	RA. [deg]	DEC. [deg]	Type	z	R_e [kpc]	n	$(g-r)_{in}$	$(g-r)_{in,1}$	$(g-r)_{in,2}$	$(g-r)_{out}$	ID
1	224.994	39.1991	I	0.0344	1.667	1.329	0.2237	0.2237	0.2237	-	1204128
2	248.761	26.1807	I	0.0424	2.312	1.726	0.1430	0.1430	0.1430	-	1213783
3	167.723	10.2944	I	0.0463	2.488	1.297	0.2084	0.2084	0.2084	-	1061491
4	236.623	11.1031	I	0.0470	1.826	0.955	0.3308	0.3308	0.3308	-	2384542
5	141.026	51.7645	I	0.0471	2.380	2.331	0.3982	0.3982	0.3982	-	0472596
6	131.908	6.5121	I	0.0510	2.209	1.536	0.2808	0.2646	0.2533	-	0945534
7	155.052	7.5456	I	0.0622	3.040	1.150	0.1212	0.1018	0.0889	-	0915461
8	148.334	10.9275	I	0.0575	3.311	0.965	0.2970	0.2714	0.2507	-	1121323
9	177.825	53.3656	I	0.0611	1.897	1.362	0.2379	0.2218	0.2049	-	0874090
10	156.328	28.0557	II	0.0210	1.663	1.819	0.3861	0.4035	0.4096	0.5208	2212669
11	235.551	23.8000	II	0.0238	2.348	1.690	0.3363	0.3090	0.2950	0.2608	1910173
12	205.011	40.4209	II	0.0241	2.530	2.147	0.4732	0.4566	0.4466	0.2916	1385682
13	167.170	0.3917	II	0.0253	2.506	1.689	0.1278	0.1092	0.1055	-0.0304	0074451
14	163.003	50.8431	II	0.0260	1.242	2.349	0.5473	0.5371	0.5306	0.4748	0850618
15	210.011	15.9206	II	0.0261	3.330	1.441	0.1392	0.0827	0.0574	-0.0430	2371952
16	168.655	31.1285	II	0.0278	2.682	2.253	0.3730	0.3563	0.3558	0.3662	1947370
17	195.307	58.1123	II	0.0281	3.279	1.926	0.2426	0.2124	0.2024	0.3390	1201340
18	193.934	48.2873	II	0.0294	3.073	2.321	0.1905	0.1840	0.1868	0.3235	1208031
19	186.988	48.4036	II	0.0310	3.495	1.197	0.2665	0.2297	0.1994	0.1385	1172989
20	236.450	30.2024	II	0.0315	4.336	2.147	0.0581	0.0120	-0.0118	-0.0437	1402015
21	128.636	53.8591	II	0.0321	4.740	1.978	0.2239	0.1953	0.1947	0.1860	0259838
22	154.947	34.3241	II	0.0325	3.563	1.321	0.4254	0.3994	0.3815	0.5536	1891268
23	195.159	39.8310	II	0.0335	2.274	1.753	0.3975	0.3637	0.3498	0.2373	1837625
24	161.464	9.7226	II	0.0335	4.472	2.363	0.2938	0.2306	0.1995	0.0338	0946423
25	213.806	34.7420	II	0.0337	1.707	1.159	0.5588	0.5414	0.5259	0.4189	1462855
26	161.719	38.9609	II	0.0339	1.478	1.853	0.0802	0.0512	0.0233	-0.0482	1179057
27	233.516	2.2105	II	0.0342	1.923	1.473	0.4702	0.4428	0.4338	0.4613	0562585
28	183.094	8.7767	II	0.0345	3.529	1.913	0.1099	0.0557	0.0193	-0.1248	0936279
29	210.459	34.3585	II	0.0350	4.192	2.199	0.1603	0.1177	0.1014	0.1013	1862317
30	230.835	8.7228	II	0.0362	2.210	1.387	0.3505	0.3220	0.2958	0.1559	1260244
31	139.237	11.0410	II	0.0391	2.123	2.204	0.3611	0.3523	0.3456	0.2726	1130618
32	179.238	1.1159	II	0.0393	2.577	1.906	0.2321	0.2191	0.2052	0.2377	0084765
33	121.834	28.6389	II	0.0394	3.948	2.390	0.2005	0.1087	0.0696	0.0060	0879500
34	170.667	36.6336	II	0.0414	1.641	1.196	0.1752	0.1648	0.1623	-0.1444	1842658
35	200.645	31.5815	II	0.0417	3.179	1.485	0.2582	0.2255	0.2072	0.1222	1949876
36	187.803	46.9533	II	0.0422	2.444	2.067	0.5899	0.5975	0.5907	0.5608	1203340
37	161.413	20.7462	II	0.0425	2.462	1.980	0.2424	0.1908	0.1700	0.2766	2282430
38	180.738	20.6599	II	0.0427	3.367	2.166	0.0905	0.0493	0.0286	0.1910	2333088
39	233.307	15.0236	II	0.0429	5.324	1.972	0.1715	0.1164	0.0972	0.1140	2303806
40	235.245	12.4913	II	0.0431	2.351	1.385	0.1625	0.1364	0.1238	0.1678	2339646
41	150.915	0.3909	II	0.0445	3.196	1.678	0.1297	0.1211	0.1276	0.1540	0073856
42	222.904	18.9244	II	0.0447	2.944	2.179	0.5971	0.6712	0.6664	0.6512	2290422
43	138.045	15.9306	II	0.0451	2.887	2.179	0.2306	0.2096	0.1923	0.0447	2305660
44	198.795	7.0535	II	0.0454	4.149	1.219	0.1601	0.1100	0.0662	0.0901	1282795
45	119.188	35.5042	II	0.0456	2.556	2.215	0.5179	0.4864	0.4696	0.3341	0467001
46	191.437	11.4179	II	0.0457	4.396	1.543	0.1144	0.0944	0.0881	0.0579	0959359
47	235.803	8.7230	II	0.0461	3.209	1.447	0.6267	0.6022	0.5902	0.7535	1426428
48	163.324	7.1946	II	0.0462	2.735	1.882	0.2638	0.2350	0.2187	0.1062	0930531
49	239.250	20.1718	II	0.0462	3.324	1.397	0.4371	0.4082	0.4057	0.4054	1965658
50	159.289	23.0513	II	0.0466	1.871	2.237	0.4694	0.4683	0.4671	0.4552	2264442
51	243.352	27.5188	II	0.0470	4.051	1.433	0.0703	0.0249	-0.0034	-0.0840	1435251
52	238.252	53.0912	II	0.0470	3.096	1.719	0.1257	0.0859	0.0635	0.0335	0217026
53	173.052	53.3796	II	0.0470	1.829	1.815	0.1593	0.1168	0.0832	0.0422	0816688
54	174.957	16.9803	II	0.0472	6.288	1.884	0.3310	0.2838	0.2523	0.0655	2394353
55	167.479	8.3364	II	0.0478	3.036	1.712	0.2802	0.2232	0.1864	0.0107	0934855
56	144.102	19.5107	II	0.0478	4.384	1.671	0.0322	0.0106	0.0019	0.2302	2256598
57	200.169	31.3341	II	0.0483	2.803	1.267	0.0865	0.0917	0.0843	0.1486	1948158
58	135.112	17.4833	II	0.0489	3.985	1.832	0.2964	0.2394	0.2132	0.1135	2230667
59	143.677	38.9626	II	0.0490	1.488	2.086	0.2940	0.2805	0.2625	0.2988	1035605

Field sample 3 (continued)											
Index	RA. [deg]	DEC. [deg]	Type	z	R_e [kpc]	n	$(g-r)_{in}$	$(g-r)_{in,1}$	$(g-r)_{in,2}$	$(g-r)_{out}$	ID
60	199.344	7.3986	II	0.0495	4.588	1.864	0.0372	0.0124	0.0042	0.1261	1284407
61	135.573	33.6371	II	0.0504	2.529	1.532	0.2034	0.1687	0.1521	-0.0373	1881189
62	249.541	28.7561	II	0.0543	5.852	1.446	0.2426	0.2238	0.2054	0.1973	1415375
63	187.759	40.2167	II	0.0570	3.007	2.176	0.2867	0.2338	0.1959	-0.2567	1856592
64	241.911	34.9636	II	0.0532	3.758	1.726	0.2665	0.2286	0.2080	0.1406	1408363
65	221.547	11.8652	II	0.0576	3.254	1.137	0.1626	0.1309	0.1124	0.1760	1419924
66	245.087	22.5736	II	0.0518	4.515	2.207	0.2566	0.2282	0.2168	0.2905	1441236
67	247.893	23.1591	II	0.0600	3.019	1.137	0.2125	0.1922	0.1783	0.1566	1434128
68	182.286	13.4356	II	0.0576	3.191	2.030	0.2391	0.2011	0.1746	0.2180	1222572
69	198.476	44.8758	II	0.0612	2.766	1.446	0.7377	0.7097	0.6873	0.7129	1237159
70	159.091	45.4331	II	0.0542	3.721	1.208	0.3097	0.2909	0.2781	0.2577	1172414
71	200.596	45.4635	II	0.0573	4.153	1.202	0.0077	-0.0327	-0.0648	-0.2134	1202526
72	164.826	44.0562	II	0.0528	3.095	1.245	0.4650	0.4391	0.4148	0.3768	1250759
73	241.125	30.3671	II	0.0563	3.605	1.537	0.0782	0.0648	0.0549	0.1203	1393344
74	245.523	31.5513	II	0.0583	3.424	1.164	0.2585	0.2392	0.2273	0.3195	1406207
75	181.069	42.3233	II	0.0534	3.296	1.323	0.2504	0.2273	0.2106	0.1563	1295346
76	215.009	8.6334	II	0.0552	5.433	2.008	0.3747	0.3358	0.3115	0.2568	1337523
77	183.366	28.0399	II	0.0556	1.256	2.339	0.6822	0.6824	0.6827	0.7084	2227456
78	171.247	22.6977	II	0.0603	3.691	1.708	0.3997	0.3605	0.3433	0.3887	2288981
79	232.188	18.5012	II	0.0542	1.582	2.027	0.4263	0.4080	0.3795	0.0348	1988605
80	212.519	24.0831	II	0.0613	3.419	1.914	0.5168	0.4818	0.4660	0.6591	2004161
81	212.706	17.8798	II	0.0536	4.222	1.687	0.1604	0.1189	0.0967	-0.3102	2363656
82	243.221	51.7756	II	0.0615	3.573	1.394	0.2716	0.2215	0.1821	0.0667	2413503
83	178.396	25.4680	II	0.0587	3.080	1.513	0.2365	0.2179	0.2031	0.2282	2324633
84	179.939	21.6173	II	0.0579	3.831	1.456	0.3871	0.3679	0.3213	0.0422	2298008
85	219.244	19.7651	II	0.0603	3.582	2.047	0.2561	0.2299	0.2184	0.1690	2316493
86	193.643	35.6047	II	0.0592	2.954	1.248	0.1574	0.1381	0.1334	0.1377	1931254
87	225.385	25.6679	II	0.0618	6.018	1.431	0.1622	0.1288	0.1008	0.0819	1934196
88	227.502	27.2235	II	0.0592	4.450	0.811	0.2609	0.2398	0.2131	0.1823	1909914
89	201.350	36.8927	II	0.0543	3.485	1.643	0.3740	0.3490	0.3422	0.3666	1863604
90	143.687	28.7704	II	0.0556	1.375	2.225	0.3320	0.3132	0.2897	0.2541	1871951
91	232.342	21.6365	II	0.0605	4.451	1.911	0.3149	0.2737	0.2460	0.2754	1974252
92	210.387	27.7007	II	0.0616	1.035	2.287	0.5061	0.4994	0.4948	0.7600	1982598
93	196.761	29.8978	II	0.0550	4.267	2.461	0.3859	0.3432	0.3174	0.2828	1972999
94	222.052	25.7745	II	0.0521	2.261	1.709	0.3213	0.3087	0.2956	0.4645	1954492
95	223.084	26.2580	II	0.0518	6.805	1.439	0.2369	0.1994	0.1837	-0.0080	1955313
96	218.290	6.3868	II	0.0586	2.005	1.598	0.0856	0.0863	0.0899	0.0810	0600692
97	229.444	2.4789	II	0.0539	2.720	2.391	0.1818	0.2453	0.2700	0.2487	0274411
98	252.657	35.1001	II	0.0600	2.736	1.239	0.4225	0.4129	0.4055	0.2950	0548548
99	122.067	28.7196	II	0.0582	2.411	1.200	0.0288	0.0161	0.0041	0.0502	0885753
100	251.854	44.9956	II	0.0597	2.937	2.244	0.2960	0.2526	0.2441	0.1147	0262223
101	170.257	61.0231	II	0.0598	3.206	1.586	0.1453	0.1166	0.1039	0.2011	0376642
102	173.571	60.7499	II	0.0616	3.165	1.608	0.0047	-0.0067	-0.0062	0.0900	0376369
103	235.303	3.2832	II	0.0564	2.508	1.894	0.4229	0.4151	0.4126	0.6911	0306310
104	141.066	3.1775	II	0.0572	6.612	1.772	0.2936	0.2369	0.2029	0.0986	0454780
105	123.811	41.0983	II	0.0613	3.424	1.474	0.3642	0.3222	0.3004	0.1565	0473585
106	126.385	41.9593	II	0.0578	2.954	1.349	0.4733	0.4644	0.4562	0.3838	0470578
107	146.487	2.0515	II	0.0623	4.408	1.032	0.5626	0.5286	0.5009	0.4361	0284635
108	202.874	47.6953	II	0.0606	4.497	1.344	0.0066	-0.0225	-0.0379	0.0927	0889278
109	144.824	1.0902	II	0.0609	3.112	2.185	0.7634	0.7127	0.6864	0.8206	0083440
110	147.439	6.2971	II	0.0612	2.518	2.376	0.4399	0.4259	0.4180	0.3176	0930080
111	120.178	46.1499	II	0.0615	2.457	1.194	0.4051	0.3918	0.3850	0.3783	0228128
112	163.668	8.6136	II	0.0516	4.465	2.471	0.3814	0.3438	0.3487	0.4262	0937733
113	146.506	34.5920	II	0.0521	3.613	1.136	0.1074	0.0744	0.0559	-0.0597	1155357
114	250.716	33.6585	II	0.0608	4.716	1.261	0.2824	0.2537	0.2354	0.2850	0999974
115	233.149	49.3842	II	0.0521	2.139	1.409	0.4594	0.4239	0.3977	-0.0688	0991897
116	182.378	59.8175	II	0.0564	1.434	1.794	0.5286	0.5176	0.5033	0.7496	0921422
117	147.841	54.9680	II	0.0601	3.882	1.060	0.1459	0.1036	0.0855	-0.0307	0918996
118	149.133	4.8738	II	0.0583	3.207	0.984	0.4059	0.3933	0.3925	0.7908	0906410

Field sample 3 (continued)											
Index	RA. [deg]	DEC. [deg]	Type	z	R_e [kpc]	n	$(g-r)_{in}$	$(g-r)_{in,1}$	$(g-r)_{in,2}$	$(g-r)_{out}$	ID
119	224.239	61.8820	II	0.0470	3.346	1.414	0.2648	0.2225	0.2016	0.1018	0501596
120	249.617	45.4970	II	0.0583	4.020	1.560	0.3369	0.3003	0.2884	0.2636	0505042
121	189.959	3.7970	II	0.0400	3.468	1.277	0.0177	-0.0009	-0.0139	-0.0649	0520516
122	219.074	5.5152	II	0.0601	1.912	2.216	0.5861	0.5779	0.5707	0.5243	0597873
123	225.284	25.4488	II	0.0597	3.811	1.903	0.1554	0.1276	0.1083	0.1648	1933545
124	137.497	2.7335	II	0.0378	1.777	2.181	0.3386	0.3051	0.2786	0.2963	0444943
125	209.620	39.4498	II	0.0363	1.965	1.912	0.3644	0.3209	0.2957	0.2447	1385787
126	201.844	12.3547	III	0.0216	2.668	2.262	0.4818	0.4663	0.4686	0.4008	1262471
127	215.667	6.1670	III	0.0222	3.056	1.545	0.4625	0.4405	0.4138	0.3727	0599051
128	237.997	21.9344	III	0.0258	1.532	1.983	0.2376	0.2341	0.2347	0.2306	1967294
129	145.129	13.5419	III	0.0287	2.232	2.135	0.0741	0.0672	0.1048	0.1695	2500713
130	177.888	27.6691	III	0.0290	2.133	1.835	0.4977	0.4659	0.4531	0.4891	2238256
131	200.107	30.6030	III	0.0320	2.837	2.382	-0.0576	-0.0872	-0.1034	0.1648	1936718
132	162.000	30.6922	III	0.0330	1.401	2.226	0.3668	0.3511	0.3457	0.4199	1962188
133	225.146	53.9690	III	0.0337	3.690	2.013	0.5443	0.4915	0.4689	0.4001	0992845
134	169.516	31.1535	III	0.0344	2.072	1.699	0.1103	0.0830	0.0686	0.0998	1947398
135	235.583	19.7529	III	0.0368	2.961	2.049	0.5982	0.4989	0.3985	0.4096	1981111
136	227.690	1.3790	III	0.0382	2.738	1.450	0.4067	0.3884	0.3853	0.6194	0266681
137	142.273	12.9612	III	0.0390	2.170	1.552	0.7293	0.6440	0.5816	0.3602	2500636
138	211.477	53.2433	III	0.0410	2.710	2.003	0.4061	0.3640	0.3476	0.2029	1196957
139	179.688	30.9622	III	0.0419	1.142	2.421	0.2737	0.2873	0.3060	0.4052	2213247
140	126.198	25.2251	III	0.0438	1.046	2.454	0.3388	0.3316	0.3242	0.2021	1152428
141	155.981	8.2977	III	0.0451	1.577	2.439	0.5516	0.5834	0.5994	0.6011	1054695
142	181.818	4.8479	III	0.0451	2.123	2.282	0.5958	0.5731	0.5641	0.5525	0458739
143	233.433	23.5734	III	0.0462	5.219	1.764	0.3758	0.3160	0.3144	0.1572	1966649
144	193.991	8.6100	III	0.0470	4.546	2.029	0.2134	0.1567	0.1332	0.1185	1291490
145	236.909	25.2697	III	0.0477	1.606	2.061	0.2815	0.2500	0.2115	0.1112	1461514
146	156.889	10.3386	III	0.0482	1.880	0.973	0.7485	0.7332	0.7198	0.8454	1071841
147	238.453	24.8176	III	0.0486	2.151	1.145	0.1584	0.1342	0.1152	-0.0792	1892821
148	198.494	8.3338	III	0.0503	1.370	2.349	0.4300	0.4192	0.4055	0.2931	1287731
149	139.035	40.8719	III	0.0505	1.716	2.006	0.0219	0.0232	0.0287	0.3437	0840063
150	222.349	26.5548	III	0.0505	2.430	1.707	-0.0910	-0.1108	-0.1186	-0.1564	1955288
151	249.316	46.7694	III	0.0619	1.849	2.059	0.4790	0.4755	0.4690	0.2552	0261404
152	232.631	0.6914	III	0.0516	1.281	1.983	0.5844	0.5802	0.5772	0.7169	0081340
153	232.601	0.6067	III	0.0515	0.950	2.424	0.6673	0.6662	0.6651	0.8946	0053290
154	220.309	17.3922	III	0.0556	1.318	2.287	0.3327	0.3229	0.3079	0.2665	2295119
155	208.274	25.1770	III	0.0579	2.067	2.332	0.3994	0.3849	0.3766	0.2578	2005089
156	184.650	24.8163	III	0.0582	1.743	0.866	0.2291	0.2260	0.2234	0.3849	2246666
157	181.146	24.9071	III	0.0588	2.679	1.619	0.2233	0.2016	0.1902	0.3234	2246557
158	200.863	2.0344	III	0.0568	1.240	1.991	0.6433	0.6161	0.6061	-0.0693	0282861
159	216.411	17.2242	III	0.0512	2.552	2.361	0.3330	0.3054	0.2926	0.2471	2341214
160	203.563	24.0760	III	0.0596	2.613	1.765	0.2047	0.1614	0.1320	0.1175	2248043
161	186.391	31.0352	III	0.0603	1.524	2.268	0.5591	0.5621	0.5630	0.7513	1986647
162	148.935	5.3201	III	0.0597	3.051	1.791	0.2643	0.2559	0.2621	0.5913	0907926
163	180.855	6.8819	III	0.0575	1.590	1.536	0.6880	0.6559	0.6238	0.6761	0926533
164	179.384	53.0672	III	0.0513	2.108	1.682	0.4068	0.3747	0.3542	0.0851	0873335
165	215.951	12.4230	III	0.0533	2.546	0.877	0.1013	0.1151	0.1288	0.3092	1427138
166	248.986	26.4191	III	0.0575	3.672	1.610	0.3545	0.2942	0.2514	-0.1574	1215378
167	157.130	45.0353	III	0.0519	2.820	2.239	0.3264	0.2927	0.2703	0.1241	1172378
168	181.152	12.2765	III	0.0586	1.588	1.648	0.4053	0.3948	0.3820	0.3072	1258671
169	251.775	29.6551	III	0.0533	2.399	0.929	0.2456	0.2422	0.2395	0.2631	0981586
170	205.582	31.8390	III	0.0611	2.014	1.468	0.3482	0.3424	0.3355	0.2628	1953724
171	182.053	35.1848	III	0.0616	1.078	2.026	0.4465	0.4396	0.4320	-0.2291	1898888
172	120.994	38.7157	III	0.0612	2.035	2.263	0.6206	0.6140	0.6095	0.6165	0370241
173	166.770	4.5587	III	0.0604	1.538	2.361	0.5527	0.5465	0.5429	0.2800	0458266
174	204.215	39.1854	III	0.0616	2.068	2.413	0.6556	0.6578	0.6602	0.7570	1838640
175	224.847	29.2548	III	0.0621	1.743	2.499	0.5007	0.4935	0.4850	0.5480	1448583
176	252.908	40.3145	III	0.0529	2.295	1.164	0.2121	0.1974	0.1873	0.2113	0583576
177	172.463	57.1874	III	0.0583	1.065	2.243	0.4028	0.3990	0.3961	0.3260	0837841

Table C5: Listing of scale lengths and break radii (each in both observed bands) of all 175 galaxies in the total cluster sample.

Total cluster sample													
Index	$h_{1,g}$ [kpc]	$h_{2,g}$ [kpc]	$R_{b,g}$ [kpc]	$h_{1,r}$ [kpc]	$h_{2,r}$ [kpc]	$R_{b,r}$ [kpc]	Index	$h_{1,g}$ [kpc]	$h_{2,g}$ [kpc]	$R_{b,g}$ [kpc]	$h_{1,r}$ [kpc]	$h_{2,r}$ [kpc]	$R_{b,r}$ [kpc]
1	1.522	-	-	1.5918	-	-	60	3.4941	1.7323	5.5227	4.4538	1.5988	5.5023
2	2.0167	-	-	1.9513	-	-	61	3.6215	1.4766	4.0947	4.5632	1.0642	4.5005
3	2.6589	-	-	2.6359	-	-	62	4.388	2.1286	12.5354	3.8861	2.2727	13.0663
4	2.0807	-	-	2.0176	-	-	63	5.7654	0.9924	9.7619	7.5603	1.2364	8.0308
5	0.8817	-	-	0.9899	-	-	64	2.7129	1.4876	6.3109	2.5075	1.4646	7.2546
6	1.5949	-	-	1.5711	-	-	65	1.6738	1.4561	3.8234	1.5957	1.3666	4.1149
7	1.3468	-	-	1.5375	-	-	66	2.4794	1.4395	7.886	2.1425	1.3431	8.5826
8	1.4644	-	-	1.5498	-	-	67	2.0255	1.3299	6.4577	2.0439	1.6679	6.9296
9	1.2627	-	-	1.2195	-	-	68	2.3053	0.9931	3.8529	2.0732	0.9993	4.0376
10	2.1077	-	-	2.1537	-	-	69	5.1139	3.0313	6.6433	3.4838	2.7794	6.9018
11	2.3965	-	-	2.4283	-	-	70	4.5662	1.0543	7.9899	3.0343	1.2448	7.6351
12	0.9474	-	-	0.8704	-	-	71	1.5073	1.004	5.1974	1.4614	1.0196	6.1758
13	1.2198	-	-	1.4278	-	-	72	5.3745	2.968	5.8357	2.8651	2.5689	6.622
14	1.3289	-	-	1.308	-	-	73	6.6623	1.2307	2.9921	6.7309	1.2954	3.8966
15	1.9159	-	-	1.9748	-	-	74	2.0376	1.6034	5.2323	2.2034	1.6309	4.9747
16	1.7552	-	-	2.959	-	-	75	4.7311	0.7825	5.9672	3.7229	0.8213	5.9063
17	1.536	-	-	1.1712	-	-	76	4.0661	1.7435	11.9589	3.8505	2.5619	9.9808
18	3.023	-	-	2.64	-	-	77	2.3956	1.5031	7.9041	2.3465	1.7127	7.7353
19	1.8267	-	-	1.6875	-	-	78	5.2716	1.5053	3.2079	3.7567	1.5161	3.3458
20	0.938	-	-	0.9124	-	-	79	6.0103	2.808	4.2927	4.4783	2.6339	4.5261
21	1.6652	-	-	1.6642	-	-	80	1.7435	1.5937	5.8088	2.0055	1.7557	6.3867
22	1.5532	-	-	1.5499	-	-	81	1.9325	0.7038	6.8679	1.9368	0.7991	7.6883
23	1.4562	-	-	1.4231	-	-	82	3.5003	0.8204	4.2825	2.9917	0.9901	4.3543
24	1.7965	-	-	1.77	-	-	83	2.352	1.7213	7.2762	2.5774	2.0656	6.9132
25	1.5338	-	-	1.4064	-	-	84	2.7552	1.1995	5.8697	2.7467	1.4596	5.9861
26	1.1687	-	-	1.2009	-	-	85	1.4413	0.9858	3.6636	1.5058	1.3428	3.8811
27	1.8139	-	-	1.8223	-	-	86	2.7218	1.5505	4.9231	2.8281	1.2473	5.3225
28	1.7338	1.1596	3.3177	1.7053	1.1654	3.2213	87	2.3004	0.8105	9.1868	2.2227	1.2116	8.2452
29	1.7966	1.2403	3.3853	1.6445	1.13	4.8211	88	5.9786	1.8823	3.8943	2.1928	1.569	4.1016
30	3.3111	1.0425	0.7724	5.6793	1.3376	6.7927	89	2.4274	1.6012	3.6448	1.8045	1.4237	4.7603
31	1.894	1.1662	8.6404	1.8204	1.1029	8.5642	90	2.3337	1.4731	9.9162	2.218	2.2038	9.1586
32	2.0862	1.0963	3.4985	2.1078	1.0866	3.3975	91	2.7682	2.0564	7.7557	2.682	2.1413	8.2551
33	2.7587	0.7294	3.2836	3.401	0.6891	3.5749	92	1.6724	1.0834	4.348	1.7286	1.097	3.9238
34	3.4924	1.6753	3.5564	2.5046	1.681	3.7225	93	5.4532	1.762	4.7109	3.7247	1.7416	4.8829
35	2.2586	1.1683	9.2225	2.0686	1.1683	7.9011	94	3.1176	1.4179	4.1097	2.8599	1.3285	4.3171
36	1.7269	1.1499	4.3859	1.6494	1.1868	4.2787	95	3.5676	2.0999	7.879	3.0013	1.8556	8.216
37	2.7822	1.5143	5.2134	2.9785	1.5999	5.3052	96	1.2351	0.8962	4.0893	1.1786	0.9988	4.3624
38	4.5017	1.1627	6.3142	3.4627	1.5256	6.1402	97	2.4063	1.3712	9.068	2.4481	1.8386	8.4743
39	2.1802	1.1937	3.6844	6.3718	1.0178	3.4441	98	3.2579	0.681	7.8985	3.8474	1.2024	7.3687
40	3.3047	1.5214	4.3286	3.1387	1.9156	4.1729	99	3.005	1.574	4.3308	2.5699	1.0025	5.9189
41	7.8624	1.2194	15.9655	8.0812	1.3184	16.3532	100	2.4169	1.1431	5.972	2.3095	1.2063	6.1676
42	1.7023	1.3882	5.6485	1.426	1.2536	5.883	101	2.9543	2.0294	6.671	2.6401	2.0453	6.6089
43	1.117	0.9406	4.0898	1.0898	0.3756	5.3654	102	2.4372	1.3247	6.5812	2.3261	1.4282	6.5694
44	4.081	2.3886	4.8594	3.3291	2.0596	5.7175	103	1.741	1.1553	6.7267	1.8691	1.3334	5.9469
45	4.0013	2.0128	5.7913	4.2929	2.1055	4.7555	104	3.302	1.1453	2.8453	2.4518	1.2084	2.8507
46	1.8416	1.0572	4.2276	1.8159	0.9604	5.431	105	4.0199	1.3539	4.6917	2.8573	1.3882	4.6025
47	2.513	1.3059	7.0126	2.2237	1.598	7.2913	106	2.5617	1.1061	6.4904	2.9372	1.3537	5.9363
48	1.4772	1.118	3.8059	1.7354	1.037	2.226	107	6.691	1.9963	4.9935	6.7603	1.863	4.8464
49	2.7396	1.3478	8.7685	2.7442	1.7774	8.8085	108	1.7431	1.0964	6.5008	1.4183	0.9755	6.8142
50	1.3844	1.0034	4.052	1.3141	1.0963	3.7324	109	4.5437	2.5737	4.5938	3.448	2.5526	5.3192
51	5.8698	2.4958	3.6026	5.2432	2.5036	3.3859	110	5.3088	1.7885	4.5499	2.9667	1.4545	5.43
52	2.9191	0.8128	5.499	1.7206	1.1597	7.0799	111	2.7831	1.4593	4.4984	1.9148	1.2259	6.0058
53	2.2828	1.6248	8.2208	3.3066	0.9099	9.3912	112	2.6415	0.9533	4.3063	3.6957	0.6421	6.6195
54	4.3544	3.1759	5.2369	3.4841	2.9801	6.1344	113	6.2271	0.984	7.0595	5.3025	1.3729	6.2433
55	3.37	1.6083	4.296	3.7061	1.7666	4.1772	114	1.6938	1.425	3.9442	2.2407	1.5647	3.2576
56	5.685	2.4359	6.5611	4.7155	1.4882	7.8017	115	2.4308	1.934	5.4556	2.4085	1.988	5.7249
57	1.4465	0.7573	6.9081	1.5763	0.7596	6.9118	116	1.7949	0.9159	4.7668	2.0241	1.0208	4.5655
58	2.4	1.3645	3.3502	2.7262	0.9532	5.2007	117	2.0301	1.3175	6.2414	1.7291	1.3685	5.4225
59	3.758	2.0997	4.16	2.7896	1.9348	4.2901	118	2.8646	1.7188	7.8046	2.8302	2.0966	6.5484

Total cluster sample (continued)													
Index	$h_{1,g}$ [kpc]	$h_{2,g}$ [kpc]	$R_{b,g}$ [kpc]	$h_{1,r}$ [kpc]	$h_{2,r}$ [kpc]	$R_{b,r}$ [kpc]	Index	$h_{1,g}$ [kpc]	$h_{2,g}$ [kpc]	$R_{b,g}$ [kpc]	$h_{1,r}$ [kpc]	$h_{2,r}$ [kpc]	$R_{b,r}$ [kpc]
119	4.7734	1.4565	2.7753	2.912	1.4069	3.1332	148	1.2165	1.5618	5.0213	1.2598	1.5259	5.8237
120	4.8657	2.1717	4.2166	3.5741	2.0416	4.8791	149	1.659	2.8103	4.0826	1.3541	2.6561	3.649
121	1.1803	1.1027	4.1682	1.238	0.9634	4.2718	150	0.8279	0.9781	2.4463	0.8465	1.0728	2.7055
122	1.6898	0.3969	6.5095	1.6462	0.7345	5.9498	151	1.1643	2.5775	3.5959	1.0886	2.422	3.4859
123	6.9686	2.0607	4.2102	3.6438	2.1453	4.8422	152	1.0131	4.4978	4.7638	1.0525	2.5445	4.5075
124	3.9757	1.9421	4.0793	3.7169	1.6926	4.4485	153	1.2676	1.843	3.0934	1.3667	1.9938	3.4588
125	2.3356	0.9409	6.7479	2.5315	1.291	6.3732	154	0.9711	1.6805	2.892	1.2349	1.603	3.3508
126	2.5142	4.9385	8.3953	1.9264	2.8502	6.3964	155	1.1228	2.0513	5.9585	1.0915	1.9971	5.9921
127	1.5374	2.2069	4.9225	1.5327	2.3104	5.2071	156	1.3018	2.0405	4.5647	1.2517	4.5112	6.3426
128	1.8816	2.1954	4.1983	1.7278	2.0564	4.1049	157	1.3873	3.2207	5.6189	1.6423	3.1708	6.5405
129	1.3732	1.8016	4.0165	1.2033	3.5085	6.6103	158	1.4049	1.8715	5.1074	1.4334	1.7294	4.5287
130	1.107	2.2661	5.3953	1.3687	3.1886	7.679	159	2.0312	2.73	8.2589	1.494	3.2332	7.6733
131	1.9703	2.0702	2.4821	2.0259	2.4574	6.0617	160	0.8862	2.727	4.5978	0.7611	2.4212	3.9678
132	1.8621	2.3198	4.4509	1.8867	2.3403	5.4582	161	1.1099	1.5341	4.5374	1.0691	1.3926	4.2803
133	2.0913	2.9629	6.0767	1.8333	3.1633	5.9302	162	1.0644	2.5265	5.1918	1.1155	2.003	5.4171
134	1.2443	2.3728	6.2509	1.0563	2.1394	4.9863	163	1.3776	2.6142	4.8305	1.5104	1.9971	4.7656
135	1.9331	2.1961	6.8071	1.8295	1.9471	5.1051	164	0.8891	2.2446	3.1546	1.1752	1.4085	3.4198
136	0.6528	1.4129	3.7634	0.6951	1.4548	4.5828	165	1.2136	1.5273	4.2805	1.2023	1.5423	3.8331
137	1.4528	1.9834	5.2213	1.3872	1.8547	5.4466	166	1.5743	2.1344	5.8982	1.3983	1.707	5.6883
138	1.4271	2.203	4.5173	1.0344	2.4597	4.2132	167	2.3537	4.9324	9.4625	2.0988	5.2788	9.3047
139	1.0421	1.6438	3.0577	1.0496	1.7996	2.8289	168	1.15	2.0088	4.8079	1.0494	2.013	3.4016
140	0.5018	1.0622	1.4919	0.4373	1.1335	1.2505	169	1.3496	1.9488	4.5051	1.2196	2.0585	4.1323
141	2.3342	2.6954	10.0127	2.306	2.7374	10.0537	170	1.4997	2.1581	5.2905	1.5823	2.6414	6.0413
142	1.1589	1.9459	4.4051	1.2581	2.0902	4.7061	171	1.705	3.5407	4.3508	1.8801	3.0553	4.1961
143	0.6567	1.1763	1.9712	0.9333	1.794	2.8879	172	1.4401	2.2633	7.8491	1.4371	2.0464	7.2279
144	1.4615	2.102	4.33	1.4813	2.1266	5.0924	173	1.735	2.8494	5.4133	1.9549	2.4804	4.4541
145	1.6157	1.925	5.3028	1.6348	2.4452	6.1933	174	1.3605	1.9864	5.1002	1.373	2.1131	4.5861
146	0.945	1.6659	2.9683	0.6881	1.6947	1.9246	175	2.287	2.7899	4.1494	2.0411	2.802	3.9784
147	2.353	3.0923	7.9161	2.1285	2.307	7.9714							

Table C6: Listing of scale lengths and break radii (each in both observed bands) of all 172 galaxies in field sample 1.

Field sample 1													
Index	$h_{1,g}$ [kpc]	$h_{2,g}$ [kpc]	$R_{b,g}$ [kpc]	$h_{1,r}$ [kpc]	$h_{2,r}$ [kpc]	$R_{b,r}$ [kpc]	Index	$h_{1,g}$ [kpc]	$h_{2,g}$ [kpc]	$R_{b,g}$ [kpc]	$h_{1,r}$ [kpc]	$h_{2,r}$ [kpc]	$R_{b,r}$ [kpc]
1	0.8365	-	-	0.8815	-	-	29	2.4166	0.8585	4.1297	2.4313	0.8964	4.4879
2	2.0981	-	-	2.2205	-	-	30	1.9146	1.4031	7.4893	2.157	1.3332	8.1887
3	1.434	-	-	1.6664	-	-	31	3.1575	1.5007	6.2759	2.9816	1.3807	5.8988
4	1.4207	-	-	1.4155	-	-	32	1.0236	0.2849	5.4294	1.7018	0.6525	3.9984
5	0.8399	-	-	0.875	-	-	33	3.1062	1.4664	5.5548	2.2586	1.213	7.4191
6	1.2666	-	-	1.2842	-	-	34	7.1386	2.2428	2.8353	3.7074	2.1943	2.8787
7	2.0432	-	-	1.9652	-	-	35	1.4363	0.7135	5.7625	1.6535	0.589	5.1553
8	1.5433	-	-	1.5462	-	-	36	6.0868	2.5558	5.9002	5.6275	2.3734	6.6061
9	1.2979	-	-	1.219	-	-	37	6.501	2.688	7.8126	4.9843	2.206	8.8937
10	1.6472	-	-	1.6607	-	-	38	2.6719	1.6178	5.2446	2.5477	1.4953	5.7726
11	1.5911	1.2555	6.8998	2.0433	0.87	6.2584	39	2.7396	1.5113	4.1501	2.7849	1.67	4.0898
12	7.7058	1.2721	2.2904	3.4224	1.3461	2.5801	40	1.5446	1.249	3.3823	1.9051	1.0158	5.6323
13	2.7531	1.4279	2.8787	2.4172	1.3955	2.7201	41	1.714	1.4443	3.5853	2.2272	1.4115	3.0327
14	2.6569	1.9683	5.6215	2.6479	1.9742	5.8375	42	2.0141	1.1759	5.8017	2.0769	1.3438	7.1687
15	3.2874	1.402	5.111	2.9363	1.2156	6.0711	43	3.0396	2.0074	9.3753	3.2968	2.0189	9.5612
16	2.1736	1.7581	7.5338	2.3001	1.817	7.584	44	0.8455	0.5293	3.6859	1.1103	0.609	3.7527
17	4.6929	3.9036	10.1017	4.9882	3.7648	9.8683	45	1.8268	0.8761	1.4949	1.7261	1.0257	1.4821
18	1.5756	1.2488	3.4944	1.7519	1.2262	3.3829	46	1.3241	0.8099	4.7762	1.4257	0.8435	4.3227
19	2.0989	1.3657	6.2277	1.9814	1.3335	7.079	47	4.1238	2.0526	9.3761	4.2982	1.7483	9.5314
20	2.0035	0.8503	7.7434	2.0603	1.4122	7.9809	48	5.4364	0.9684	5.7709	3.8787	0.9061	6.2256
21	2.5828	1.1727	8.6398	3.0844	1.2761	8.3604	49	2.6438	1.7381	4.4219	2.8208	1.5479	5.3355
22	2.0745	1.2491	1.6164	1.5769	1.1448	4.0008	50	3.9999	1.4502	4.3226	2.9938	1.3675	4.8487
23	2.1753	1.538	6.2512	2.4657	1.4323	6.7827	51	1.8103	1.0135	1.6456	1.5901	0.8714	1.7663
24	3.0125	0.9925	6.8915	2.5929	1.4239	6.5159	52	3.0579	1.5158	4.2436	2.8068	1.4992	4.5604
25	1.1611	0.9357	3.8499	1.2289	0.8387	4.6381	53	1.2142	0.775	5.8025	1.5483	0.7584	5.9427
26	1.5198	1.2177	2.8391	1.5404	1.1808	2.9314	54	3.2063	1.0877	1.8829	2.3412	1.0477	2.2048
27	3.6229	2.2915	7.0063	3.3779	1.9215	7.9979	55	5.8737	2.5421	8.4105	4.8937	2.4327	9.0201
28	7.566	2.2145	4.8287	7.6027	2.2393	5.6202	56	2.3151	1.0484	5.6379	2.841	1.0535	5.6321

Field sample 1 (continued)													
Index	$h_{1,g}$ [kpc]	$h_{2,g}$ [kpc]	$R_{b,g}$ [kpc]	$h_{1,r}$ [kpc]	$h_{2,r}$ [kpc]	$R_{b,r}$ [kpc]	Index	$h_{1,g}$ [kpc]	$h_{2,g}$ [kpc]	$R_{b,g}$ [kpc]	$h_{1,r}$ [kpc]	$h_{2,r}$ [kpc]	$R_{b,r}$ [kpc]
57	1.9983	0.7781	2.7765	1.6055	1.0027	2.7766	115	2.2146	1.4492	6.4415	2.4739	1.3608	7.1646
58	4.1316	1.3267	4.1026	4.5374	1.3233	3.9627	116	6.3023	1.9008	4.9987	4.7875	2.0203	5.0497
59	1.8094	0.9097	3.6256	1.9821	0.998	3.7139	117	1.686	1.2626	4.8524	1.8433	1.3158	5.0365
60	2.8628	1.6007	7.3947	3.3724	1.7701	7.2711	118	2.8235	2.0992	2.9484	2.6263	1.9455	3.3173
61	1.6009	1.1951	3.8489	1.771	1.1583	4.692	119	3.5053	1.6007	8.3146	3.5308	1.8005	8.2778
62	2.2575	1.431	8.0282	2.6397	1.6434	5.8147	120	6.2659	2.8553	10.7615	6.7094	3.0087	10.8852
63	3.341	2.3929	9.012	3.0496	1.7691	8.7865	121	2.5226	1.3664	7.1803	2.6888	1.475	7.1276
64	3.3358	1.206	2.1044	2.5349	1.2861	2.1227	122	2.2125	0.9154	8.7313	2.2604	0.4487	8.8698
65	2.7441	1.9319	6.9578	2.8411	1.784	7.0946	123	3.1853	1.4042	6.7215	2.7889	1.3434	6.8442
66	2.9143	1.1519	3.5905	3.0512	1.2712	3.5487	124	5.6642	2.4464	8.9612	4.6585	2.3315	7.87
67	1.3383	1.0633	4.7359	1.4303	0.9994	4.7537	125	3.2585	1.8661	8.145	4.2023	2.4788	6.873
68	2.7747	1.9783	4.3989	3.3463	1.8873	3.3527	126	2.2174	2.5204	7.1477	1.9268	2.8524	6.0104
69	4.4014	2.1229	3.4116	3.1741	1.8833	4.4377	127	0.5397	1.0569	4.2101	0.8503	1.3591	4.0232
70	5.0924	1.125	4.7936	4.0338	1.223	4.8202	128	2.7764	2.9712	8.2833	2.5982	3.3535	7.908
71	0.9093	0.5989	3.6713	1.0608	0.5939	4.4854	129	2.0281	3.2308	9.1083	1.9996	3.1711	8.3994
72	2.1513	0.6808	6.9039	2.2092	0.7029	6.9959	130	1.831	2.2579	7.2746	1.7956	2.5568	6.9255
73	2.9697	0.9831	4.6377	2.8043	1.0767	4.6895	131	0.5961	1.0419	1.6303	0.7227	1.0461	3.0156
74	2.5537	0.6605	8.0521	2.6295	0.8615	7.8909	132	3.076	3.7274	13.0094	3.1074	3.948	12.7274
75	5.4537	2.2405	5.5825	4.1776	2.371	5.8133	133	3.1905	4.4061	6.6499	2.7476	4.7071	6.4758
76	1.9882	0.7258	6.4782	2.2257	0.805	6.5557	134	2.0093	2.6665	3.3713	1.8599	2.5729	3.4928
77	5.0044	1.0464	3.6063	1.9609	1.0884	3.3361	135	0.8691	1.0202	1.871	0.7241	1.2075	1.1597
78	0.8983	0.6278	4.5032	1.1532	0.3888	4.7117	136	1.4672	1.7905	6.3773	1.5556	2.0101	6.7403
79	4.3903	2.2718	6.5655	3.6878	1.6352	8.5917	137	1.6603	1.7588	5.8675	1.4831	1.8639	5.2938
80	5.1456	2.9273	6.2676	4.256	2.5846	7.1583	138	0.6046	1.1238	0.8157	0.6184	1.3322	0.8156
81	3.3297	0.9371	14.2013	3.4682	1.0424	14.7411	139	1.3878	1.4902	3.6751	1.3885	1.6162	3.3728
82	1.8989	1.3322	1.8284	1.8331	1.285	2.7074	140	1.4972	2.8253	3.8391	1.5256	3.4344	3.9604
83	5.7558	2.1009	8.2047	5.1624	1.8873	8.6357	141	0.6573	0.717	2.0597	0.6587	0.9179	2.7043
84	3.7778	2.4464	7.3412	3.7171	2.2282	7.7158	142	1.2643	1.8185	3.0225	0.867	1.5996	1.0678
85	2.0754	1.467	3.6064	2.1761	1.4628	3.4393	143	1.4102	1.9422	4.0558	1.381	2.3813	5.0938
86	4.1405	0.6743	2.414	4.0779	0.7176	2.5134	144	1.1168	1.4463	3.7727	1.1802	1.5373	3.1934
87	3.9183	1.5823	2.9882	3.9894	1.5436	3.7167	145	1.7892	2.5188	9.5608	1.9633	2.2777	9.6021
88	3.2875	1.3368	5.7058	3.3781	1.2968	5.8852	146	0.8633	1.0899	2.3507	0.7273	1.3301	2.0031
89	1.9769	0.8703	3.4099	1.9094	0.9837	2.2334	147	1.1854	2.04	6.1521	1.3642	2.2631	5.6977
90	2.1442	0.7883	2.6143	1.8613	0.7488	2.679	148	1.0426	1.5412	4.1876	1.0898	1.7865	5.4537
91	2.6188	2.0328	7.9924	2.6167	2.1067	7.7473	149	2.6517	3.4367	8.8391	2.6375	3.4969	7.4422
92	1.6113	1.0747	4.9983	1.83	1.0756	5.706	150	1.0649	1.6328	2.6986	1.0568	1.5991	2.9038
93	2.8451	0.693	1.6286	3.3726	0.7865	1.5715	151	2.1807	2.5454	7.5147	2.2242	2.5655	7.9768
94	1.4042	0.6559	6.4752	1.7247	0.522	6.4358	152	1.8275	2.0512	6.9211	1.1652	2.0555	6.8605
95	4.4788	2.8108	4.5556	3.6741	2.7825	5.22	153	1.7383	2.7316	7.4741	1.6727	3.3112	6.0859
96	2.6899	1.9405	6.9105	2.072	1.6372	7.6471	154	0.8422	1.0582	2.5537	0.802	1.1922	2.4062
97	3.6514	0.9475	3.4374	3.0966	0.7913	3.9701	155	0.9065	1.4332	4.6682	0.9709	1.323	4.4191
98	5.9288	1.1829	1.4644	3.1965	1.2888	1.577	156	1.694	2.3626	9.547	2.0871	2.4613	10.1695
99	2.3476	1.2172	3.6771	2.7151	1.2737	3.3505	157	1.5315	1.8655	5.5484	1.3939	1.804	6.0223
100	6.0314	2.2894	4.7313	4.8635	2.4294	4.2276	158	1.4346	2.6957	4.0778	1.3214	2.5805	3.533
101	1.8476	1.0455	6.1179	2.1221	1.3023	6.0222	159	0.8032	1.5976	6.682	0.853	1.7975	7.4124
102	3.4984	1.0789	7.4124	3.1798	0.9883	7.801	160	1.0971	1.639	7.6968	1.3317	1.8407	7.5835
103	3.9594	1.974	8.8045	3.889	1.9526	9.0113	161	2.2777	2.9568	7.3407	2.0478	2.66	6.7859
104	1.8614	1.4021	6.1496	2.1727	1.4739	7.2189	162	0.721	1.2757	1.6954	0.8458	1.5538	1.7487
105	6.3361	2.7139	5.6001	5.3526	2.334	5.604	163	1.7718	1.8012	7.5718	1.6572	2.1646	6.9443
106	1.7934	1.143	1.9509	1.7142	1.2148	4.4115	164	0.6622	0.8382	2.3112	0.607	1.1983	2.4405
107	5.9742	2.0652	3.6784	5.2793	2.2067	3.8515	165	1.1351	1.2326	3.6716	1.1669	1.4199	3.7831
108	3.3922	1.0768	6.3048	3.9507	1.1068	6.5459	166	0.8923	1.0589	3.1067	0.7404	1.5201	4.4515
109	2.3902	1.1635	2.9897	2.354	1.2101	3.0556	167	0.6668	0.816	4.358	0.6605	1.2031	3.9111
110	1.8533	1.4656	6.825	1.8935	1.1388	6.9713	168	0.9682	1.5132	2.4571	1.1032	1.7392	2.9759
111	4.2967	1.7869	5.9591	3.9638	1.6136	6.3522	169	0.8244	2.6245	4.3452	1.334	1.8129	5.3266
112	4.424	0.5858	3.3725	3.1807	0.6211	3.4568	170	0.893	1.9811	2.7686	0.8305	2.0317	2.7879
113	3.733	1.1599	2.7581	4.2899	1.3385	2.5092	171	2.287	3.7327	9.4455	2.5419	3.1907	9.5267
114	3.3954	1.4098	7.816	3.1692	1.3968	8.029	172	1.5142	4.2094	2.6132	1.5716	2.9517	2.9538

Table C7: Listing of scale lengths and break radii (each in both observed bands) of all 172 galaxies in field sample 2.

Field sample 2													
Index	$h_{1,g}$ [kpc]	$h_{2,g}$ [kpc]	$R_{b,g}$ [kpc]	$h_{1,r}$ [kpc]	$h_{2,r}$ [kpc]	$R_{b,r}$ [kpc]	Index	$h_{1,g}$ [kpc]	$h_{2,g}$ [kpc]	$R_{b,g}$ [kpc]	$h_{1,r}$ [kpc]	$h_{2,r}$ [kpc]	$R_{b,r}$ [kpc]
1	1.4816	-	-	1.5247	-	-	60	5.5352	2.5674	4.9389	3.4597	1.9148	7.835
2	1.2405	-	-	1.2534	-	-	61	2.3655	1.6031	2.7878	2.6825	1.4852	2.6287
3	1.465	-	-	1.3931	-	-	62	3.6894	1.528	4.1191	3.0415	1.3483	3.9019
4	1.784	-	-	1.7463	-	-	63	2.2893	1.1203	2.6989	2.3261	0.9516	2.6178
5	1.016	-	-	0.9875	-	-	64	3.1491	1.8965	4.8273	2.7258	1.8116	4.9298
6	1.4178	-	-	1.2459	-	-	65	6.5358	1.6226	4.9278	7.1301	1.5602	4.3853
7	1.8705	-	-	1.9736	-	-	66	5.1668	1.8912	4.084	3.8691	1.7375	4.0116
8	1.6404	-	-	1.4697	-	-	67	3.7002	1.728	1.8312	2.5211	1.537	1.9796
9	2.2679	-	-	2.2073	-	-	68	3.2557	1.4783	6.8994	2.7927	1.1091	7.4889
10	0.8343	-	-	0.8303	-	-	69	4.6114	1.6802	4.2057	2.92	1.4671	4.8378
11	3.7989	1.7597	4.171	3.3766	1.5532	4.5196	70	1.6695	1.3293	2.2124	3.6593	1.1962	1.02
12	2.9522	1.4216	6.0495	3.1685	1.2643	4.8864	71	1.3033	1.1038	5.7149	1.2736	0.6552	6.1568
13	3.9559	1.0102	4.4482	4.595	0.8112	4.0299	72	4.2392	1.9299	5.1798	3.987	2.1189	3.8718
14	2.5302	1.7333	7.4139	2.3374	1.7125	9.2721	73	4.1044	1.4945	7.8523	3.429	1.1978	8.018
15	3.7028	1.4919	3.1764	2.8719	1.3855	3.235	74	2.7653	1.053	3.855	2.0996	0.6763	3.8621
16	3.3714	1.8897	6.8996	3.3806	1.8001	6.8575	75	1.8022	1.1751	3.9721	1.9054	1.0415	3.8207
17	2.3424	2.035	3.1182	2.4864	1.8932	2.7918	76	3.0663	1.4561	4.5528	2.0252	0.9326	6.0194
18	3.0398	2.7852	6.4614	2.84	2.1509	7.8949	77	2.8468	1.2637	7.8798	2.5175	1.4697	7.0076
19	6.801	1.1898	4.2891	6.2703	1.0401	5.0114	78	5.3513	2.8269	5.8828	4.6341	2.3499	5.6975
20	1.3962	1.1192	2.8212	1.2478	0.7864	3.3304	79	4.5695	2.3634	8.3999	4.0874	2.0693	8.9109
21	1.8974	1.1884	5.5702	1.9175	0.9476	5.4689	80	4.9491	2.406	3.1408	3.1758	1.9797	3.1444
22	3.6256	2.4017	8.0491	3.3412	2.233	8.2626	81	2.5067	1.9832	9.636	2.4352	1.3704	9.2704
23	3.0149	1.2204	2.866	2.9582	1.0751	2.8511	82	2.8348	0.6599	6.758	2.5217	0.3923	6.6164
24	2.461	1.9389	7.1924	2.755	1.5553	6.5348	83	4.0922	1.8855	4.6901	4.6715	1.849	3.7327
25	4.2622	3.4293	6.7932	5.6738	3.4297	5.1809	84	3.8373	2.2103	5.2457	6.2178	2.1861	4.0675
26	2.4369	1.3555	5.6904	2.1391	1.1814	5.95	85	5.7036	1.8915	4.1906	3.7788	1.5683	4.3879
27	1.8611	1.6101	4.72	1.9299	1.2932	4.8835	86	2.0257	1.4711	4.5693	2.009	1.28	4.6863
28	3.9998	2.029	4.8279	2.7683	1.5691	6.9994	87	3.0327	1.1956	4.007	3.0261	1.0135	3.7365
29	3.3243	1.1332	5.5594	2.8839	0.9991	5.5553	88	6.9978	1.7932	2.1223	6.4326	1.643	2.0209
30	2.9892	1.5785	3.9911	2.5416	1.3138	4.8394	89	1.7428	1.203	4.1665	3.0385	0.8798	3.873
31	4.1337	1.9743	6.3926	3.5128	1.6399	6.8068	90	4.1398	1.5189	5.933	3.921	1.3708	5.5759
32	2.1936	1.574	7.8119	2.4547	1.3153	6.4625	91	2.0109	1.2669	7.5189	2.0304	1.1325	7.2609
33	5.0034	3.2714	6.8777	5.7733	2.9283	5.5345	92	2.3532	1.2165	4.6217	2.5618	1.2188	3.9279
34	4.9468	1.6759	8.3475	4.6541	1.3039	8.6791	93	4.3242	1.3675	2.8254	3.3312	1.1297	3.8946
35	1.7744	1.1521	6.5274	1.8662	0.9852	6.8907	94	2.7807	1.7951	4.5888	2.3297	1.3671	5.1116
36	1.4479	1.104	5.0223	1.398	0.8596	4.3868	95	4.7517	1.4614	3.6611	3.7924	1.2561	3.5642
37	2.0109	1.5218	5.2997	1.9152	1.3778	4.8773	96	2.7532	2.2733	4.2399	2.4337	1.5437	6.9071
38	6.2883	2.0494	6.7709	3.26	1.8826	7.864	97	3.9822	1.3092	2.9942	3.4541	1.3208	2.7035
39	2.6162	1.5925	9.1419	2.3523	1.3246	10.303	98	2.6443	1.1379	5.7943	2.1547	1.0043	5.5102
40	5.5679	2.6727	6.3658	4.2281	2.5163	6.7008	99	2.431	1.5885	5.0496	2.267	1.5326	4.6991
41	3.5672	1.9478	5.5737	3.1285	1.6636	5.5749	100	2.3061	1.6288	6.2122	2.3685	1.4124	6.118
42	4.1264	1.0274	0.8531	1.023	0.6159	4.7327	101	4.4152	2.5554	6.1078	3.5911	1.9829	7.0997
43	7.1129	1.5626	8.9907	5.6038	1.4788	9.2589	102	2.0667	1.6628	6.9909	2.1874	1.5142	4.3397
44	5.482	3.1443	11.6153	4.5939	2.8671	11.9451	103	2.7975	2.1603	4.4397	2.3437	1.6636	5.6837
45	3.4558	2.4225	4.6865	5.0133	2.2418	6.0575	104	4.6645	2.7573	6.7843	5.5575	2.188	6.0744
46	3.27	2.4493	6.6167	3.1516	1.9754	6.3283	105	3.3384	1.6014	5.4794	3.472	1.3841	5.266
47	2.2277	1.4606	4.3631	1.9942	1.3003	4.708	106	3.512	1.6593	3.5062	2.2546	1.2076	3.5885
48	3.3951	1.8977	3.9376	4.2622	1.7562	3.4397	107	1.4843	1.0543	4.9959	1.5711	0.934	5.0481
49	5.799	2.6688	7.2304	4.8791	2.4698	7.3853	108	3.6685	1.8228	5.2543	3.052	1.5256	5.4036
50	3.3355	1.8832	4.1522	3.1958	1.8013	3.8382	109	2.4276	2.1482	8.8429	2.5845	1.8041	9.1079
51	1.7801	1.5661	6.7443	1.7827	1.2727	7.4112	110	2.1807	1.6525	5.7074	2.1021	1.4758	5.8237
52	2.5496	0.9308	2.9283	2.7523	0.7132	3.1713	111	2.1512	1.3843	5.4077	2.0325	1.1567	6.0261
53	1.5976	1.2821	6.3262	1.6866	1.1098	7.1392	112	7.0202	2.5303	4.8073	3.5553	2.4053	5.3045
54	2.7377	1.7282	3.7301	3.163	1.4514	4.0603	113	2.2566	1.2089	5.7552	1.9822	1.168	5.9298
55	6.6039	1.9993	4.3183	6.4059	1.8101	4.5921	114	4.0243	1.4453	4.7605	3.3949	1.2478	4.741
56	2.5325	1.737	9.7388	2.4192	1.3475	11.1438	115	1.8066	1.3197	4.6409	1.7565	1.1799	4.7557
57	4.1047	2.6646	7.3928	3.5516	2.439	7.2476	116	2.3862	1.348	3.5652	2.2306	1.16	3.5408
58	3.0712	1.3286	4.708	2.0474	1.0303	4.9936	117	5.3804	1.7643	5.6483	4.4349	1.5093	5.7964
59	6.5351	2.9163	7.2426	5.6194	2.399	7.7973	118	6.4162	1.6777	4.2498	4.7894	1.5806	4.3208

Field sample 2 (continued)													
Index	$h_{1,g}$ [kpc]	$h_{2,g}$ [kpc]	$R_{b,g}$ [kpc]	$h_{1,r}$ [kpc]	$h_{2,r}$ [kpc]	$R_{b,r}$ [kpc]	Index	$h_{1,g}$ [kpc]	$h_{2,g}$ [kpc]	$R_{b,g}$ [kpc]	$h_{1,r}$ [kpc]	$h_{2,r}$ [kpc]	$R_{b,r}$ [kpc]
119	7.2262	1.9807	5.7089	5.5944	1.9109	5.5108	146	1.4859	1.8961	3.4409	1.1042	1.4324	5.2665
120	2.2247	0.9597	4.2305	1.886	0.6792	4.8339	147	1.5657	1.7075	3.0479	1.3783	1.5445	3.7113
121	1.5644	0.9712	2.5997	1.5508	0.6807	4.3251	148	1.1417	1.1729	1.5143	0.8994	1.3434	2.7575
122	2.05	1.7764	4.9833	1.9776	1.5395	5.1326	149	1.6074	1.8491	4.7117	1.3344	1.8995	4.9746
123	1.9191	1.8852	4.5002	1.8785	1.8328	5.4535	150	1.0203	0.9059	1.2367	0.7902	0.8086	1.1806
124	1.0374	1.5015	3.9953	0.8165	1.0866	3.2571	151	0.875	1.5262	2.0507	0.6475	1.4241	2.5009
125	2.1455	2.1387	6.2742	1.8739	2.1355	5.2457	152	1.6733	2.4282	3.8369	1.4639	2.396	4.4527
126	0.8247	1.1997	2.048	0.8501	1.1483	2.7628	153	1.1816	1.4947	6.6688	1.2625	1.8876	7.5458
127	1.009	0.9537	3.8674	0.7796	0.8429	3.8558	154	0.9581	1.6915	5.7781	0.703	1.8647	6.0458
128	1.3868	2.4428	4.7199	1.083	2.2279	4.5427	155	1.2798	1.3728	2.6161	0.775	1.1837	3.8058
129	1.1939	1.4431	1.3427	0.7859	1.2957	1.8748	156	1.0875	1.1563	2.3103	1.0279	1.2587	2.8748
130	0.5887	0.6065	2.5281	0.5976	0.8604	3.2355	157	2.3833	3.8805	5.7636	2.0495	3.6205	6.6142
131	1.3173	1.5056	6.0598	1.1455	1.3927	5.9556	158	1.7317	1.5495	4.5763	1.5977	2.1154	5.7488
132	1.5413	2.649	4.0499	1.4918	2.5411	4.9241	159	1.3599	1.5383	3.057	1.4958	2.6357	6.4152
133	1.7282	2.0312	6.3591	1.4217	1.6231	6.5389	160	1.9057	2.5777	4.841	1.768	2.5452	5.3366
134	1.4192	1.3962	2.724	1.2539	1.529	3.4349	161	0.8542	1.5865	5.6798	1.5899	2.0498	7.5482
135	1.1512	1.2521	2.928	0.8547	1.2488	4.2412	162	1.9102	2.7059	4.9569	1.3858	2.5982	5.0332
136	1.0808	2.5701	2.7829	1.0715	2.3503	4.4954	163	1.438	1.5659	2.4789	0.9596	1.522	2.555
137	1.6877	1.9146	4.9756	1.6765	2.0632	5.8762	164	0.9738	2.0213	5.5774	0.8185	2.0096	5.7575
138	3.0772	4.7351	6.4423	2.6462	4.3416	6.9245	165	2.8457	4.2906	6.6113	2.4195	4.0823	6.8306
139	2.3897	3.4199	9.3856	2.0759	2.2712	9.9258	166	1.3635	1.9398	4.5263	1.3091	1.5265	5.2902
140	1.2923	1.5946	3.239	0.5731	1.5195	2.0063	167	2.2346	2.9186	7.4767	1.84	2.8229	6.8446
141	1.765	1.6917	5.1832	1.6178	1.8556	6.7572	168	1.2639	1.8062	4.4295	1.2217	1.6029	5.315
142	1.7682	2.0552	10.7533	2.1832	2.5337	10.6298	169	1.9186	2.0255	5.305	1.7441	2.1267	5.2438
143	1.0337	0.8443	3.0696	0.9482	0.9647	5.2898	170	0.6429	0.8374	2.0101	0.5072	0.935	2.9733
144	1.8522	2.4086	6.1242	1.7068	2.2113	7.0472	171	1.5997	1.9453	5.7365	1.0389	2.1293	6.0995
145	3.2611	3.6688	10.7345	2.7975	3.2525	11.7368	172	1.915	4.1719	3.2015	1.7539	4.9282	3.6789

Table C8: Listing of scale lengths and break radii (each in both observed bands) of all 177 galaxies in field sample 3.

Field sample 3													
Index	$h_{1,g}$ [kpc]	$h_{2,g}$ [kpc]	$R_{b,g}$ [kpc]	$h_{1,r}$ [kpc]	$h_{2,r}$ [kpc]	$R_{b,r}$ [kpc]	Index	$h_{1,g}$ [kpc]	$h_{2,g}$ [kpc]	$R_{b,g}$ [kpc]	$h_{1,r}$ [kpc]	$h_{2,r}$ [kpc]	$R_{b,r}$ [kpc]
1	1.0678	-	-	1.1306	-	-	30	1.6276	1.2349	4.0304	1.45	1.222	4.2891
2	1.4189	-	-	1.4475	-	-	31	2.3017	1.3873	3.6776	2.5188	1.1845	3.9571
3	1.4982	-	-	1.7333	-	-	32	3.3937	1.2106	3.9901	2.7085	1.3278	4.0236
4	0.9593	-	-	0.9772	-	-	33	2.717	2.3257	4.2151	2.749	2.4516	3.76
5	1.524	-	-	1.4227	-	-	34	1.0647	0.7184	5.3328	0.9814	0.9368	7.4206
6	1.6482	-	-	1.7149	-	-	35	2.2815	1.712	4.5516	2.1786	1.7117	4.214
7	1.9825	-	-	1.8807	-	-	36	5.7639	0.9014	8.8999	6.1031	1.9898	8.4448
8	1.6197	-	-	1.5815	-	-	37	2.0048	0.8423	6.6746	1.8811	1.0755	6.7012
9	1.0853	-	-	1.0509	-	-	38	2.8697	1.2753	5.9162	2.5351	1.438	6.35
10	1.2345	1.0932	3.6612	1.3766	1.1822	3.548	39	4.8307	2.5357	3.612	3.7236	2.4594	4.1303
11	2.2303	1.3809	3.0065	1.8865	1.3803	3.1653	40	2.5111	0.8414	3.4911	2.327	0.9626	3.4708
12	4.0803	0.8898	6.4187	2.1661	0.9889	6.6299	41	2.0359	1.3034	6.8202	2.149	1.2093	7.0045
13	1.501	0.7007	7.3676	1.2215	0.6094	7.1724	42	6.1022	1.806	5.5783	5.8949	2.048	5.3789
14	1.2175	1.0348	3.3867	1.1989	1.0515	3.4903	43	1.7683	1.0885	8.0322	1.761	1.0583	8.0806
15	2.7003	1.7124	4.3782	2.3531	1.6638	4.4928	44	5.9374	1.6504	4.4822	4.5963	1.7816	4.4096
16	1.6616	1.2334	3.8553	1.8139	1.2365	3.6697	45	1.457	0.2728	7.8258	1.5462	0.2889	8.4338
17	8.2125	1.3566	4.4019	4.1734	1.4517	4.8858	46	3.0467	1.5049	9.0047	3.2156	1.2374	10.2529
18	2.105	0.4821	9.0359	2.0148	0.4266	8.8407	47	2.6184	1.7312	6.2251	2.5809	0.7534	8.2978
19	6.1323	1.4792	4.2615	5.9256	1.5094	4.0909	48	2.052	1.6623	4.5552	2.0773	1.6555	3.7445
20	2.6853	1.6126	8.6927	2.6306	1.5342	8.8776	49	3.2633	1.5104	3.7962	4.9894	1.686	2.9158
21	3.9439	1.3285	6.5039	5.7099	1.7718	5.0084	50	6.3646	2.1813	5.0997	7.1166	2.0941	5.3278
22	5.2676	0.9217	4.6215	2.161	1.4255	5.2343	51	3.1442	1.5116	10.5555	2.8479	0.529	11.7815
23	2.0268	1.4442	3.814	1.7906	1.3851	4.0842	52	3.72	1.1962	5.7071	3.1743	1.3867	5.5528
24	3.62	1.952	5.888	3.0596	1.7593	6.1586	53	2.0175	1.0435	2.3531	2.0048	1.1687	2.2174
25	2.9049	0.677	5.8506	1.3094	0.6185	6.6258	54	4.5689	2.3468	8.1096	4.137	2.6199	6.6621
26	0.7922	0.5181	5.3656	1.0407	0.5836	5.1955	55	2.129	1.3648	5.8031	1.971	1.2898	5.6834
27	1.8894	1.339	4.5275	1.8277	1.3701	4.4514	56	2.9783	1.3018	8.4503	2.8397	0.9325	9.9165
28	3.2564	2.0649	4.5016	2.2904	1.5682	7.1864	57	2.5541	1.415	2.9429	1.8894	1.5871	3.3844
29	2.911	1.6183	7.2912	2.8236	1.2539	7.6103	58	7.0767	1.9041	4.3003	5.2659	1.8217	4.4214

Field sample 3 (continued)													
Index	$h_{1,g}$ [kpc]	$h_{2,g}$ [kpc]	$R_{b,g}$ [kpc]	$h_{1,r}$ [kpc]	$h_{2,r}$ [kpc]	$R_{b,r}$ [kpc]	Index	$h_{1,g}$ [kpc]	$h_{2,g}$ [kpc]	$R_{b,g}$ [kpc]	$h_{1,r}$ [kpc]	$h_{2,r}$ [kpc]	$R_{b,r}$ [kpc]
59	1.3917	1.018	5.3009	3.4525	0.7782	4.5677	119	2.6521	2.0144	4.9589	2.2288	1.9407	5.4681
60	3.7486	0.9864	11.4976	3.5611	1.2757	11.6012	120	3.0175	2.4968	5.2479	2.6647	2.3622	4.281
61	1.9369	0.9868	5.5094	1.7398	0.403	7.0213	121	2.7888	2.1841	9.0678	2.5945	2.4012	9.0154
62	4.3387	3.5488	8.5731	3.8914	3.6311	9.1993	122	2.0951	1.5514	5.5556	1.9791	1.6738	5.1832
63	3.2221	2.2144	12.3918	2.9778	1.4124	12.7983	123	4.5069	2.2691	3.7368	5.3201	2.7862	4.0238
64	3.5333	2.106	5.1879	3.2937	2.1019	4.8571	124	1.3028	1.1515	5.0832	1.3805	1.1975	5.0264
65	2.6934	1.1916	5.4256	2.4441	1.2672	5.7083	125	1.6296	1.4069	4.4188	1.5345	1.4059	4.5252
66	3.7507	1.3338	6.4391	3.2855	1.1566	7.1252	126	1.465	2.087	3.5735	1.3968	1.8674	3.7008
67	2.6428	1.661	3.9035	2.3271	1.7021	3.9131	127	1.329	1.7957	3.3026	1.2736	1.7902	3.3977
68	2.6804	1.6381	3.2031	2.1923	1.2988	5.304	128	0.8316	1.7882	3.0756	0.8554	1.726	3.103
69	1.9215	1.351	7.8191	2.201	1.4606	7.4124	129	1.0277	1.652	2.8586	1.1805	1.7492	3.2267
70	2.9308	1.9403	4.3874	2.5963	1.7916	5.4362	130	1.2445	1.4765	2.9197	1.21	1.5231	2.7998
71	3.1926	2.0003	6.046	2.6615	1.909	6.2631	131	0.9996	1.7415	5.8302	1.0063	1.7491	5.7299
72	3.2756	1.0353	9.5789	2.3517	1.441	9.0881	132	0.9002	1.3251	2.486	1.0397	1.4027	2.5179
73	3.0175	2.058	5.422	2.6979	1.7361	7.653	133	2.3641	2.7242	5.4223	2.2571	2.85	6.5032
74	2.7377	1.7769	8.6201	2.5093	1.3643	9.0322	134	1.1676	1.5427	3.3994	1.1984	2.6555	5.2186
75	4.7894	1.4028	5.9615	5.0686	1.4679	5.4336	135	1.9386	2.0043	5.7923	1.3359	2.5698	4.0494
76	4.1218	1.8522	7.8918	3.6772	1.9186	7.858	136	1.6717	2.3098	5.7729	1.6688	2.3043	5.972
77	1.2385	0.9041	3.6254	1.3461	0.9708	3.6883	137	1.4326	1.8788	3.7704	1.1554	1.8386	3.3524
78	4.5969	1.2002	5.9478	4.1042	1.4156	5.7523	138	1.5399	1.8585	3.5203	1.6355	1.8182	5.1677
79	2.2842	1.3641	5.4225	1.5589	1.2869	5.5276	139	0.9166	1.1556	2.3366	0.8512	1.2355	2.1348
80	2.1121	1.0089	7.4561	1.8315	1.148	7.1848	140	1.2075	2.3573	4.4084	0.9108	1.8586	2.9228
81	2.966	1.2941	12.1293	2.7094	1.6652	10.6858	141	1.3524	1.804	2.769	1.4349	1.8368	4.5651
82	2.7925	2.0535	4.8521	2.4407	1.8313	5.6974	142	1.2647	2.1892	4.3502	1.1264	1.926	3.9728
83	1.4771	0.9859	6.4323	1.5173	0.993	5.5346	143	2.6596	3.4939	4.6853	2.5779	3.3185	5.2574
84	3.2701	1.9918	7.3154	2.9167	2.3315	6.4422	144	3.2715	3.6085	10.0873	2.6887	3.2566	9.9658
85	7.38	1.3438	6.4573	6.4938	1.4301	6.2675	145	0.9022	1.6667	3.25	0.9252	1.7295	3.3924
86	2.2142	1.4348	4.6418	2.5747	1.2641	4.5442	146	1.2523	1.4722	3.9549	1.1735	1.9593	4.075
87	6.0943	2.8901	5.991	5.9602	2.815	6.4394	147	1.3727	2.8606	6.1531	1.1653	2.3441	6.1299
88	5.8615	1.9492	4.913	7.2975	1.8951	4.5949	148	1.2851	1.4631	3.2012	1.3205	1.4295	3.337
89	2.4687	1.7181	7.1657	2.5814	1.5068	7.6554	149	1.1491	1.2888	5.0745	1.1896	2.0249	5.6902
90	1.3327	1.0455	3.3318	1.3163	1.0641	3.1825	150	1.5129	1.9503	8.2065	1.5245	1.8118	8.1028
91	2.9593	1.8841	6.3209	2.6089	1.9148	6.9255	151	1.4029	2.1614	1.8036	1.406	2.4351	6.9792
92	1.2378	0.6102	3.6722	1.496	0.6067	4.2676	152	1.1554	1.405	4.0802	0.8945	1.2817	1.2537
93	3.7243	1.6131	14.408	3.5549	2.5124	14.0725	153	0.6464	0.8301	3.6748	0.8878	1.3147	3.7153
94	1.5413	1.3125	4.5306	1.4851	1.2188	6.8947	154	0.9686	1.1859	2.8943	0.959	1.1609	2.9695
95	5.4832	1.4698	13.7195	5.1741	1.5146	14.4301	155	1.3827	1.9036	4.3744	1.6369	1.9515	5.1306
96	1.379	1.2196	5.0624	1.7264	1.2634	2.8619	156	0.9231	1.3684	5.5609	1.0526	1.4947	5.0665
97	3.329	1.6041	5.4472	4.7026	1.6901	4.899	157	1.5581	2.6386	5.9604	1.945	3.1255	5.8597
98	2.2559	1.1963	6.995	2.0244	1.3328	6.9031	158	0.9862	1.3989	3.5303	1.0611	1.7502	5.449
99	2.2678	1.1737	3.4867	2.2735	1.2076	3.6522	159	1.7647	1.923	6.2612	1.6615	2.038	6.075
100	2.6151	1.127	7.4647	1.9572	1.6451	5.7307	160	1.4571	1.6381	5.3335	1.4679	1.8984	4.6972
101	2.5127	1.5524	6.9147	2.8177	1.8578	6.4279	161	1.3629	1.4461	5.6501	1.1576	1.6033	4.1315
102	2.3242	1.8462	5.144	2.729	1.6511	6.7321	162	1.476	2.1868	8.2096	1.7788	3.2294	8.2668
103	1.8021	0.9429	7.449	1.6979	0.8648	7.904	163	0.9833	1.3556	3.9338	1.0106	2.0101	4.4943
104	5.1547	2.0099	9.7362	4.2543	1.9646	9.7347	164	1.97	3.2384	7.2224	1.4239	3.119	6.926
105	2.7295	2.0697	4.9681	2.3422	1.8733	5.2529	165	1.6428	1.811	6.5262	1.6496	2.275	7.1002
106	2.9895	1.2288	3.7795	2.8496	1.0324	4.1839	166	2.4054	3.7294	9.587	2.1996	3.2895	9.1482
107	4.4694	2.1758	5.1112	3.5759	2.1499	5.4107	167	1.8885	2.5139	6.7333	1.9893	2.7599	8.1403
108	3.9039	2.4091	5.2382	3.1505	2.0542	8.4416	168	0.9301	2.0554	6.1522	1.2713	1.6987	6.2798
109	2.7613	2.5255	8.2527	2.7311	1.5251	11.6614	169	1.3562	2.1716	4.4343	1.8077	2.0676	8.7386
110	2.009	1.328	9.2501	2.009	0.9119	10.1275	170	1.083	1.9255	3.7304	1.1646	1.9188	3.6378
111	2.2748	1.3534	2.5203	2.8172	1.405	2.8808	171	1.6152	1.9104	3.6703	1.1465	1.905	5.5924
112	2.3749	2.0526	8.3488	2.589	2.1982	6.4778	172	1.5651	2.2593	4.5392	1.8765	2.3702	5.495
113	2.8671	1.1921	6.9061	2.3889	0.9443	8.5188	173	1.5221	2.0033	7.1187	1.3957	1.5007	5.9477
114	3.3949	1.0394	10.2521	4.4965	0.6936	10.3492	174	1.368	1.8296	6.9878	1.3752	1.8768	6.6131
115	2.1435	0.6511	5.2871	2.453	0.5301	6.6548	175	1.2152	1.4105	4.4002	1.3351	1.6207	4.6851
116	1.1519	0.8439	4.4486	1.1776	0.6055	5.1719	176	1.4866	1.8271	6.4057	1.4055	1.8456	5.3667
117	2.6945	1.1806	9.1363	2.4057	1.1153	9.6873	177	0.9251	1.3523	2.5724	0.7311	1.151	2.4441
118	2.1789	0.9769	8.8423	2.1343	0.9328	9.8227							